Juha Korhonen

Master's Thesis

Using Volumetric-modulated Arc Therapy and Cone-beam Computed Tomography Image Guidance with Six Degrees of Freedom in Patient Positioning for the Radiation Therapy of Patients with Bladder Cancer

AALTO UNIVERSITY

School of Electrical Engineering

Thesis submitted for examination for the degree of Master of Science in Technology.

Helsinki June 29th 2011

Supervisor:

Prof. Raimo Sepponen

Instructor:

Ph.D. Mikko Tenhunen

Aalto University
School of Electrical
Engineering

AALTO UNIVERSITY
SCHOOL OF ELECTRICAL ENGINEERING

ABSTRACT OF THE
MASTER'S THESIS

Author: Juha Korhonen

Title: Using Volumetric-modulated Arc Therapy and Cone-beam Computed Tomography Image Guidance with Six Degrees of Freedom in Patient Positioning for the Radiation Therapy of Patients with Bladder Cancer

Date: 29.6.2011 Language: English Number of pages: 7 + 63

Department of Electronics

Professorship: Applied Electronics Code: S-66

Supervisor: Prof. Raimo Sepponen

Instructor: Ph.D. Mikko Tenhunen

The radiation therapy of bladder cancer patients is challenging especially because of the changing volume and shape of the bladder. With the on-line adaptive method, it is possible to aim the treatment accurately to the bladder, but the use of the method demands special features from the treatment unit.

The goal of this Master's Thesis was to assure the functionality of the new linear accelerator Elekta Axesse in Helsinki University Central Hospital (HUCH) and to investigate the prospective benefits of the features; volumetric-modulated arc therapy (VMAT), cone-beam computed tomography (CBCT) and six degrees of freedom, for the treatment of patients with bladder cancer. Furthermore, it was a goal to introduce comprehensive instructions for the treatment process, including strategies for treatment planning, plan verification, CBCT imaging and patient positioning.

In order to assure the functionality of the treatment unit, phantoms were developed. The one constructed around the matrix detector was used for the VMAT plan verification process, and the internal organ phantom was generated in order to investigate the CBCT imaging and the accuracy of patient positioning. The VMAT treatment plans were created using the treatment planning system Monaco.

As a result of the Thesis, the equivalence between the calculated and delivered VMAT treatment plans was shown to be in 3 % and 3 mm scales with 95 % of point doses. The accuracy and functionality of the CBCT system were shown to work in 0.1 cm and 0.1° scales. In addition, new presets were created especially for imaging bladder cancer patients with the CBCT. Into the treatment planning system was attached the VMAT treatment plan template which is also a part of the created instructions for the complete radiation therapy process of patients with bladder cancer. Using the instructions, five patients with bladder cancer were treated during the spring 2011.

As a conclusion of the Thesis, the Elekta Axesse linear accelerator makes it possible to treat the bladder cancer patients very reliably and accurately with radiation therapy.

Keywords: Radiation therapy, volumetric-modulated arc therapy, cone-beam computed tomography, six degrees of freedom and on-line adaptive method.

AALTO-YLIOPISTO
SÄHKÖTEKNIIKAN KORKEAKOULU

DIPLOMITYÖN
TIIVISTELMÄ

Tekijä: Juha Korhonen

Työn nimi: Intensiteettimuokattu kaarihoito ja kartiokeilatietokonetomografia kuusiulotteisella potilasasettelulla virtsarakkosyöpää sairastavien potilaiden sädehoidossa.

Päivämäärä: 29.6.2011 Kieli: Englanti Sivumäärä: 7 + 63

Elektroniikan laitos

Professuuri: Sovellettu elektroniikka Koodi: S-66

Työn valvoja: Prof. Raimo Sepponen

Työn ohjaaja: Dos. Mikko Tenhunen

Virtsarakkosyöpää sairastavien potilaiden sädehoito on haasteellista erityisesti virtsarakon tilavuuden ja muodon vaihtelun vuoksi. Kuvantaohjatun adaptiivisen menetelmän avulla on pystytty kohdistamaan sädehoito tarkasti virtsarakkoon, mutta menetelmän käyttäminen vaatii kuitenkin erityisiä ominaisuuksia sädehoitolaitteelta.

Tämän työn tavoitteena oli varmistaa Helsingin yliopistollisen keskussairaalan (HYKS) uuden Elekta Axesse sädehoitolaitteen toiminta kliinisessä ympäristössä ja tutkia sädehoitolaitteen erityisominaisuuksien; intensiteettimuokatun kaarihoidon, kartiokeilatietokonetomografian ja kuusiulotteisen potilasasettelun, etuja virtsarakkosyöpää sairastavien potilaiden sädehoidossa. Hoitojen toteuttamiseksi oli tavoitteena esitellä annossuunnittelun, suunnitelmien laadunvarmistamisen, potilaan kuvantamisen ja potilasasettelun sisältämä sädehoito-ohje.

Sädehoitolaitteen toiminnan varmistamiseksi kehitettiin testikohteita, joista matriisi-ilmaisimen ympärille kehitettyä systeemiä käytettiin annosjakaumien laadunvarmistukseen ja kliinisesti yhteensopivaa testikohdetta kuvantamisen ja potilasasettelun tarkkuuden selvittämiseen. Intensiteettimuokattujen kaarihoitosuunnitelmien kehittämiseen käytettiin Monaco hoidonsuunnittelujärjestelmää.

Tämän työn tuloksena laskettujen ja toteutuneiden intensiteettimuokattujen kaarihoitosuunnitelmien välinen vastaavuus osoitettiin olevan 3 %:n ja 3 mm:n sisällä 95 %:ssa mittauspisteistä. Kuvauslaitteen ja potilasasettelun toiminta varmistettiin 0,1 cm:n ja 0,1°:n tarkkuudella. Laitteeseen luotiin erityisesti virtsarakkosyöpää sairastavien potilaiden kuvantamiseen sopivia asetuksia. Hoidonsuunnittelujärjestelmään lisättiin kaarihoitosuunnitelmapohja, joka on myös osa virtarakkosyöpää sairastavien potilaiden hoitamiseksi kehitettyä sädehoito-ohjetta. Ohjeen perusteella hoidettiin viisi potilasta HYKS:ssa kevään 2011 aikana.

Tämän työn perusteella voidaan todeta, että Elekta Axesse sädehoitolaite mahdollistaa virtsarakkosyöpää sairastavien potilaiden hoitamisen erittäin luotettavasti ja tarkasti.

Avainsanat: Sädehoito, kuvantaohjattu adaptiivinen menetelmä, intensiteettimuokattu kaarihoito, kartiokeilatietokonetomografia ja kuusiulotteinen potilasasettelu.

Preface

This project was named based on the investigation contract between Elekta Instrument AB and Clinical Research Institute HUCH Ltd, and was performed in the Department of Oncology of Helsinki University Central Hospital. I want to thank Elekta, the Clinical Research Institute and the Department of Oncology for calling me into this interesting and challenging project in the beginning of the cooperation between the parties, and making it possible for me to complete my Master's Degree within it.

I want to thank all the physicists, engineers, oncologists and radiographers with whom cooperation has been excellent. Especially, I wish to thank the chief physicist Mikko Tenhunen for supporting me not just with the project, but also during all the other steps in the beginning of my career.

In addition, I would like to thank my family and closest friends. It would have been a lot of more difficult to reach this far, if my parents would have not reminded me of the significance of studies during the times when ball games, especially hockey, were more appealing than books. I want to thank my fiancée and my friends about the positive energy they bring into my life. This energy makes also my daily work more vigorous.

Helsinki June 29th 2011

Juha Korhonen

Table of contents

Lists of symbols and abbreviations

List of symbols

D_m	measured absorbed dose using matrix detector
D_w	absorbed dose in water
J_{100}	percentage dose of maximum dose at depth of 100 mm
$J_{100/\ 200}$	ionization ratio between depths 100 and 200 mm
K_{Acc}	measurement accuracy of matrix detector
K_C	calibration factor for measured dose distributions by the created verification system
K_{DR}	relative difference between daily and reference dose rate
K_m	factor for calibrating the ionization chambers of matrix to the chamber of absolute dosimetry
$k_{p,\ t}$	correction factor for the ionization chamber's calibration factor's pressure and temperature dependence
K_R	relative factor between a measured or calculated point dose and the measured point dose with gantry angle 0°
k_r	recombination coefficient
K_T	factor for eliminating the effect of attenuation by the treatment table
K_γ	factor for correcting the dependence of measuring angle of the chambers of the matrix
M	charge measured by ionization chamber
m	readout of the electrometer
MD	measured absorbed dose using matrix in different investigations
$N_{D,\ w,\ Q}$	calibration factor for ionization chamber
TM	traversed distance of radiation in matter to the measuring point
α	gantry angle
β_{Arc}	size of an arc
β_T	size of the sector of an arc where attenuation by the treatment table need to be considered

List of abbreviations

CBCT	Cone-beam Computed Tomography
CT	Computed Tomography
DVH	Dose Volume Histogram
EUD	Equivalent Uniform Dose
Gy	Gray
HUCH	Helsinki University Central Hospital
ICRU	International Commission on Radiation Units and Measurements
IMRT	Intensity Modulated Radiation Therapy
MLC	Multileaf Collimator
MV	Megavolts
OBI	On-Board Imager
PDD	Percentage Depth Dose
PMMA	Polymethyl Methacrylate
PTV	Planning Target Volume
VMAT	Volumetric-modulated Arc Therapy

1 Introduction

The treatment of patients with bladder cancer using radiation therapy involves peculiar challenges. Pivotal problems are caused by organ motion in the pelvic area and the varying volume of the bladder. Furthermore, the vicinity of organs at risk and the incontinence of the patients set some constraints on treatment. By observing these challenges the on-line adaptive method for basis of the radiation therapy of patients with bladder cancer has been developed. The method is based on image-guided radiation therapy, in which a three-dimensional image of the patient positioned on the treatment table is required before delivery of the treatment.

The challenges of radiation therapy for bladder cancer patients and the use of the on-line adaptive method establish high requirements for the treatment unit. A linear accelerator should be equipped, at least, with a high level on-board imaging system and be able to deliverer dynamical fields. With recently installed linear accelerator Elekta Axesse (Elekta Instrument AB, Sweden) at the Department of Oncology of Helsinki University Central Hospital (HUCH) it is possible to face the requirements. The linear accelerator is equipped with cone-beam computed tomography (CBCT) device, treatment table with six degrees of freedom and it is capable for volumetric-modulated arc therapy (VMAT).

In order to bring a new treatment unit into clinical use, it is essential, that verifications between planned and delivered dose distributions are done exactly. Using the Elekta Axesse linear accelerator, the plan verification process encounters new challenges caused by the rotational character of VMAT. For this purpose it is crucial to create a reliable verification system before starting treatment of patients. In addition, clinical verification of the matching accuracy of the CBCT system with the planning computed tomography (CT) image and the co-operation between the CBCT system and the mobile treatment table has to be assured. Also the delivered doses of the CBCT images have to be determined.

VMAT treatments require special properties also from the treatment planning system. At the same time, with the new linear accelerator, also a VMAT capable Monaco treatment planning system (Elekta CMS Software, Germany) was installed. The use of a new planning system with new kinds of treatment methods signifies challenges to identify suitable ways to work with the system to obtain feasible solutions for treatment. It is important for the clinic to create a gold standard, i.e. a template, for specific patient cases in treatment planning. In the case of patients with bladder cancer, it is desirable to create a reliable template for the whole treatment process including also a strategy for accurate patient positioning.

2 Theoretical Backgrounds and the Goals of the Project

2.1 Photons in radiation therapy

The properties of electromagnetic radiation such as attenuation, absorption and interactions in tissues provide the basis for dose calculation in radiation therapy. Between photons and absorbing, materials encounter processes of interactions that have

an effect on the attenuation of radiation. The energy of the radiation and the properties of the material have essential influences on processes, which do not border on to the interactions of primary photons, but also there are following secondary- , tertiary, etc processes. With the photon energies used in radiation therapy, the photons lose their energy to electrons most of all caused by three different interactions. First, by Compton scattering, in which a photon loses some of its energy in interaction with an atomic electron. A scattered photon moves on as a photon with a longer wavelength than before and the emitted electron loses its energy in the following interactions in matter. Another significant mechanism is pair production. In this process a photon interacts strongly with the electromagnetic field of an atomic nucleus and gives up all of its energy in the process of creating a pair consisting of a negative and a positive electron. These commonly short-lived positrons generate photons around them while absorbing in matter. Third, a noteworthy phenomenon is the photoelectric effect. In this process the entire energy of a photon is absorbed by an atom in an interaction, where the energy is re-transferred to ejected orbital electrons. Throughout among these processes is formed absorbed dose in matter. It is defined as the energy absorption of one Joule of ionizing radiation imparted by one kilogram of matter, and it is announced in units of Gray (Gy). [1][2]

In addition to just knowing the phenomena of ionizing radiation in matter, it is crucial to be able to determine how the overall dose is distributed in practise. This can be examined using dose measurements and analyses of different dose graphs. For example by percentage depth doses (PDD), which describe the percentage doses in matter compared to the dose at maximum point with a certain field size and energy. By PDDs, for example, a ratio between doses at depths of 100 and 200 millimetres, i.e. ionization ratio, can be determined. It is also important to investigate dose distributions at a certain depth in matter outside the middle axis. This is possible by so-called profiles, which can be normalized in two ways depending on what it is desired to investigate. The first way is to normalize many profiles of a field to the value at the depth of maximum dose. In this case it is possible to investigate the attenuation of a field as a function of depth. Normalizing can also be done to the dose at the middle axis of each depth. With this off-axis-ratio it is possible to investigate how dose is distributed compared to the middle axis. It can be investigated even more visibly with so-called decrement graphs, which are formed by merging the points at which there are the same relative doses. Significant graphs in dose distribution analysis are also isodoses, which can be constructed when dose distribution is normalized into a specific point dose. All the other point doses in the investigated area are compared to the specified point dose. The ones with the same relative doses are merged to form a graph; isodose. [1][2]

By the physical properties of ionizing radiation and the information analyzed by measurements, it is possible to change photon flux into overall dose at every point of the irradiated area to form dose distributions. These can be calculated nowadays by treatment planning systems' calculation algorithms, in which all possible kinds of fields and plans should be modelled. In the traditional external beam photon radiation therapy the dose calculation and delivery of the radiation beams are based on static fields. In general, the static fields have almost uniform intensity across a field. Occasionally, for example wedges have been used in order to change beam intensity profiles to meet the goals of a composite plan. This process is called intensity modulation, which is nowadays possible to perform with variously shaped computer-controlled intensity modulation systems such as dynamic multileaf collimators (MLCs). Using dynamic

MLC, several treatment fields with nonuniform fluence can be optimized by a proper treatment planning system to form composite dose distribution into the target volume. By using this intensity modulated radiation therapy (IMRT), also the dose calculation works in a different way. By so-called inverse planning the treatment goals, criteria and beam directions are inserted into the software by the user. Using the information, the treatment planning system tries to calculate optimal fluence profiles for each field by creating suitable movements for the dynamic MLC. The resulting composite dose distributions should include a high dose in the target volume and an acceptably low dose in the surrounding healthy tissues. Dose distributions can have irregular shapes, for example concave ones, which can be observed by isodoses in three dimensions. In the trajectory of the IMRT technique the amount of dynamical features have increased by adding a rotational property of the gantry while beam is on. Generally, this method is called intensity modulated arc therapy. From it has evolved volumetric-modulated arc therapy, in which also simultaneous variations of dose rate and gantry speed are allowed. [1][2][3][4][5][6]

2.2 Radiation therapy as a treatment for patients with bladder cancer

Traditionally, the standard treatment for patients with muscle-invasive urinary bladder cancer is radical cystectomy. However, some patients have inoperable tumours or their medical conditions make them unfit to undergo the cystectomy. For these patients radiation therapy is an effective treatment. Conventional radiation therapy technique for this group of patients includes one planning target volume (PTV) designed by one treatment planning CT image. In order to take into account the maximum changes of the bladder's shape, size and position, the margins of the PTV have had to be designed wide enough to ensure sufficient dose coverage. All of the treatments, i.e. fractions, are realized by the one and only treatment plan. This method implies irradiation of large volumes of healthy tissues especially by the fractions during which the bladder volume is relatively small, i.e. when the bladder is empty. [7][8][9]

The development of the technologies and methods of image-guided radiation therapy have made it possible to identify and correct problems arising from inter- and intrafractional variations in patient setup and anatomy, including the shapes and volumes of the treatment target, organs at risk and the surrounding normal tissues. By these improvements the on-line adaptive method has been introduced for the basis of the radiation therapy treatment of bladder cancer patients. With this method constant changes in bladder volume and positions of internal organs in the pelvic area have been taken into consideration by the bladder localization before every fraction and also by having several treatment plans created for different PTVs. Using four CT images taken within an hour after urinating, four different target volumes can be planned. Before every fraction the prevailing situation of the bladder is tracked down by a CBCT image. The position and shape of the bladder is compared to the four contoured bladder shapes by the four planning CT images. The plan created by the bladder shape, which is most equivalent to the daily bladder shape, is then treated. This method can reduce the dose to the organs at risk, while maintaining the dose coverage of the target volume at a similar level, compared to the conventional treatment technique. [2][7]

In radiation therapy of bladder cancer patients in HUCH the on-line adaptive method has been in use since 2009. The treatment offered in 2009 and 2010 was realized using

Varian Clinac iX (Varian Medical Systems Inc., Palo Alto, CA, USA) linear accelerator, which is equipped with the On-Board Imager (OBI) CBCT system. In treatment planning the IMRT technique has been used with seven treatment fields with 6 and 15 MV photon energies. The treatment planning process has been realized using the treatment planning system Eclipse (Varian Medical Systems Inc., Palo Alto, CA, USA) with kernel based pencil beam convolution calculation algorithm. The objectives set by International Commission on Radiation Units and Measurements (ICRU) in report 50 have been used as the goals for target dose. The planned target doses have been between 55.8 and 65 Gy, for which one of the limiting factors has been the amount of radiation that the bowels are exposed to. [7]

2.3 The Goals of the Project

The comprehensive goal of the project is to introduce instructions for suitable working process for the radiation therapy of patients with bladder cancer in HUCH by utilizing the new Elekta Axesse linear accelerator with its features. In order to achieve this goal, there are many partial issues, which have to be investigated. By introducing strategies individually for all the parts of the working process, the comprehensive working strategy can be constituted.

Before beginning to plan patient treatments the equivalence between the VMAT treatment plans created by the Monaco treatment planning system and delivered by the Elekta Axesse linear accelerator have to be configured. To achieve this goal it is relevant to create a reliable verification system. For the treatment of patients with bladder cancer also the accuracy of image guidance has to be ensured. So, it is also a goal to assure the performance of the CBCT system by image quality, automatic matching capabilities and precise patient repositioning. Furthermore, it is an aim to find such combinations of parameters for CBCT imaging, which would make it possible to perform images with good enough image quality with as low irradiation as possible.

After achieving the goals concerning the operations of the equipment, the concentration of the investigations can be focused on the use of the equipment. For treatment planning it is a goal to find suitable settings and parameters, which would form the basis of a workable template for VMAT treatment planning of patients with bladder cancer. Also introduction of a suitable strategy for performance of the CBCT imaging and patient positioning is set as a target. In the end, by all the reached goals, comprehensive instructions for the radiation therapy of bladder cancer patients should be introduced including strategies for VMAT treatment planning, plan verification and patient positioning.

3 Basics of the Equipment Used in the Project

3.1 Linear accelerator Elekta Axesse

Elekta Axesse is a linear accelerator with modern features and equipment for radiation therapy. The one in HUCH was installed recently in October 2010. The accelerator includes three photon energies, which can be delivered by varying dose rates even

while the gantry is rotating. The gantry can be rotated a complete 360° circle by starting from gantry angle of 180° with a maximum speed of 360° in a minute. Treatment plans can be realized in the clock-wise direction of rotation. The fields can be shaped by dynamic MLC, which includes a set of 40 leaf pairs, in which each leaf is four millimetres wide. The leaves are able to move with a speed of 2.5 centimetres per second even while the gantry is rotating and the beam is on. The dose rate variations can be irradiated up to 600 monitor units per minute with the energy of 6 megavolts (MV). These features of the linear accelerator make it possible to use VMAT in treatment planning. In VMAT treatment planning the used arc is split into segments, which also represent the control points of the treatment. An example of the movement of the dynamic MLC during a segment is shown in image 1. The realization of a VMAT treatment plan is controlled by the treatment unit's computer by the instructions of the plan made by a treatment planning system. The computer of the treatment unit controls the progression of a plan by monitoring the treated monitor units, dose rate variations and the actual movements of the leaves as well as rotating the gantry during the segments. [2][3][4][5][10]

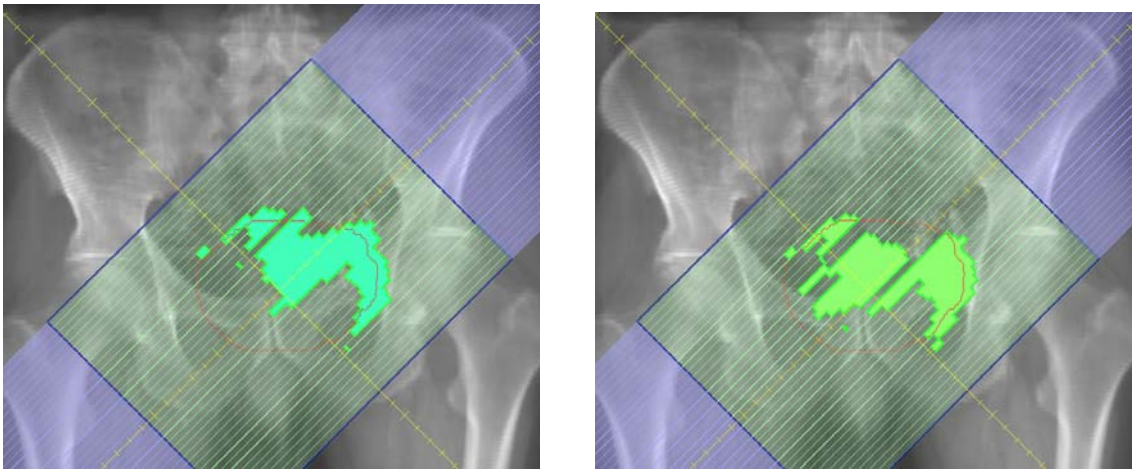

Image 1: Function of dynamic MLC in VMAT treatment plans. On the left the start position, and on the right the end position, of dynamic MLC in a segment with 4° gantry rotation and 9.5 monitor units.

The linear accelerator, which is shown in image 2, is equipped with two kinds of on-board imaging systems. With these systems it is possible to obtain on-line information about patient positioning, and so improve the accuracy of delivery of the treatment to its target volumes. A megavoltage electronic portal imaging device provides planar imaging using the accelerator's treatment photon energies. A flat-panel image detector is positioned opposite the source of megavoltage radiation. Even though the detector is a modern matrix system with amorphous silicon photodiode detectors, the image quality is relatively poor with megavoltage class photon energies. Because of this, the linear accelerator is also equipped with an on-board kilovoltage imaging system to produce high quality three-dimensional volumetric images. This CBCT system called Xvi includes its own x-ray tube positioned 90° clock-wise from the gantry and flat panel area detectors mounted opposite the x-ray tube. The CBCT system performs numerous planar projection images from multiple directions as the gantry rotates at least 180°. With these radiographs the software of the CBCT system constructs a three-dimensional volumetric image using a filtered back-projection algorithm. There are a number of pre-programmed presets for imaging in Xvi. However, some of the parameters can be manually adjusted by a user to have an effect, among other things, on

image quality and delivered dose. The CBCT images, also denoted localization images, can be matched with a reference image, which is a planning CT image, manually or by one of the matching algorithms of the software. These algorithms are designed to concentrate on recognizing differences in electron densities within a specified range between tissues. With the information obtained from the matching process, a patient can be re-positioned if necessary. [2][10][11]

Image 2: Elekta Axesse in HUCH. The gantry is set at a position of 0°. Opposite to the gantry is the flat-image detector for megavoltage radiation. The x-ray tube is on the right in the image and the detector for kilovoltage radiation is opposite to it. In the sealing is an infrared stereo tracking camera and on the treatment table is attached a frame of passive reflectors. On the wall on the very left in the image are the lasers for longitudinal and vertical patient positioning.

To get the full advantage out of the three-dimensional image of CBCT for patient positioning, the treatment unit is equipped with a treatment table system called Hexapod. The carbon fibre treatment table is positioned on top of two motorized movement units. Hexapod is able to be moved in all six degrees of freedom, which makes it possible to correct both translational and rotational positioning errors as shown in image 3. In the translational directions the range of movement accuracies are 0.1 mm in the maximum range of translations +/- 3 cm, +/- 3 cm and +/- 4 cm in x-, y-, and z-directions, respectively. In the rotational directions the range of movement accuracies are 0.1° in the maximum range of +/- 3° in all directions. The table position is computer-controlled via the iGuide software that the treatment table system's computer is running. The table is guided by an infrared stereo tracking camera installed in the sealing of the treatment room. The camera detects the positions of five passive reflectors, which are positioned on a frame attached to the treatment table. [10][11][12][13]

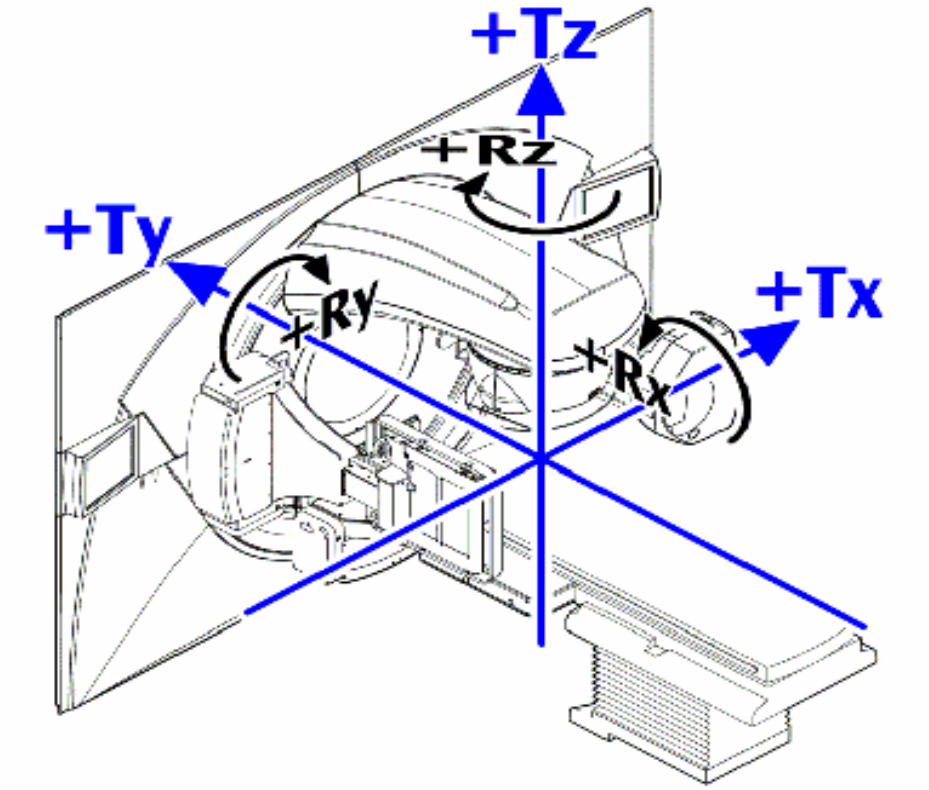

Image 3: Coordinate system of Elekta Axesse [10]. In the coordinate system the lateral direction is set as x, longitudinal as y and vertical as z.

3.2 Treatment planning system Monaco

Due to many degrees of freedom in VMAT treatment planning, the optimization process is computationally challenging. The treatment planning system needs to be able to calculate optimal dose distributions by considering the limitations of the accelerator and by trying to solve dose delivery challenges by using multiple dynamic property of the accelerator at the same time. These push calculation algorithms to their limits and raise calculation times even compared to conventional IMRT. Inverse plan optimization in IMRT is traditionally performed by dose volume histogram (DVH) optimization objectives. This method lets the user set dose levels for different contoured volumes of anatomical targets and organs of interest. The nonlinear responses of tumours or organs to radiation dose are not, however, adequately represented. In cases where a small number of voxels in a tumour volume receive a very low dose, it would not have any significant effect on the result of the plan. However, as a result the tumour control probability would be greatly diminished. This issue is relevant especially with arbitrary inhomogeneous dose distributions, which are reconstructed by inverse planning. The losses of tumour control and the capability of an organ to survive, if some parts of it lose capability to function, are considered in biological optimization. The biological information can be supplied in terms of tumour or normal tissue complication probability models or equivalent uniform doses (EUDs). The EUD of the target tissue is defined as the biologically equivalent dose that, if given uniformly, will lead to the same cell kill in the tumour volume as the actual nonuniform dose distribution. [3][4][5][6][14]

The Monaco treatment planning system is a tool, which utilizes not only the physical effects of radiation, but also EUDs and the biological properties of the tissues. The user has a possibility to set the cell sensitivity of Poisson's cell kill model. Organs at risk can be set as serial or parallel constraints depending of the properties of the tissue to function after a certain level of exposed radiation into them. The user is able to influence the amount of volume of a structure, which can be sacrificed, and also affect the strengths of the limits of the constraints. The system uses a two-step VMAT optimization process. In the first phase of optimization the treatment planning system creates the user specified arc by segments, which operate also as control points at the treatment unit's computer during treatment. Then the calculation algorithm of the first phase optimizes the fluence distributions for the segments. At this phase the fluence distribution is calculated by the pencil beam convolution algorithm, which considers dose to be produced by the sum of narrow cylindrically symmetry beams. The dose at a point in the patient is calculated by summing the calculated dose distribution of all pencil beams to the examination point. Because the algorithm is kernel-based two-dimensional method, the accuracy is limited especially in the presence of heterogeneities, but the calculation times are relatively short. Inside the limits of the accelerator, the user may influence, for example, the dose rate, minimum dose per segment and calculation grid spacing by changing these parameters in the optimization properties window of the software. By influencing these, the user is able to optimize the best possible solution by making compromises, for instance, between plan quality and treatment time [4]. In the second calculation phase, the treatment planning system takes into account the deliverability of the accelerator, which is limited, for example, by restrictions on MLC and gantry movements, as number one in priority. The optimal field shapes are then generated in order to produce as smooth composite dose delivery as possible [5]. As a result, plan quality might be adversely affected in comparison to the fluence distribution calculated in the first phase. The second phase calculation can be done by a voxel based Monte Carlo method which enables more accurate dose distribution calculation than the analytical algorithms. The Monte Carlo method calculates the number of electrons created in each voxel by the primary photon beam and particles created in interactions. The final calculated dose distribution is formed by the most presumable distribution of the absorbed dose. The user may affect the calculation accuracy and time by modifying some parameters of calculation properties like the Monte Carlo variance and grid spacing. [1][2][3][15][16]

3.3 Dosimetric equipment

The ionization chambers are standard detectors of dosimetry in radiation therapy. The basic theory of the chambers is based on the cavity theorem of Bragg-Gray. The chambers are constructed by a cavity of gas, containing two electrodes with different potentials. The electrodes capture the generated charge carriers. Ionization is defined by the relative current, which is determined by an electrometer. Ionization chambers of absolute dosimetry are calibrated in secondary laboratories by national radiation authorities under a known field of radiation usually with ^{60}Co-calibration. The calibration is based on determined absorbed dose in water by international primary laboratories in so-called standard conditions of pressure 101.3 kPa and temperature 20 °C. In use of ionization chambers it is essential to consider many issues concerning either the chamber or the measurement circumstances. These are, for example, the correction factor of interference, a correction factor for a chamber's calibration factor's

pressure and temperature dependence, as well as a recombination coefficient. Recombination of ions and electrons is caused by pulsation in the linear accelerator's radiation during high instantaneous velocities of dose-rate. By a recombination coefficient the finite of a chamber's collecting-efficiency is taken into account. So, by taking into account these issues and by knowing ionization ratio and the relativity of the irradiated dose and electrometer, it is possible to calculate absolute dose using the equation

$$D_w = N_{D,w,Q} \cdot m \cdot k_{p,t} \cdot k_r \quad (1)$$

where D_w is the absolute dose of photon energy at the measuring point of a chamber, $N_{D,w,Q}$ is calibration factor, m is the readout of an electrometer, k_r is the recombination coefficient and $k_{p,t}$ is a correction factor for the chamber's calibration factor's pressure and temperature dependence. This correction factor $k_{p,t}$ for daily environmental conditions can be calculated by equation

$$k_{p,t} = (T / T_0) \cdot (p_0 / p) \quad (2)$$

where T is measured temperature in kelvins, T_0 is 293.2 K, p is measured pressure in pascals and p_0 is 101.3 kPa. [1][2][17]

One of the basic parts of quality control equipment in radiation therapy is a water phantom, which includes a cubic shape water tank with a capacity of about 200 litres. This system can be positioned in the treatment room under the gantry when the gantry angle is set as 0°. In the water tank there is a holder for an ionization chamber, which can be moved in three dimensions. With this moving ionization chamber it is possible to measure, for instance, point doses, percentage depth doses and profiles. On the top corner of a water phantom, there is also a holder for a reference chamber which monitors the dose rate. The measured data is recorded and analyzed by the equipment's software. [1][7][18]

In order to measure dose distributions in a two-dimensional level, ionization chamber arrays can be used. These so-called matrix detectors have a number of separate ionization chambers positioned usually into a shape of a square. The ionization chambers of these devices are open to outside air, and they are calibrated in certain air pressure and temperature conditions usually with ^{60}Co-calibration. The devices are planned to measure radiation entering the device from towards, either by positioning device on the treatment table and setting the gantry angle at 0°, or by attaching the device to the head of the gantry by a fixation device. The measured data is evaluated by algorithms of the device's software. The measured dose distribution is then available for analyses and comparisons with calculated dose distributions. [19][20]

Film dosimetry is a common field in two-dimensional relative dosimetry. A pivotal assumption in film dosimetry is that the dose to the film is reflected in the resulting optical density of the film. These radiochromic films have an ability to produce a permanent visible colour change upon irradiation. By the polymerisation process, in which energy is transferred from an energetic photon to a colourless photo monomer molecule, and chemical changes, the image formation of a measured dose distribution occurs. To actually get the dose distribution available for analysis, the film is measured by special scanners called transmission densiometers. Even though the conventional

challenges in film dosimetry caused by the accuracy of densiometers, sensitivity of the films to ultraviolet radiation and the sensitivity of the relationship between dose and optical density, the film dosimeters have a high spatial resolution and relatively low energy spectral sensitivity. [21][22]

4 Methods, Materials, Measurements and Calculations

4.1 Verification system for VMAT treatment plans

One of the most crucial issues in the process of radiation therapy is the equivalence between treatment planning and the actual delivery of the treatment. The calculated dose distributions in units of Gray should be delivered by a relative amount of monitor units, which describe the sensitivity of the linear accelerator's interior ionization chamber i.e. monitor chamber. The grounds of the automatic calculations of the relative monitor units by treatment planning systems are in the number of measurements done with each linear accelerator. With these results, the accelerator-specific calibration factor is determined for all of the energies. It is necessary to establish, that the adjusted treatment planning system works the way it should be by creating dose distributions, which linear accelerators are able to generate. This verification is essential to realize before starting patient treatment. Dose distribution measurements are also important in the long term to assure that the calibration factors remain updated. [1][2][23]

The verification procedures for treatment plans with static fields are mostly done by measuring created dose distributions by positioning the measuring device, like matrix, straight towards the gantry [19]. The property of VMAT treatment plans with a moving gantry while radiation is on creates totally new challenges for the treatment plan verification process. It is possible to realize plan verifications of VMAT treatment plans by creating quality assurance plans in which movements of the gantry are inhibited, and so the radiation beams are delivered only by a static gantry angle 0° [19]. However, this eliminates obviously one significant part of realization of a VMAT treatment plan, and means that it is neither possible to test or consider the functionality of moving gantry and its effect on dose distribution.

It would be desirable to be able to realize VMAT treatment plan verifications also with rotation of the gantry. This gives a boost to start investigations of the possibility to create a suitable and reliable way of measuring dose distributions by matrix with a rotating gantry of 360°. This creates two additional challenges, which need to be considered in measurements: first, the measuring accuracy of the matrix relative to the direction of radiation, and; second, the effect of attenuation by the treatment table. To investigate these issues, a reproducible system should be created, which could work also as a phantom for VMAT treatment plan verification.

In order to create a verification system there is a need of a specified measuring device. For this purpose, 2D-Array seven29 (PTW Freiburg GmbH, Germany) is decent. It is a two-dimensional matrix detector with 729 ionization chambers, which are arranged to make a regular matrix of 27 · 27 chambers [19]. The sizes of the chambers are 5 · 5 · 5 mm^3, the gaps between the chambers are 5 mm and the material around the chambers is polymethyl methacrylate (PMMA), which makes a 5 mm thick layer on top of the chambers and a 10 mm thick layer underneath the chambers [19][23][24]. To build a

system around the matrix there should be a suitable material with known properties to set around it. For this case the properties of water-equivalent RW3 material, so-called solid water, are reasonable [25]. Seven 1 cm thick slabs with a covering area of 30 · 30 cm are placed both on top and under the matrix. Construction of the created system is shown in image 4. To make this system an efficient and reliable measuring tool for treatment plan verification, there are a couple of things that need to be investigated. Besides the before-mentioned dependence of the measuring angle of the matrix and the effect of attenuation by the treatment table, there should be evaluated repeatability accuracy of the matrix, the effect of changing environmental conditions and the dose-rate of the accelerator. Also to be able to compare the measured dose distribution with the calculated one, it is necessary to calibrate the matrix with the treatment planning system. By finding factors which calibrate these issues out, and so make measured and calculated dose distributions relative to each other, it is possible to realize the configurations of the introduction of energies and also the quality assurance measurements of VMAT treatment plans.

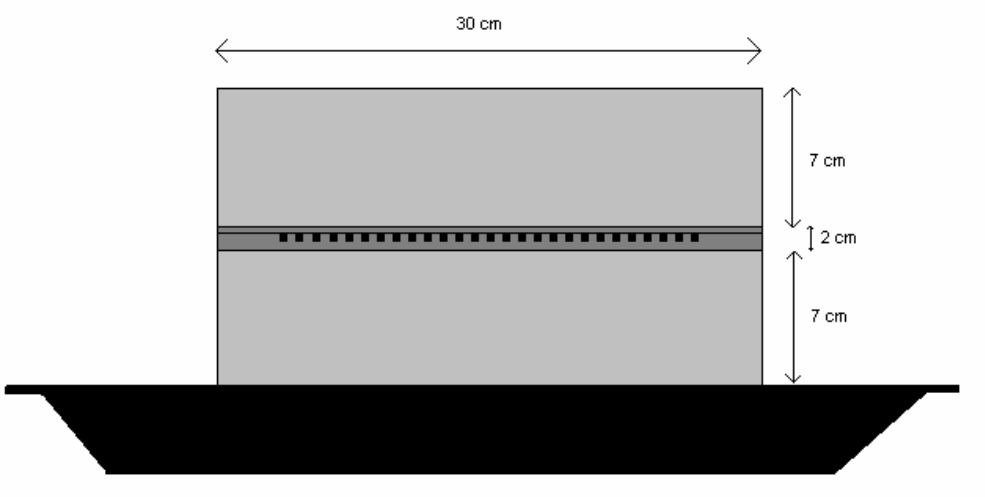

Image 4: Cross section of the created VMAT treatment plan verification system positioned on the treatment table.

4.1.1 Calibration factor for measured dose distributions

An issue that needs to be considered always with a matrix, or with whatever measuring device, is the reliability and accuracy of the measuring device. By solving the repetitive accuracy it is possible to analyze the results of other measurements within a certain tolerance. Before all the measurements, also changing environmental conditions need to be considered. Air pressure and temperature are measured and inserted to the matrix's software called VeriSoft, which automatically correlates the measurement device for daily conditions by calculating a calibration factor for measured doses [19]. The daily dose rate of the linear accelerator is taken into account always before investigations by measurements with the energy, that is going to be used in measurements by radiating 100 monitor units with a field size of 10.4 · 10.4 cm by a gantry angle of 0° and source to detector distance of 100 cm to the isocenter of the matrix system. The positioning of the system for these measurements is shown in image 5. If the measured value is more different than the repetition accuracy of the matrix from the dose at the measuring day of the absolute measurements, a correlation needs to be done before any relative measurements are realized. Comparable measurements of absolute dosimetry to

measurements done by the matrix in similar circumstances are done also because the treatment planning system is configured by absolute dosimetry measurements. With this calibration factor it is possible to compare the calculated and measured dose distributions. As mentioned in the previous chapter it is also essential to define the correlation factor for measuring the angle dependence of the matrix and the effect of attenuation by the treatment table. With these three factors it is possible to calculate a combined correlation factor for measured dose distribution to be comparable against the calculated one using the following equation

$$K_C = K_m \cdot K_T \cdot K_\gamma \qquad (3)$$

where K_C is the correlation factor for measured dose distribution to compare with the calculated one with the used arc, K_m is the calibration factor to make the matrix comparable with absolute dosimetry, K_T is correlation factor for elimination of the effect of attenuation by the treatment table and K_γ is the correlation factor of the measuring angle dependence.

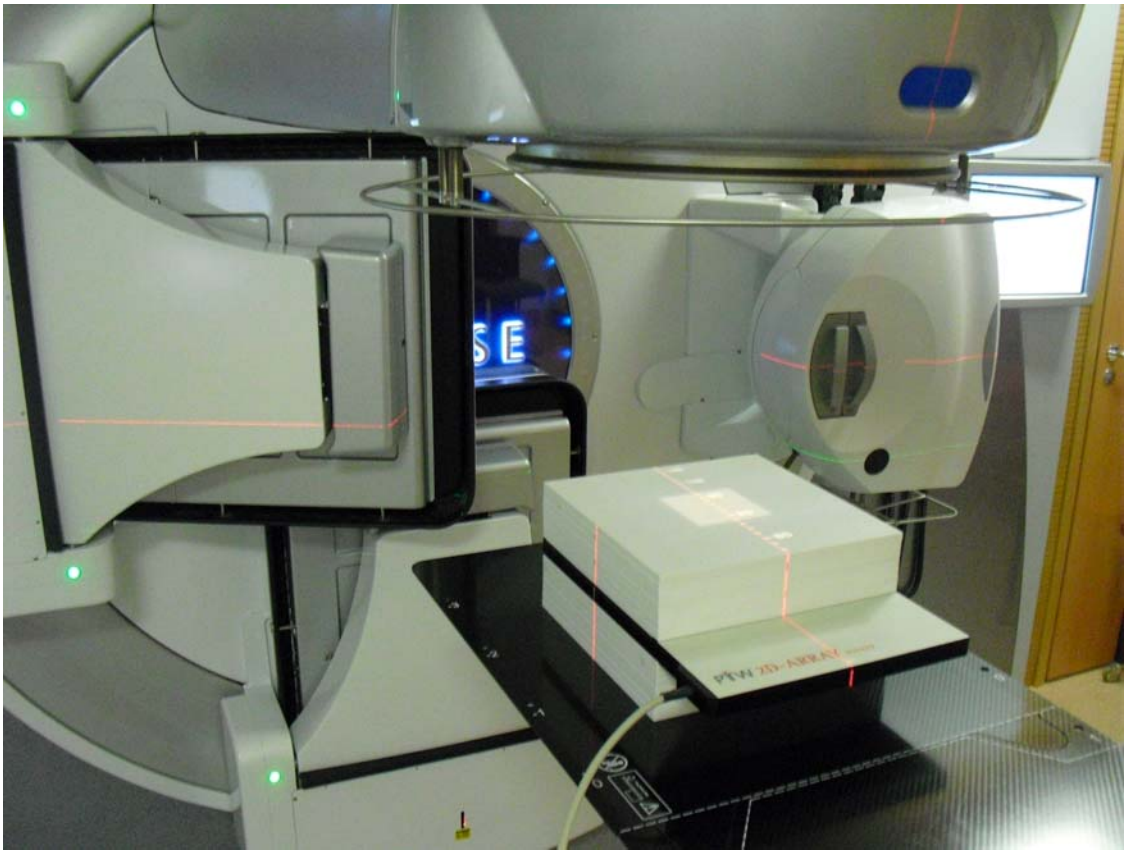

Image 5: The created VMAT treatment plan verification system positioned on the treatment table.

Calibration of chambers of the matrix to the chamber of absolute measurements, repetitive measuring accuracy of chambers of the matrix and observation of daily dose rate

Determination of the calibration factor to make measurements done by the matrix comparable with absolute dosimetry is accomplished by comparing results of consecutive measurements of the matrix and by a calibrated ion chamber in similar

circumstances with photon energies of 6 and 10 MV. The used ionization chamber is called Farmer NE 2571 (serial number 1840) and the used electrometer is called dosimeter NE Farmer 2579/1 [2]. The ionization chamber is positioned into a water phantom called Blue Phantom^2 with Omni-Pro-Accept software (IBA Dosimetry GmbH, Germany) [18]. Before the measurements air pressure and temperature of water are measured and a correction factor for the chamber's calibration factor's dependence on daily conditions is calculated by equation 2. Then percentage depth doses with both energies are measured. From the recorded data ionization ratios between depths 100 and 200 mm, and a percentage dose of maximum dose at depth of 100 mm are collected. Using the ionization ratio a daily calibration factor for the ionization chamber is checked from the calibration certificate [26]. Then the absolute measurements are done according to national guidelines of quality controlling [27]. The ionization chamber is set at 10 cm deep, which means that the measuring point is at a depth of 9.7 cm. Reference chamber is set at the corner of the 10.4 · 10.4 cm field, source to skin distance is set as 100 cm and the output of the linear accelerator is set to 300 monitor units. Measurements are repeated three times. Measured maximum dose per 100 monitor units can be calculated using the equation

$$D_{w,\,max} = N_{D,\,w,\,Q} \cdot m \cdot k_{p,\,t} \cdot k_r \cdot (1/J_{100}) \cdot (1/3) \quad (4)$$

where $D_{w,\,max}$ is the absorbed dose in water at the maximum point, $N_{D,\,w,\,Q}$ is the calibration factor, m is the readout of the electrometer, $k_{p,\,t}$ is a correction factor for the pressure and temperature dependence of the chamber's calibration factor, k_r is the recombination coefficient and J_{100} is a percentage dose of the maximum dose at a depth of 100 mm. With $D_{w,\,max}$ it is possible to estimate the daily dose rate of the accelerator because the accelerator is adjusted to produce dose of 1.000 Gy at the point of $D_{w,\,max}$ by 100 monitor units. Using equation 4 without dividing terms with a value of J_{100}, it is possible to calculate the dose in water at a depth of 10 cm. Next, the matrix is set on the treatment table. Seven centimetres thick layer of solid water slabs is set underneath and a 9.2 cm layer on top of the matrix. So, the measuring point of the middle chamber is then set at a depth of 9.7 cm. The source to skin distance is set to 100 cm. Field size and monitor units are kept exactly same as in the previous measurements. The measurements with the matrix are also repeated three times. The calibration factor to make the matrix comparable with absolute dosimetry K_m can be calculated using equation

$$K_m = D_w / D_m \quad (5)$$

where D_w is an average of three repeated measured absorbed doses with the absolute chamber and D_m is an average of three repeated measured absorbed doses with the matrix. [1][2][17]

The matrix is also positioned on the treatment table the way it is in the created verification system for VMAT treatment plans. The reference dose for checking the daily dose rate and the random error of the chambers of the matrix are evaluated by repetitive measurements. The matrix is irradiated by energies of 6 and 10 MV with 100 monitor units using a gantry angle of 0° and a field size of 10.4 · 10.4 cm. Measurements are repeated ten times and each time the measured dose of the middle chamber of the matrix is recorded. An average of ten measurements is calculated. The average is set as a reference dose for the daily dose rate measurements. Always before

starting to investigative measurements, the possible effect of the daily dose rate can be estimated using equation

$$K_{DR} = MD_{Ref} / MD_d \quad (6)$$

where K_{DR} is the relative difference between the daily dose rate and the reference dose rate, MD_{Ref} is the measured dose on the day of the absolute measurements and MD_d is the measured dose on measuring day. If the factor K_{DR} is larger than the measurement accuracy of the matrix, the measured absorbed doses are calibrated by the factor K_{DR}. The accuracy of repetitive measurements can be estimated using the following equation

$$K_{Acc} = \Delta MD / MD_r \quad (7)$$

where K_{Acc} is the measurement accuracy of the matrix, ΔMD is an average of ten measurements and MD_r is the smallest or the largest measured dose.

Factor for elimination of the effect of attenuation by the treatment table

Investigation is planned in order to separate the influence of attenuation by the treatment table from the measured dose distributions. The investigative measurements are started by positioning the created verification system at the isocenter after moving the treatment table laterally at zero position and by preparing accelerator system with a field size of 10.4 · 10.4 cm and 100 monitor units. Measurements are done with energies of 6 and 10 MV. Measurements need to be done with gantry angles, from which radiation traverse through the treatment table to the measuring point of the middle chamber of the matrix 8.5 cm above the surface of the treatment table. These gantry angles are between 110° and 250°. In image 6 is shown the measurement situation with a gantry angle of 110°. Because the exact same lateral symmetry of the treatment table, it is not necessary to measure effects from both lateral sides. Measuring the gantry angles are at intervals of 10°. In order to consider the changing shapes at the lateral sides of the table, so that the effects of different parts of the table can be solved, measurements are done also with gantry angles of 107.5°, 112.5°, 115° and 125°.

Image 6: Starting angle of the investigations into the effect of attenuation by the treatment table.

After measuring the doses with above-mentioned gantry angles, the created system is turned upsides down. With this set up the measurements are done with gantry angles, which are comparable to the ones used through the treatment table. Then the factor for eliminating the effect of attenuation by the treatment table can be calculated by equation

$$K_{T,\alpha} = MD_{180° - \alpha} / MD_{\alpha} \quad (8)$$

where $K_{T,\alpha}$ is the factor for eliminating the effect of attenuation by the treatment table from a particular gantry angle α and MDs are the measured doses with relative gantry angles. With the calculated correlation factors a graph is drawn.

From the graph an average factor for eliminating the effect of the table can be calculated by extracted factors between 5° steps, which belong in the sector of the arc. In order to determine the calibration factor K_C of the created verification system, the factor K_T can be then calculated using equation

$$K_T = ((K_{\Delta(T,\alpha)} - 1) \cdot (\beta_T / \beta_{Arc})) + 1 \quad (9)$$

where K_T is the factor for eliminating the effect of attenuation by the treatment table for the used arc, $K_{\Delta(T,\alpha)}$ is an average factor to eliminate the effect of attenuation by the treatment table, β_T is the size of the sector of the arc in which attenuation by the treatment table needs to be considered and β_{Arc} is the size of the arc.

Measurements in order to determine angle dependence for chambers of the matrix

Also the measuring angle dependence of the chambers of the matrix is investigated separately. The relation between the gantry angle and the direction of the radiation to the middle chamber of the matrix in the created system is shown in image 7. The investigations are done by comparing the measured doses by different gantry angles to the ones measured by gantry angle 0° with relative amounts of solid water that radiation traverses through to the measurement point of the middle chamber of the matrix. The length of traversed matter can be calculated by trigonometric function of cosine

$$TM_{\alpha} = 7{,}5 \text{ cm} / (\text{Cos } \alpha) \qquad (10)$$

where TM_{α} is the length of traversed matter from a gantry angle of α. These calculations are done between steps of 10° from gantry angle 0° to 180°. The calculated length of traversed matter is rounded up by a 1 mm scale. The calculated amounts of traversed matter are placed on top of the matrix and the measurements are done by energy of 6 MV by 100 monitor units and a field size of 10.4 · 10.4 cm. With the results of these comparable measurements, and by taking into account the gantry angle dependent effect of attenuation by the treatment table, it is possible to calculate a factor to calibrate the chambers' angle dependence out using equation

$$K_{\gamma,\,\alpha} = MD_{0°,\,TM\alpha} / (MD_{\alpha} \cdot K_{T,\,\alpha}) \qquad (11)$$

where $K_{\gamma,\,\alpha}$ is the correction factor for the measured dose with a gantry angle of α, $MD_{0°,\,TM\alpha}$ is the measured dose by a gantry angle of 0° with the length of traversed matter from gantry angle α, MD_{α} is the measured dose by gantry angle α and $K_{T,\,\alpha}$ is the factor for eliminating the possible effect of attenuation by the treatment table with gantry angle α. With factors $K_{\gamma,\,\alpha}$ a graph is drawn. From the graph it is possible to calculate a factor for correcting the dependence of the measuring angle of the chambers of the matrix K_{γ} for the arc used. This can be done by calculating the average of factors $K_{\gamma,\,\alpha}$ within the used arc between gantry angle steps of 10°. [28]

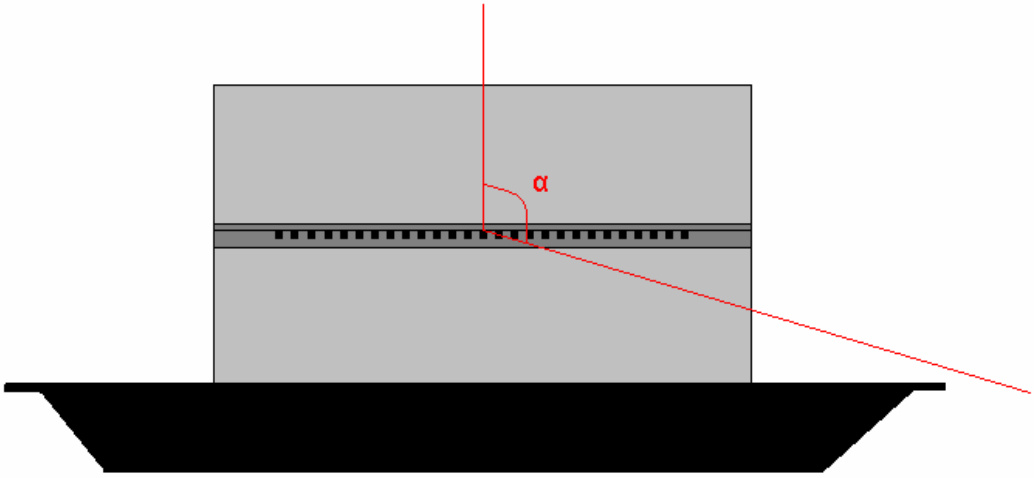

Image 7: The relation between the gantry angle and the direction of the radiation to the measuring point of the middle chamber of the matrix in the created system.

Dose calculations using treatment planning systems

The created verification system is investigated also by calculations done by treatment planning systems. With these investigations it is possible to analyze the features of the created verification system, and to compare the results of the measurements with calculations. It is also possible to compare the accuracies and features of the calculation algorithms of the treatment planning systems. The calculations are done by the Monte Carlo algorithm of Monaco 2.0.3 and kernel-based analytical anisotropic algorithm of Eclipse 8.6. The calculations are done by similar fields as in the measurements using energy of 6 MV. The calculations are done by steps of gantry angles between 10°, but between gantry angles from 60° to 120° the used steps are 5°. The calculated dose by every field is estimated at the same point, where the measurement point of the middle chamber is. By using the same parameters as in the investigations of the dependence of the measuring angle and the effect of attenuation by the treatment table, it is possible to take these results under the same analyses. All these measured and calculated doses are inserted in a graph with the same scale, in which the measured dose with a gantry angle of 0° is set as 1,000. All the other measured and calculated doses are set against this value using equation

$$K_{R,\alpha} = MD_{0^\circ} / D_{\alpha} \tag{12}$$

where $K_{R,\alpha}$ is a relative factor compared to the measured dose with a gantry angle of 0°, MD_{0° is measured dose with a gantry angle of 0° and D_{α} is the measured or calculated dose with a gantry angle of α. The measured doses with gantry angles, in which the effect of attenuation by the treatment table is relevant are also corrected by correlation factor $K_{T,\alpha}$, and inserted as a graph in the same graphics along with the others.

4.2 The Ball Test

It is pivotal to assure the reliability of cooperation of Monaco treatment planning system version 2.0.3 and Elekta Axesse linear accelerator in treatments of VMAT plans with all energies. This goal can be represented briefly by dividing it into three categories of the essential properties and phases of VMAT planning and treatment. These are quality assurance of the treatment planning system's fluence distribution optimization module, quality assurance of the treatment planning system's sequencer and quality assurance of the accelerator's dynamic dose delivery process [23].

To investigate these issues the ball test is created. The idea is to have a mutual concept in the investigated plans, that is, first of all challenging for the system to realize, and secondly, easy to manipulate by little changes in treatment planning without losing the main parts of the concept. The ball test is realized with the created plan verification system. The search of the answers is started with treatment planning by creating, calculating and investigating plans. A suitable spectrum of these plans is treated and measured. Estimations of implementation capability of the system are done by equivalences between the calculated fluence distributions and the measured dose distributions.

4.2.1 Treatment planning of the Ball Test

The main goal for treatment planning in the ball test is quality assurance of treatment planning system's fluence distribution optimization module. However, in treatment planning it is also a goal to create plans, which are suitable for dose distribution measurements. For these purposes a plan with a regular size target ball added in with an alterable constraint ball is constructed. The balls' middle points are positioned towards the top of the matrix's middle chamber. The construction is shown in image 8. For all the plans the radius of the target ball is set as six centimetres and the target dose at 2,0 Gy. However, constraint ball's maximum dose is placed first in priority for the treatment planning system. This dose limit is changeable for the plans so that the capability of the system to perform with high gradients can be investigated. Also the constraint ball's radius differs between plans. All the other parameters in treatment planning are set suitable for clinical treatment planning and are kept constant in all the plans. Calculations are performed with two phase optimization. After the first phase calculation using the Pencil beam convolution algorithm, the second phase is calculated using the Monte Carlo algorithm.

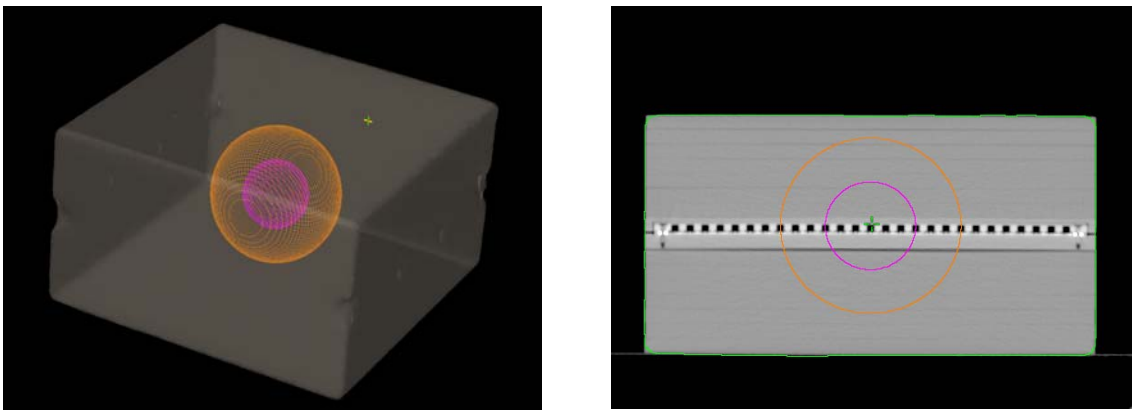

Image 8: Construction of the ball test. At left three dimensional view, and at right a transversal slice at isocenter, of a CT image, in which the target ball is drawn by orange and constraint ball with radius of three centimetres is drawn by pink.

By forcing plans to the limits of the calculation algorithms, it is possible to find out; first of all, the limits of the treatment planning system, but also to analyze whether pushing the calculation system by challenging constraint-target dose differences, i.e. gradients, matter to actually treated dose distributions by decreasing the equivalence between the calculated and treated dose distributions. These are investigated by plans where the constraint ball's radius is set as three centimetres. For the first plan, the constraint ball's dose limit is set off. With this plan, called R3D100%, the calculation algorithms can concentrate on just producing uniform dose distribution for the volume of target ball. For the second plan the constraint ball's dose limit is set to two thirds of the target dose. In this plan, called R3D66%, the calculation algorithms have to struggle with the limit of the constraint ball while producing enough dose to the target area. With the three centimetre radius constraint ball it is investigated how low the dose limit can be pushed, so that calculation algorithms are able to finish the calculation and at which point of dose limit the calculation system warns the user that a plan is infeasible. The plan with the lowest dose limit of the constraint ball, which calculation algorithms calculate without warnings, is named as R3Dmin%. It is also investigated how well the

calculation algorithms are performing by changing the size of constraint ball, and whether it matters to the accuracy of production of the dose distribution. These are all investigated with the constraint ball's dose limit of two thirds of the target dose. Calculations are done with constraint balls' radius' of one and five centimetres. These plans are named as R1D66% and R5D66%, respectively.

4.2.2 Dose distribution measurements with matrix

By measuring the dose distributions of the created plans and comparing the results with the same plan's calculated fluence distribution at the coronal slice on top of the chambers, quality assurance of the treatment planning system's sequencer and accelerator's dynamic dose delivery process with VMAT treatment plans can be done. The measured dose distributions by the created verification system will be correlated by the calculated calibration factor for a 360° VMAT treatment plan with used energies. Evaluations of dose distributions are done by a gamma index method. 95 % of the chambers in the area of radiation should pass typical accuracy limits of 3 mm and 3 % between the calculated and measured point doses to confirm equivalence between the calculated and delivered dose distributions [23][24]. In this test an area, where the planned dose is about at least 50 % of the target dose, is considerer separately. This area includes the 225 most centrally located chambers of the matrix. By comparing the percentages of the passed chambers between the plans, it is possible to analyze the possible effect of high gradients or different size of constraint on the realization accuracy of the plans.

Also repetition accuracy of a treatment is tested by measuring dose distribution of the delivered plan R3D66% three times consecutively with the energies used. In the results the repetitive measuring accuracy of a chamber, which is measured during the investigations for the created verification system, is also taken into consideration. However, the measured dose distributions of the same plan delivered repetitively are compared by a gamma index method with accuracy limits of 0.5 % and 0.5 mm. The plan R3D66% with energy of 6 MV is measured also three times after re-positioning the created system in order to estimate any possible error in arrangements made by the user.

4.2.3 Dose distribution measurements with radiochromic film

In the dose distribution measurements done by the matrix, the size of the chambers and intervals between them set uncertainty into spatial resolution. A higher-resolution detector such as radiochromic film might be preferable for such measurements of dose distribution [2]. However, the clinical practicality of the matrix encourages the use of it as a dose distribution measurement device in the long-term. In order to ensure the required accuracy of the matrix, both spatially and by dosimetry, it is important at least to determine possible relative inaccuracies in spatial resolution, and also with dose, compared to radiochromic film dosimetry.

For this investigation the film dosimetry equipment and methods used in HUCH are brought into play. The used film is Gafchromic EBT2 (International Specialty Products, NJ, USA), which is developed specifically for dosimetric working in a radiation

therapy environment, and can resolve features with spatial resolution to at least 0.1 mm [21]. The 0.25 mm thick film is handled and measured by the instructions from the manufacturer [21]. The output factor of the exact film used in the measurements is determined by the ratio of the detector response per monitor unit for a given field, to that, for the reference field at a reference depth [2]. The daily dose rate of the linear accelerator, which is used for calibration to be congruent with the analyzing methods used in HUCH, is checked by a monitor test device called LinaCheck (PTW Freiburg GmbH, Germany) [29]. In the measurements five different amounts of doses are used, which are decided to be in a broad enough range compared to the impending dose distribution in order to ensure accuracy of the calibration especially in the most significant range of doses. With a relative amount of monitor units for each dose, three measurements are done by field size of 5 · 5 cm to 3 · 3 cm pieces of the same sheet of film as the dose distribution measurement is done. The pieces of film in the calibration measurements are positioned in the middle of a 10 cm pile of solid water slabs with a source-to-detector distance of 100 cm. These fifteen pieces of film are scanned three times each with DosimetryPRO Advantage red densiometer (Vidar Systems Corporation, VA, USA) [30]. The densiometer is linear in the condition of the investigation with its 16-bit scale of colouring, which provides a spatial resolution of 0.08 mm [30]. By taking an average of these doses the system can be calibrated to be able to analyze the actual measured dose distribution of the investigation. It is also scanned three times, and the average is used.

The film measurement is done by the plan R3D66% with energy of 6 MV. The five doses for calibration measurements are 1.0, 1.3, 1.7, 2.0 and 2.4 Gray. In the actual dose distribution measurement a 19 · 15 cm piece of the sheet of film is positioned into the created verification system on top of the matrix. So, the measuring points of the chambers of the matrix are 0.5 cm under the film. At the level of the film the target ball is 11.96 cm and the constraint ball 5.92 cm in diameter. Compared to the measuring level of the chambers, changes in the positions of the outer and inner gradients are 0.02 cm and 0.04 cm, respectively. However, the plan is measured by the matrix at the same time, and the measured dose distribution by the film is compared to the measured dose distribution by the matrix. The attention is paid most of all to the sharpness of the gradients. This investigation also offers an indication of the reliability and accuracy of the created verification system.

4.3 Verification of clinical test VMAT treatment plans

Before starting to plan VMAT treatments for patients, also five clinical test plans are created by planning CT images of previously treated patients. Verification of these clinical test VMAT treatment plans are performed by measuring dose distributions with the created system by quality assurance mode without rotating gantry and using the original plan. Quality assurance mode with a static gantry angle of 0° is measured four times with different isocenters to increase resolution relating to the gaps between the ionization chambers of the matrix. First measurement is done by positioning the isocenter in the middle of the matrix and the next one 5 mm aside from the middle point by moving the treatment table. Then the last two measurements are done likewise by changing the place of the isocenter, so that measurements are done with isocenter in every corner of a square. These dose distributions are merged by the software of the matrix. The second phase of these plan verification measurements is done by measuring

the actual treatment plan by it's actual planned rotating gantry with the created VMAT plan verification system. The calibration factors for the measured dose distributions in each case are entered to the system. The measured dose distribution maps are compared with the calculated ones. 95 % of the chambers inside about an area of 50 % isodose should pass accuracy limits of 3 mm and 3 % between the calculated and measured point doses [23][24]. Also the percentages of passed point doses with the same accuracy limits inside about an area of 10 % isodose are calculated.

If the results of the ball test and the clinical tests are acceptable, VMAT treatment planning for clinical cases can be launched. Additionally, all of the VMAT treatment plans of every patient are delivered in their actual forms and measured with the created system. Also one of the treatment plans of each patient is measured by quality assurance mode without rotation of the gantry. The results are analyzed, before starting the treatment with the plans.

4.4 Patient positioning using the CBCT system and the robotic treatment table Hexapod

From a clinical point of view, there are two main goals in CBCT imaging of patients with bladder cancer. First, to use such an imaging preset which enables sufficient image quality to determine daily position of the bladder with as little dose as possible. Second, to be able to make adjustments on patient positioning by position of the bladder instead of just extrinsic markers clinically accurate enough to realize treatments as planned. In order to reach these goals a possibility to create new CBCT imaging presets with different properties is investigated. Also tests for imaging, automatic matching and patient positioning accuracies need to be performed before determining strategies for CBCT imaging and position correction of the patients. It would be desirable to use the grey-value algorithm in automatic matching, because by the use of it, the matching could be done automatically by the positions of the internal organs. In addition the encouraging results of investigations about the accuracy of the grey-value algorithm to be precise, and even more accurate than the bone algorithm in automatic matching, motivates the investigations using it [11]. By introducing practical strategies for the whole process of CBCT imaging and patient repositioning also the total treatment time could be reduced.

4.4.1 Different presets for the CBCT imaging

The most suitable presets, i.e. imaging settings including for example tube current and voltage, installed in Xvi for CBCT imaging in bladder cases are presets called Prostate M10 and Prostate M10 Fast using counter clock-wise direction of gantry rotation. From the information offered by the manufacturer the Prostate M10 Fast produces less absorbed dose into a patient and is twice as rapid compared to Prostate M10 preset [10]. Still image quality remains high, which encourages investigating the possibility of decreasing the dose and speeding up the imaging at the expense of the image quality of the preset. However, image quality comes as number one in priority in the investigations, because it has to be clinically good enough to visualize clearly most of all the walls of the bladder.

The creation project of the presets is realized by modifying the parameters of the Prostate M10 Fast preset. The parameters can be adjusted only in limited scales, set by the manufacturer, which have to be considered while changing the parameters of the presets [10]. However, it is possible to modify many of them as long as the limited scales of the parameter combinations are respected. The parameters that are most reasonable to concentrate on modifying, in order to achieve the goals, are tube voltage, current, time, degrees of rotation, speed of the gantry and number of frames. By varying the parameters several presets are constructed. Into all the presets the imaging direction is set in the counter clock-wise direction. However, the presets, which are introduced clinically, have to pass first of all tests of image quality and automatic matching, and in addition the measurements of produced absorbed dose.

Image quality and accuracy of automatic matching between the presets

By the created presets the CBCT imaging needs to be performed by imaging as human-like structure as possible in order to visualize the results of the presets. A phantom is created using the real organs of a pig and a cow bought from a butcher. Kidneys, liver, heart, tongue, pieces of fat and thigh bone of a pig are inserted into a plastic bag with the cartilage of a cow. Also a small plastic bag filled with air and one filled with urine are plot in between the organs. A piece of aluminium, which is the same size as gold seeds used in the prostate for tracking, is inserted into the heart. The plastic bag with the substances is covered with cow's blood and sealed. The bag is inserted into a water proof cool box made out of expanded polystyrene. It is filled by water and put into a freezer, so that the entireness would stay stable in the box as an ice cube. During the measurements the cool box is sealed with a cover, so that melting of the ice is sufficiently slowed down at least for couple of hours. The created internal organ phantom is imaged by CT to have a reference image for the investigations, which is shown in image 9. An isocenter is set to the piece of aluminium, and markings are drawn on the box by the positioning lasers.

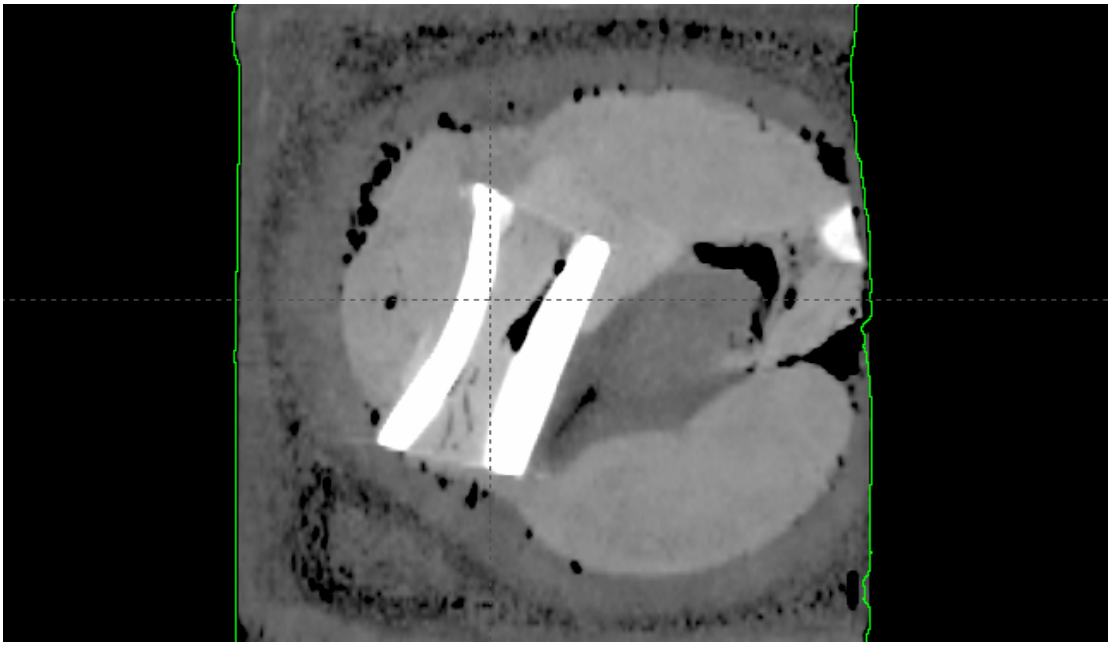

Image 9: Transversal view of a CT image of the created internal organ phantom.

In the investigations the internal organ phantom is positioned on the treatment table, as shown in image 10, and CBCT imaging is performed by the created presets. With the ones, which create images with a level of image quality high enough for clinical applications, are then brought to the next step of the process. Using these presets, as well as with presets Prostate M10 and Prostate M10 Fast, imaging is performed to realize a comparable accuracy test of automatic matching between images performed by the presets. The test is done three times by positioning the internal organ phantom on the treatment table, so that the isocenter is moved a little at least in three dimensions. The variations are between 3 - 10 mm in translational directions and 0.3 - 1.0° in rotational directions. CBCT imaging is performed with each preset, and the image is compared to the reference CT image by automatic matching done by the grey-value algorithm of the software, which is adjusted to match the images by an area, which includes all the substances of the phantom. The suggested position corrections are written down, and compared to the ones suggested by the other presets in order to determine if the modification of the presets matter to accuracy of matching. In order to approve the created presets for clinical use by the automatic matching capabilities the results of automatic matching should recommend the same, or at least not alternations, over the limitations of the scales, positional corrections for all the presets.

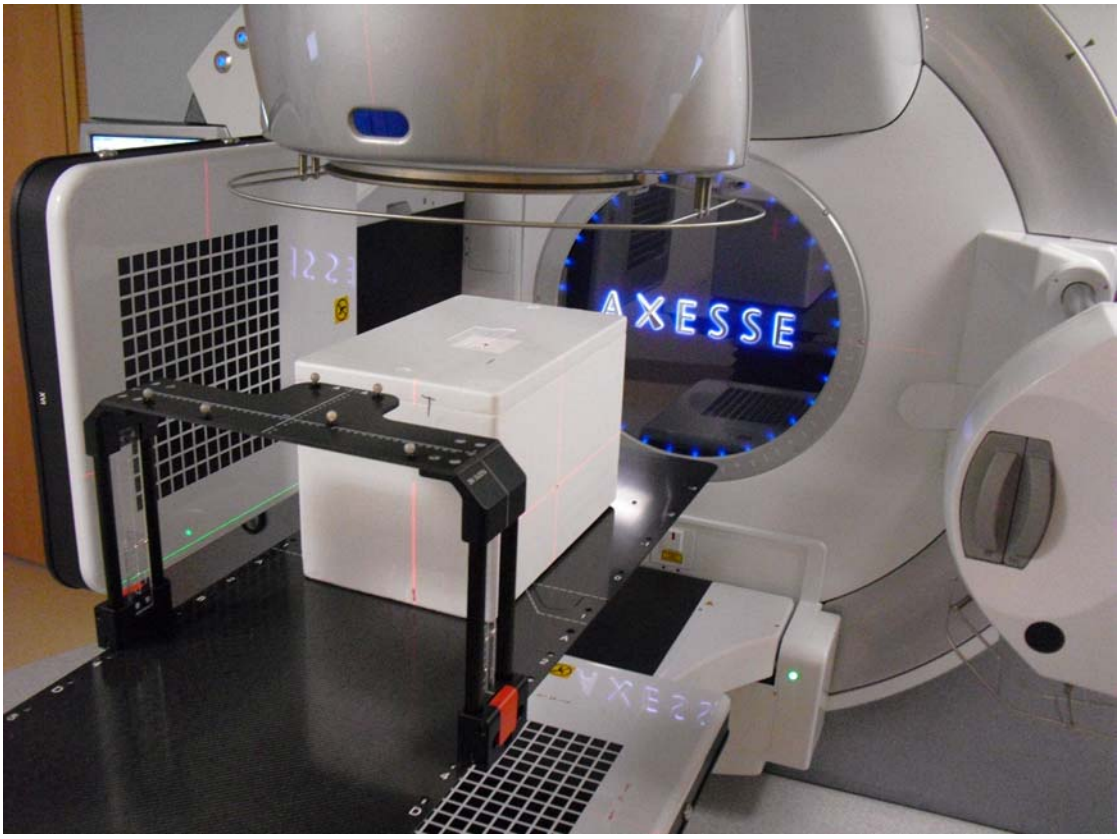

Image 10: The internal organ phantom positioned on the treatment table for CBCT investigations.

Irradiated dose using the CBCT imaging with different presets

The irradiated doses of the CBCT images performed with the presets, which are accepted into clinical use for bladder cases by image quality and matching accuracy tests, are measured with the CT thorax phantom, which is shown in image 11. The

phantom is cylinder shape with a radius of 16 centimetres, and it is positioned on the treatment table, so that the isocenter is set in the middle of the phantom. The material of the phantom is PMMA, in which there are openings for ionization chambers in the middle and also at depths of one and five centimetres from the surface. The used ionization chamber is the same as in the absolute dose measurements. It is positioned in the openings so that the longitudinal laser spots to the middle of the chamber. With each preset the doses are measured in the middle and at highest dose position at a depth of one centimetre from the surface. The position on the surface is determined by measuring with one of the created presets dose at three points on the surface; just on top of the treatment table, the opposite side from the table and at lateral side. With the one preset measurements are also done three times when the chamber is positioned in the middle, so that the measuring accuracy of the chamber and the repetitive irradiated dose by the imaging can be considered in analyses of the results.

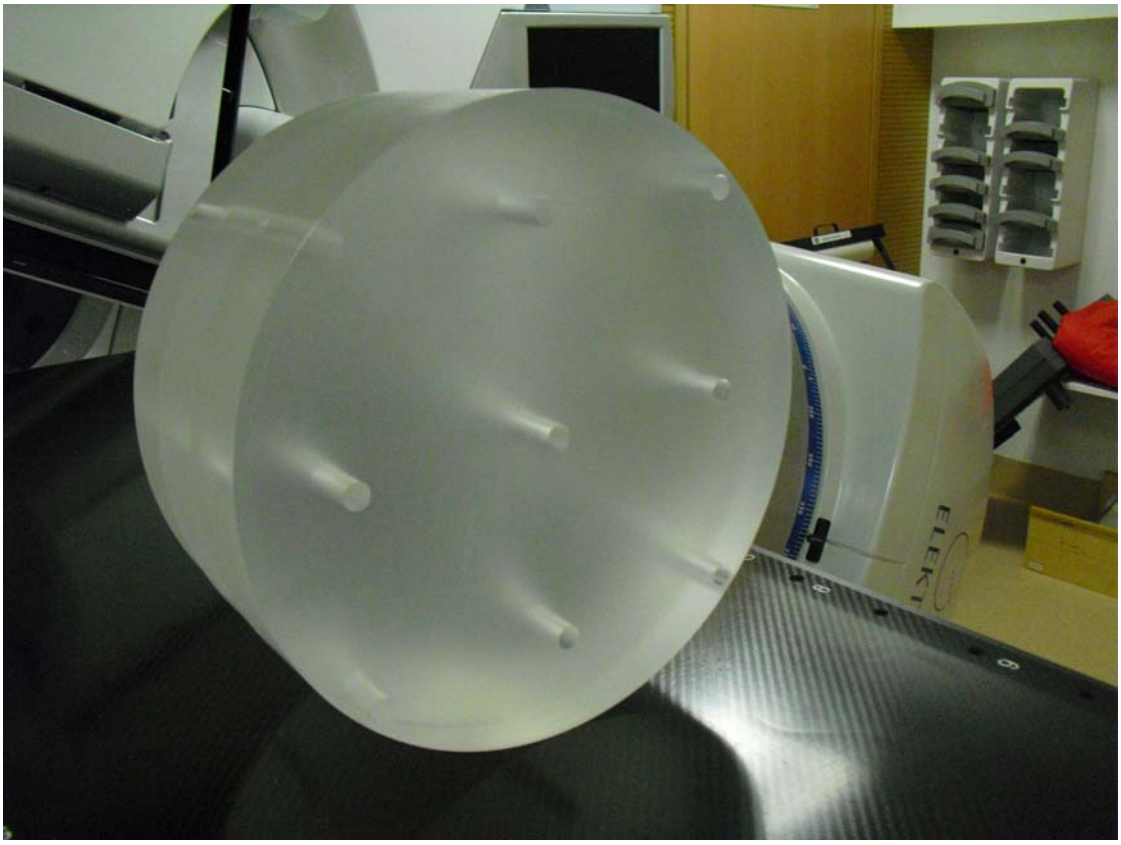

Image 11: CT thorax phantom used in measurements of CBCT dose.

4.4.2 Automatic matching accuracy with grey-value algorithm

Investigations on the accuracy of automatic matching are done by the internal organ phantom by positioning the phantom slightly apart from the isocenter of the treatment unit, and then imaging it using the CBCT preset Prostate M10 Fast in counter clock-wise direction. The CBCT image is compared by automatic matching with the grey-value algorithm of Xvi to the reference CT image. The grey-value algorithm is used in investigations because it concentrates on small changes in electron densities in the image, which make it the most feasible for matching by position of the organs. The recommended position corrections are compared to the actual position, where the

phantom was positioned. The positional errors are adjusted one by one to evaluate one direction at a time using a CBCT image. The directions are decided by taking into consideration the rotational direction of the imaging device, so that the directions against the frames and also along the frames are investigated. So, the individually investigated translational directions are longitudinal and lateral. Also, the rotational accuracies around lateral and vertical directions are investigated. For all of the directions the investigations are done by two divergences to also evaluate whether the amount of error matters to the matching accuracy. In the translational directions the set divergences of the phantom from the isocenter are 0.5 cm and 2.0 cm. In the rotational directions the transfers are 0.5° and 2.0°. So, all of the divergences are inside the moving range of the Hexapod treatment table Also investigations are made by adjusting the phantom using both 0.5 cm translational transfers and both 0.5° rotational transfers once. The same is done also by 2.0 cm and 2.0° transfers. In order to evaluate the possible range of errors made by the user in positioning of the phantom using lasers, adjustments and imaging are done three times using the 2.0 cm transfer in the lateral direction and using the 2.0° transfer around the vertical direction. After automatic matching, the results of it are also analyzed manually for every case.

4.4.3 Movement accuracy of the CBCT equipment

The repositioning accuracy of the CBCT system is also important to determine [12]. Clinically it is essential that the cooperation between CBCT imaging, matching by the software and the realized movements of the Hexapod treatment table work precisely together. The cooperation is investigated by double-checking the position of the internal organ phantom after realizing the recommended position corrections of automatic matching. Therefore, the phantom is positioned on the treatment table slightly apart from the actual isocenter at least in three dimensions. The movements are not more than 1.0 cm in translational directions nor over 1.0° in rotational directions. The CBCT imaging is performed by Prostate M10 fast. The image is matched by automatic matching of Xvi with the grey-value algorithm. The recommended position corrections are inserted into the iGuide software, by which the movements of the Hexapod treatment table are realized. After the movements of the treatment table, CBCT imaging is performed again, and automatic matching is implemented. It is observed if the position corrections recommended are null or at least inside the step ranges of the system. The process is carried out five times with different phantom positions in each case.

4.5 Planning of the treatment process for the radiation therapy of patients with bladder cancer

Because of the substantial improvements of the on-line adaptive method in the radiation therapy treatments of bladder cancer patients, the treatment planning process is built around the demands of the method. To answer the demands, the features of the linear accelerator Elekta Axesse and the treatment planning system Monaco are challenged. With VMAT planning it is a goal to find a suitable template, by which the target dose can be reached with minimum healthy tissue irradiation within as short treatment time as possible. There are also significant demands on accurate CBCT imaging with a minor dose and accurate patient positioning by six degrees of freedom. The final goal is

to be able to create instructions for the whole treatment process of patients with bladder cancer.

The radiation therapy planning process for patients with bladder cancer is started by considerations of accurate patient positioning. There have been encouraging results of investigations to improve visualization of the bladder tumour in CBCT images using fiducial markers [31]. Therefore, an urologist injects drops of a x-ray contrast agent called lipiodol through a flexible cystoscope into the bladder wall days before planning CT imaging. About an hour before the CT imaging is started, patients are instructed to drink a lot of water and to urinate minutes before positioning on the CT imaging table. The first image is performed immediately, and the other three in intervals of fifteen minutes. With the help of the images, the isocenter is set and marked by tattooing points on patients' skin at the crossroads shown by the positioning lasers. With each CT image an oncologist contours relative planning target volumes (PTVs) by the position of the tumour volume. [7]

In actual treatment planning process, VMAT treatment plans are realized for every PTV individually. The goal is to implement a template in the treatment planning system for bladder cases. The template should include a suitable work-flow for the planning process and practical parameters for optimization. The investigations are realized by thorough treatment planning for patients with bladder cancer. As minimum criteria for the planning process, the objectives set by ICRU report 50 are used [32]. Using these objectives the minimum dose in the PTV should be at least 95 % and the maximum dose smaller than 107 % of the planned dose. After these criteria are filled, the concentration is on decreasing the dose in organs at risk and shortening the treatment time. It is important to explore the trade-off between plan quality and the efficiency of its delivery carefully for each individual case [4]. Especially with very complex cases in VMAT treatment planning, there might have to be compromises made between the quality of dose distribution and treatment time [4]. In order to realize these goals, concentration is focused on properties and parameters in the windows of treatment planning system called beam setup, segment shape properties, IMRT calculation properties and prescription.

Before starting the treatment, the VMAT treatment plans are verified by dose distribution measurements. The verification method used in actual treatment plans is decided by the results of the ball test and verifications done by the clinical test VMAT plans. If the results indicate that the created verification system is reliable, it is introduced as a tool for the clinical treatment plan verification process. However, at least one plan of each patient is also measured using the previous method with quality assurance mode without gantry rotation. By analyzing the results, it is a goal to introduce a systematic long-term work-flow for the VMAT treatment plan verification process.

In the treatment process, the patient is positioned carefully on the treatment table by the radiographers using the tattooed markings on the patient's skin and lasers on the walls of the treatment room. The frame of the infrared reflectors is attached to the Hexapod treatment table on a place, where it is not between the radiation source and target volume, and the motorized table is set in its zero position so that the maximum range of corrections could be applied in all directions. The CBCT imaging is then performed to determine the on-line position and volume of the bladder. The used imaging preset is

decided by the results of the CBCT investigations. However, the CBCT imaging is performed always in the counter clock-wise direction in order to get the gantry close to the starting angles of the treatments in the end of imaging. Furthermore, the used matching and positioning correction strategy are resolved by the results of CBCT investigations. If the automatic matching with the grey-value algorithm is clinically accurate, the possibility of using automatic matching can be utilized. Because of the shifting places and volumes of organs in the pelvic area, the smallest PTV plus five millimetres is used as an automatic matching volume, and results of the automatic matching are reviewed manually. Any possible corrections to the patient position are made by the motorized table with six degrees of freedom, if the position correction investigation results are encouraging. If the dose of the CBCT images is noted to be relatively negligible with some presets, imaging is performed also immediately after the treatment. In these images the image quality is not crucial because imaging is not performed for accurate patient positioning. These images would provide information about the changes in bladder volume and movements of the organs that have occurred during the treatment. It is a goal to introduce function strategies also for these CBCT relating questions in the instructions for radiation therapy treatment of patients with bladder cancer.

5 Results

5.1 Results of the investigations on the created verification system

5.1.1 Defined calibration factor for measured dose distributions

Always before starting investigative measurements the daily conditions were determined. Air pressure and temperature were measured and entered into the matrix's software. The relative measurements of dose rate were made with the energies used that day. Except on one measurement day, the calculated difference between daily dose rate and the reference dose rate using equation 6 was less than the measurement accuracy of the matrix. So, no corrections were made by this reason except on that one day. After daily conditions had been checked, the measurements and calculations were carried out as explained in section 4.1.1. These investigations were able to determine the calibration factors for the measured dose distributions. For 360° VMAT treatment plans with 6 MV energy calibration factor $K_{C,\ 6x}$ is 1.036 and with 10 MV energy $K_{C,\ 10x}$ is 1.045. The factors behind these numbers are represented in the section by details.

Results of calibration of the chambers of the matrix in order to be comparable with the chamber of absolute dosimetry and repetitive measuring accuracy of the chambers of the matrix

Measurements were made first with the water phantom. The air pressure and temperature of the water inside the water phantom were measured and inserted into equation 2 to calculate the correction factor for the absolute chamber's calibration factor's pressure and temperature dependence. The percentage depth doses were measured with energies of 6 and 10 MV. These are shown in image 12. The absorbed doses in water were calculated for both energies using equation 4, where the doses at maximum points for energies of 6 and 10 MV were 0.999 Gy and 1.000 Gy,

respectively. Furthermore, the doses at a depth of 10 cm in water were 0.681 Gy and 0.730 Gy, respectively. Using the equivalent measurements with the matrix, the calculated doses with 6 and 10 MV were 0.693 Gy and 0.734 Gy, respectively. A calibration factor to make the matrix comparable with the absolute dosimetry was calculated using equation 5, from which $K_{m,\,6MV}$ was determined as 0.983 and $K_{m,\,10MV}$ as 0.995.

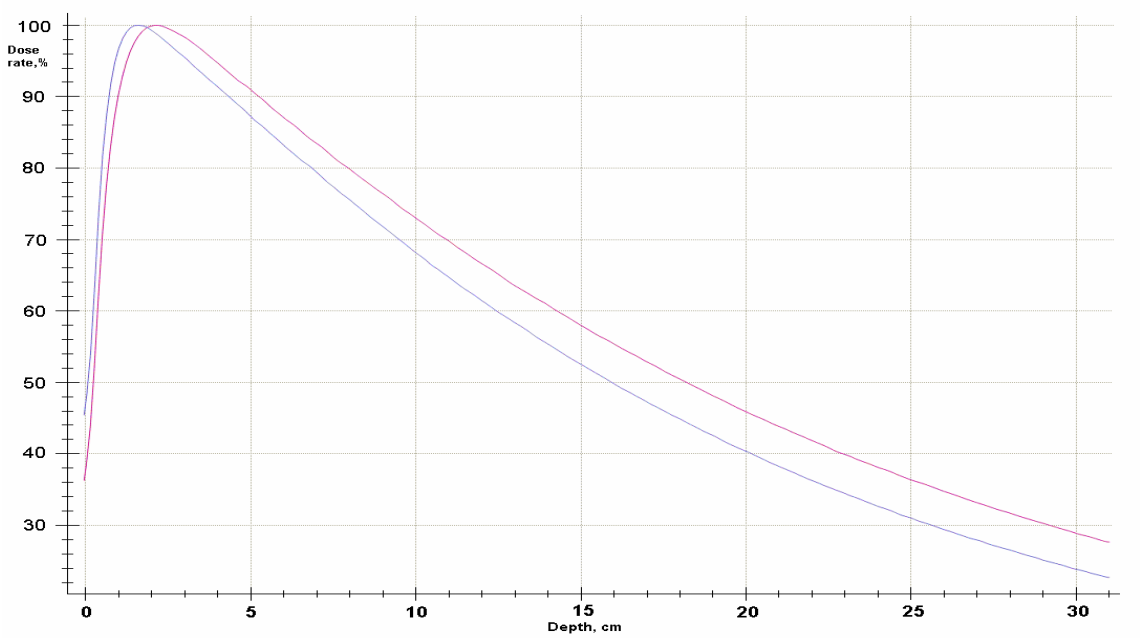

Image 12: Measured percentage depth doses. Blue graph represents the PDD of 6 MV and pink graph the PDD of 10 MV.

The ranges of the measured doses of ten repetitive measurements made by the matrix with energies of 6 and 10 MV were from 0.884 to 0.888 Gy and from 0.935 to 0.938 Gy, respectively. Moreover, the calculated averages were 0.8857 and 0.9368 Gy, respectively. By dividing the farthermost measured dose by the average it was calculated that the precision of the repetitive measurements are 0.2 % with both energies.

Results of investigations on factor for eliminating the effect of attenuation by the treatment table

Using the measured doses the factors $K_{T,\,\alpha}$ were calculated using equation 8. These results are shown in image 13 as a graph. The average effect of attenuation by the treatment table was calculated for both energies. Then the factor for eliminating the effect of attenuation by the treatment table from dose distribution measurements with the created verification system for 360° VMAT treatment plans were calculated using equation 9 with both energies. The calculations reveal that $K_{T,360°,6MV}$ is 1.012 and $K_{T,360°,10MV}$ is 1.009.

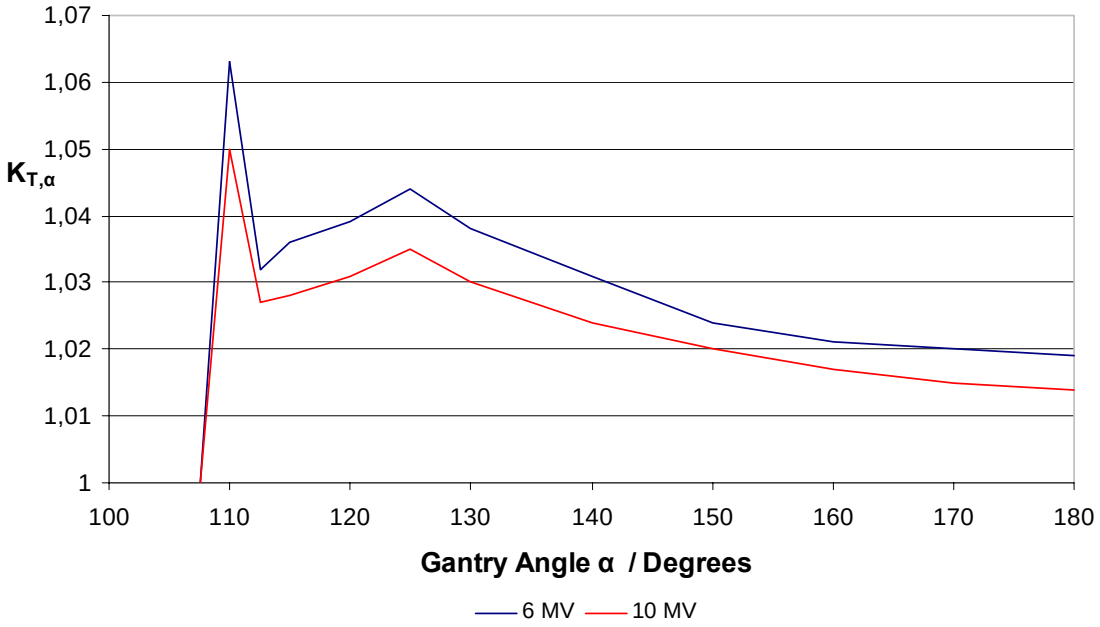

Image 13: Factors to eliminate the effect of attenuation by the treatment table from different gantry angles.

Angle dependence of the chambers of the matrix

The correction factors for dependence of the measuring angle were calculated using equation 11 after finishing the measurements. A graph reconstructed by the calculated factors is shown in image 14. Using all these factors an average was calculated to get the factor K_{γ} for correcting the dependence of the measuring angle of chambers for the 360° VMAT treatment plan verification with the created system. As a result of the calculations, the value of $K_{\gamma, 360°}$ was specified as 1,041.

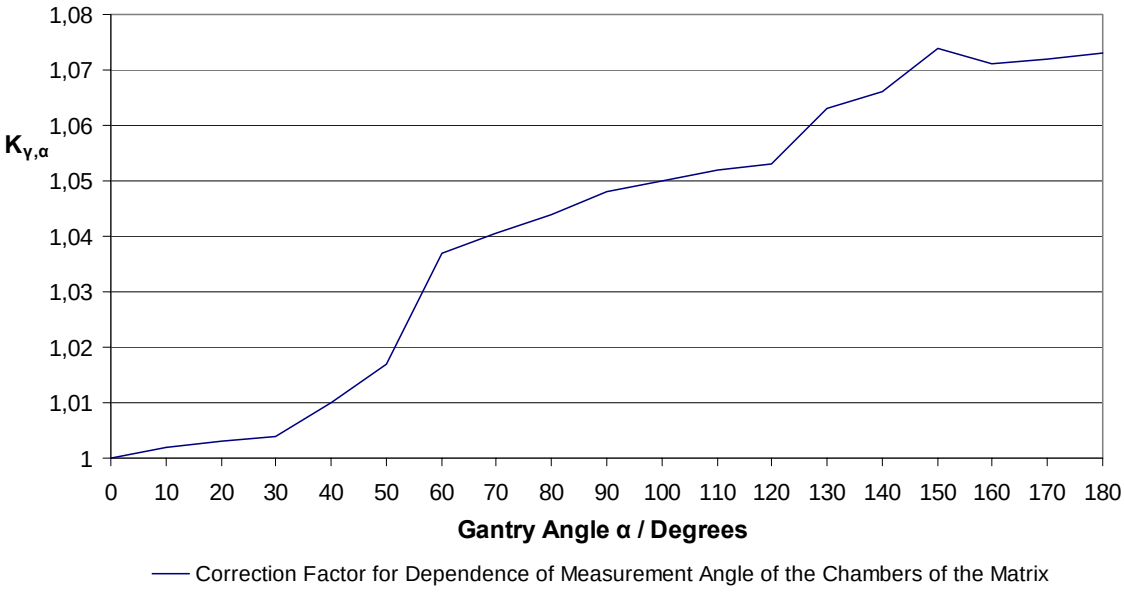

Image 14: Factors to correct the measuring angle dependence of the chambers of the matrix.

Results of measurements and calculations done with the created verification system

These measurements and calculations were realized also as described in section 4.1.1. All the investigated point doses were compared to the measured dose with a gantry angle of 0° using equation 12. Based on these factors, four graphs were reconstructed and one further graph by eliminating the effect of the attenuation by the treatment table from the measured doses. These graphs are shown in image 15.

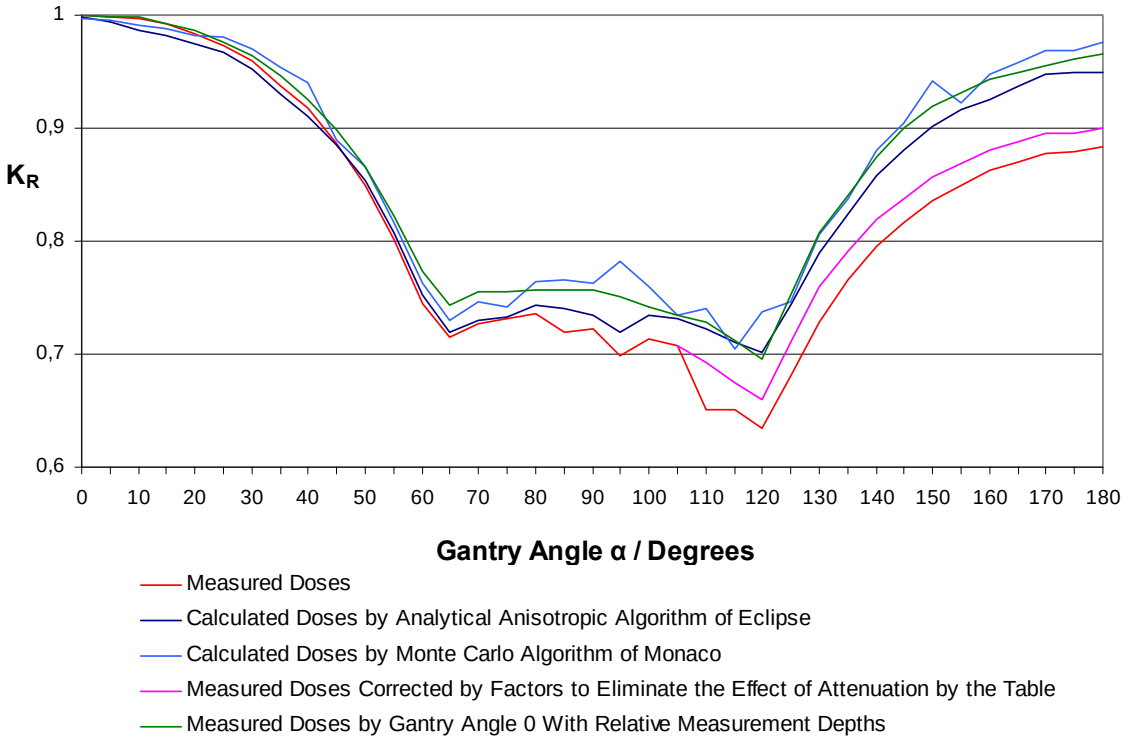

Image 15: Measurements and calculations made for the created verification system for VMAT treatment plans with energy of 6 MV. The measured doses are compared to calculations performed using analytical anisotropic algorithm of Eclipse and Monte Carlo of Monaco. Also the graphs of the measured doses correlated by table attenuation factor and measured doses from the gantry angle of 0° with relative measurement depths are shown. K_R represents a relativity factor compared to the measured dose from a gantry angle of 0°, which is set as 1.000.

5.2 Results of the Ball Test

5.2.1 Comparisons between calculated plans

In the planning process emphasis was placed on estimating the capability of the planning system to optimize fluence distribution with changing target sizes and limited constraint doses. It was also a goal to find the limits of the treatment planning system, where it will give an infeasibility warning to reach the set goals or not even reconstruct the fluence distribution map. This was tested using the constraint ball of radius 3 cm inside the target ball of radius of 6 cm. With both used energies the treatment planning system was able to optimize fluence distribution without problems till the situation, where the constraint ball's dose limit were set at 60 % of the target dose. The dosage

statistics reached in targets and constraints are shown in table 1, for energy of 6 MV, and in table 2, for energy of 10 MV, in all investigated situations. The planning system was able to calculate also treatment plans even with the smaller constraint ball's doses till 40 %, but it informed the user with a warning sign "infeasible" in the column of the constraint ball in the optimizing window. These plans were not even able to be treated at the linear accelerator. The accelerator's software gave inhibit error of mlc. The treatment planning system was not even able to optimize plans with the smaller constraint ball's dose than 40 % of the target ball's dose.

Table 1: Statistics of calculations with energy of 6 MV. 100 % target dose is 50 Gy.

6 MV		Constraint		Target	
Constraint's radius / cm	Constraint's dose limit	Volume where dose limit is crossed / %	Hot Spot / Gy (% of dose limit)	Volume where target dose is reached / %	Hot Spot / Gy (% of dose limit)
3 cm	100 %	-	-	97.0	54.5 (109)
3 cm	66 %	54.5	37.4 (113)	6.6	50.8 (102)
3 cm	60 %	38.8	33.2 (111)	0.0	44.8 (90)
5 cm	66 %	69.6	35.9 (109)	0.0	46.0 (92)
1 cm	66 %	60.0	36.3 (110)	69.0	55.2 (110)

Table 2: Statistics of calculations with energy of 10 MV. 100 % target dose is 50 Gy.

10 MV		Constraint		Target	
Constraint's radius / cm	Constraint's dose limit	Volume where dose limit is crossed / %	Hot Spot / Gy (% of dose limit)	Volume where target dose is reached / %	Hot Spot / Gy (% of dose limit)
3 cm	100 %	-	-	99.0	55.8 (112)
3 cm	66 %	61.1	37.0 (112)	8.9	51.5 (103)
3 cm	60 %	43.0	33.5 (112)	0.3	50.0 (100)
5 cm	66 %	68.4	36.0 (109)	0.0	45.5 (91)
1 cm	66 %	60.1	36.7 (111)	63.7	54.0 (108)

5.2.2 Comparisons between measured and calculated dose distributions

Results of measurements made using the matrix

All the treatment plans of the ball test were measured and calibrated according to the way introduced in section 4.2.2. The percentage proportions of the point doses measured by the chambers, which passed the accuracy limits in the area of 15 · 15 most middle chambers, and in the whole irradiated area of 27 · 15 chambers, are introduced in table 3 for every measured plan. Nine plans out of ten passed the accuracy limits of 3 % and 3 mm with at least 95 % of accepted point doses in the 225 closest chambers to the isocenter. By examining the results of plan R3D66% with energy of 6 MV it can be observed, that 99.1 % of the 225 most centrally located chambers to the isocenter, and 99.0 % of the 405 chambers, which were in the irradiated area, passed the accuracy limits. This can be observed also from image 16 showing a coronal slice of the measured dose distribution of plan R3D66% at the level of the measuring points of the chambers. In the image, the red squares indicate that the measured dose by the chamber did not pass the set accuracy limits. The profiles of the plan at the isocenter are shown in images 17 and 18.

Table 3: Percentage of accepted point doses measured by the chambers inside about an area of 50 % isodose. In parentheses the percentage of accepted point doses in the whole irradiated area.

Constraint's radius/ cm and dose/ %	6 MV			10 MV		
	100 %	66 %	Min.	100 %	66 %	Min.
5 cm		96.4 % (97.3 %)			96.4 % (90.6 %)	
3 cm	100.0 % (99.5 %)	99. 1 % (99.0 %)	98.7 % (98.5 %)	100.0 % (99.1 %)	99.6 % (91.4 %)	94.7 % (88.9 %)
1 cm		98.7 % (97.5 %)			99.6 % (96.8 %)	

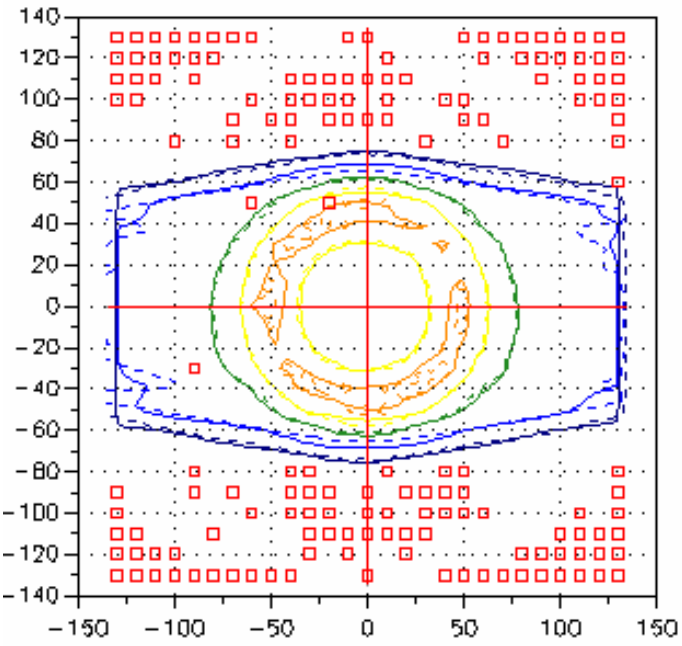

Image 16: Coronal slice of measured dose distribution of plan R3D66%6MV at the level of the measuring points of the chambers. Profiles: orange = 100 %, yellow = 80 %, green = 50 %, blue = 20 % and dark blue = 10 % of the target dose. Red squares indicate that the measured dose by the chamber did not pass the set accuracy limits.

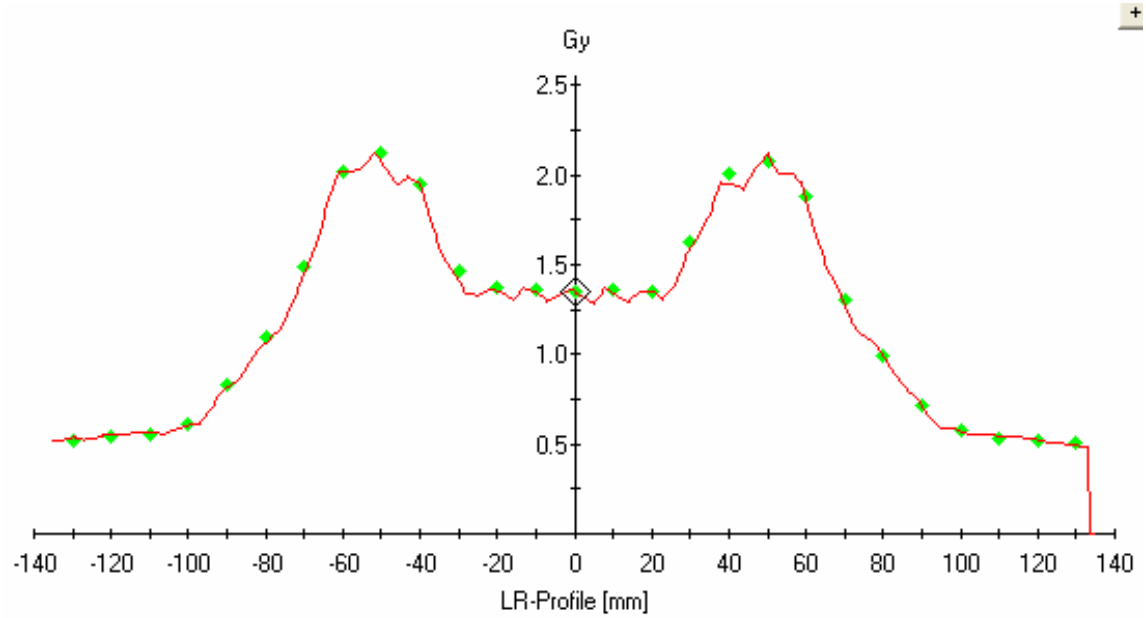

Image 17: Profiles of left to right directions at the isocenter of the calculated and measured dose distributions of plan R3D60%6MV. The red line signifies the calculated dose profile and squares measured point doses of the chambers. The green squares indicate the passed point doses and the red squares the failed ones.

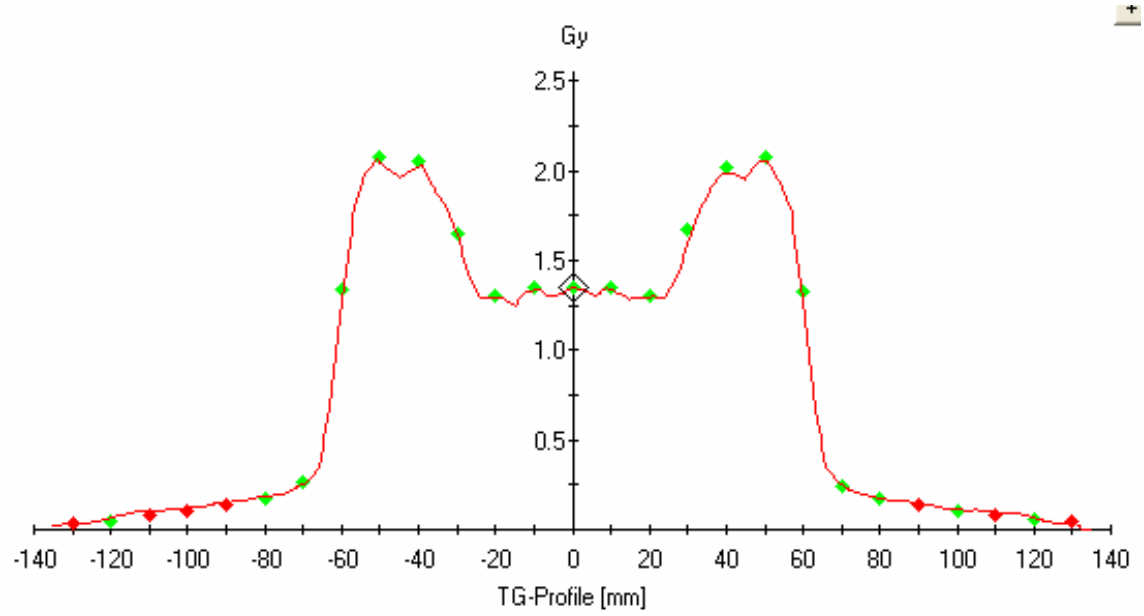

Image 18: Profiles of gantry to table directions at the isocenter of the calculated and measured dose distributions of plan R3D60%6MV. The red line signifies the calculated dose profile and squares the measured point doses of the chambers. The green squares indicate the passed point doses and the red squares the failed ones.

By turning attention to the middle columns of table 3, it can be seen with both energies, that by removing the dose limit of the 3 cm radius constraint ball, all the point doses of the 225 most centrally located chambers are passed. By examining the column in the other direction, where the dose limit of the constraint ball was tightened as low as the treatment planning system permitted without warnings, the percentage of passed point doses descended. By changing the radius of the constraint ball from 3 cm to 5 cm with a dose limit of 66 % of the target dose, the number of passed point doses also decreased. By reducing the radius of the constraint ball with the same dose limit to 1 cm, the number of passed point doses also decreased with energy of 6 MV; however with 10 MV, the number of passed point doses remained the same with the 225 most centrally located chambers, and increased by considering all the chambers in the area of irradiation.

In order to investigate the reliability of the congruency of the measured dose distributions in repetitive treatments, plan R3D66% was measured three times with both energies, and also another three times by repositioning with energy of 6 MV. By comparing all cases of measured dose distributions from the same session, using the accuracy limits of 0.5 mm and 0.5 %, 100 % of the 225 most centrally located chambers' point doses passed. Also more than 95 % of all the 405 point doses measured by the chambers in the irradiated area passed the accuracy limits. By comparing the measured dose distributions of 6 MV before and after re-positioning, more than 95 % of the point doses measured by the 225 most centrally located chambers passed the accuracy limit of 0.5 % only by relaxing the distance accuracy limit to 1.5 mm.

Results of measurements made using radiochromic film and the matrix together

The used sheet of a radiochromic film was irradiated, measured and calibrated as explained in section 4.2.3. Plan R3D66% was measured by the film and the matrix together. The isodoses of the dose distributions measured by the film and the matrix are shown in image 19. From the image, the resolution limitations of the measuring devices can be observed. In the isodose measured by the matrix the measuring points can be observed by squares as a uniform dose, because the point doses of the chambers are not averaged with the ones around them. Both detector systems' profiles at the isocenter in the directions of left to right and gantry to table are shown in images 20 and 21, respectively. In these images the measured dose by the matrix is represented by green graphs in which the measured point doses using chambers are shown by steps in the graphs. The red graphs represent the measured doses by film. The borders of the film can be observed by the end of the graphs earlier, than the graphs of profiles measured by the matrix.

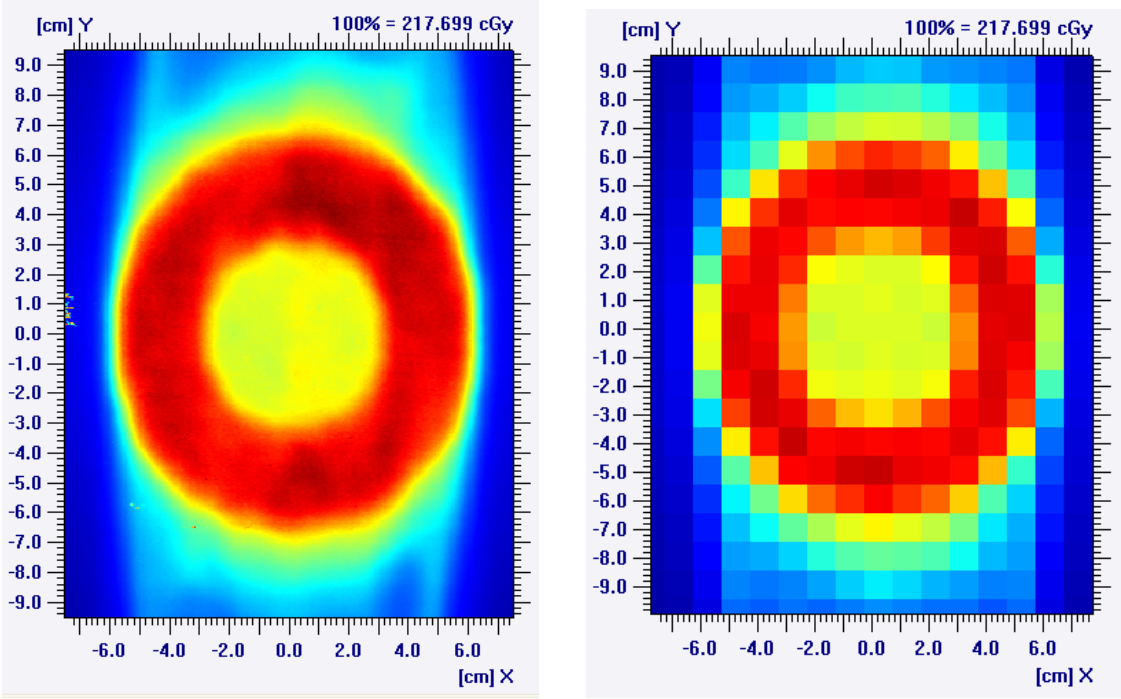

Image 19: Isodoses of the measured dose distributions. On the left the measured dose distribution by radiochromic film on top of the matrix and on the right the measured dose distribution by the matrix, where the measured dose by each chamber is shown as squares with uniform dose in the area.

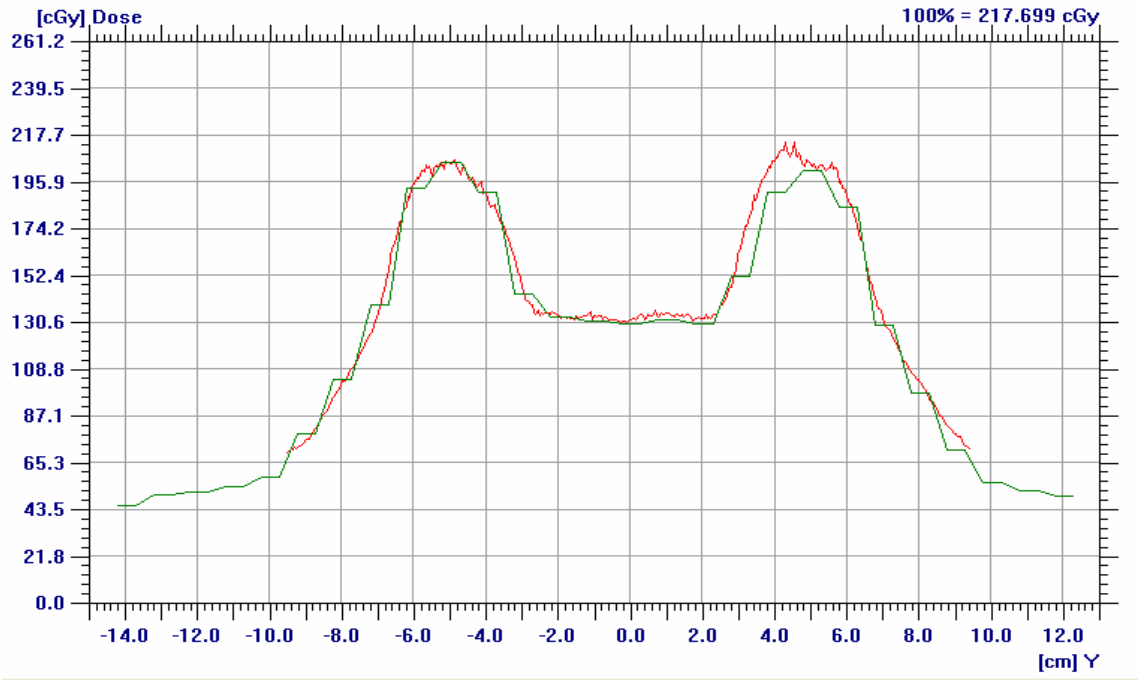

Image 20: Profiles of left to right directions of measured dose distributions of plan R3D60%6MV. The red line signifies the measured dose profile using the film and the green line the measured point doses by the chambers.

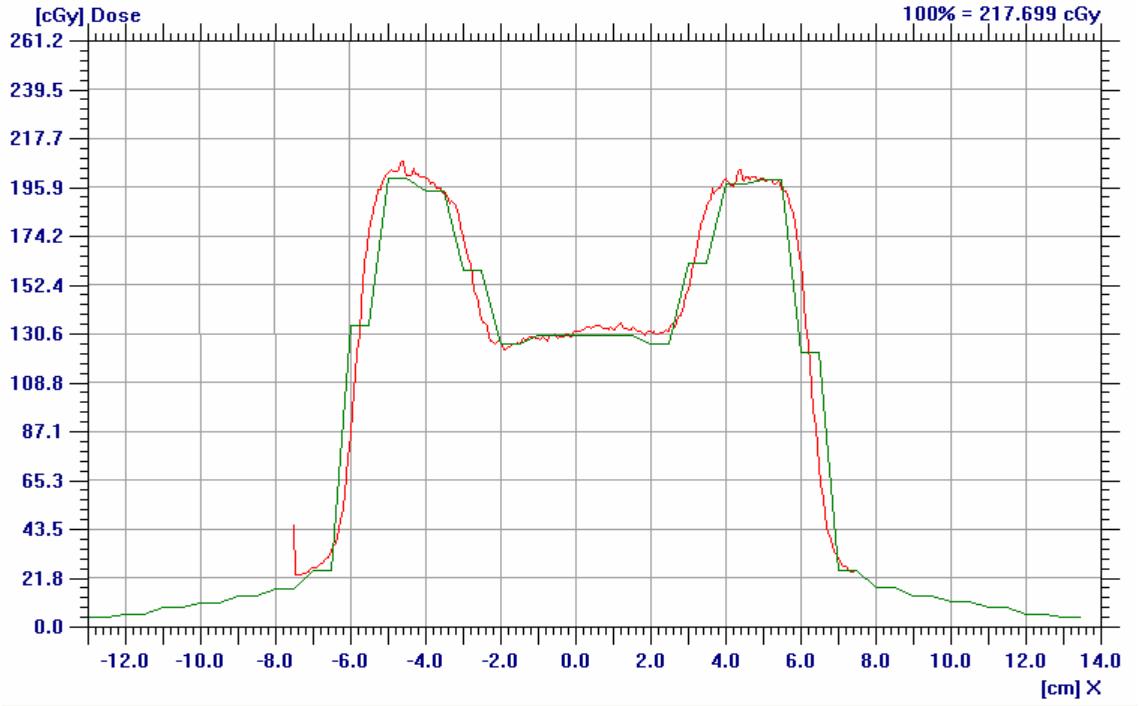

Image 21: Profiles of gantry to table directions of measured dose distributions of plan R3D60%6MV. The red line signifies the measured dose profile using the film and the green line the measured point doses by the chambers

5.3 Results of comparisons between calculated and measured dose distributions of clinical test VMAT treatment plans

Five clinical test plans were measured with the created verification system using both 6 and 10 MV energies. The dose distributions of all the test plans were measured as planned with 360° gantry rotation and by quality assurance mode without gantry rotation. The dose distributions were analyzed as discussed in section 4.3. For the measured dose distributions, the determined calibration factors were used. It was calculated that the percentage of the chambers, which had measured acceptable point doses inside the set accuracy limits in an area of about 50 % isodose were between 95.3 % and 100.0 % with the 6 MV energy plans, and between 95.1 % and 100.0 % with the 10 MV energy plans. The percentage of passed point doses in an area of about 10 % isodose was between 93.8 % and 96.8 % with the 6 MV energy plans, and between 93.4 % and 95.5 % with the 10 MV energy plans. The results of the verifications measured by quality assurance mode without gantry rotation correlated very well with the corresponding 360° plan verifications.

5.4 Results of investigations on patient positioning

5.4.1 Created presets for the CBCT imaging

There were three presets created, which were sufficient for clinical imaging of patients with bladder cancer. These presets were named as Bladder A, B and C. It was noticed during testing that the parameters which affect the imaging time cannot be decreased from the values in preset Prostate M10 Fast in order to avoid significant artefacts in the images. Therefore, the imaging time with all the sufficient created presets was 60 seconds, and the focus was on decreasing the amounts of volts and amperes per second in order to minimize irradiated doses.

Results of automatic matching accuracy between the presets

Investigations to compare the equivalence of automatic matching between the created and the original presets were realized as explained in section 4.4.1. The preset Prostate M10 was chosen as the reference preset. The recommended position corrections in six dimensions by the other investigated presets were compared to the ones recommended by the reference preset. Using the three measurements with different positions of the internal organ phantom, there was not suggested more than 0.01 cm or 0.1° different corrections from the ones recommended by the reference preset. Nor were larger differences than those between the recommendations by any other presets. The results of the measurements are shown in table 4.

Table 4: Comparisons of matching accuracies between the presets. Prostate M10 is the reference preset.

Preset	Measurement 1	Measurement 2	Measurement 3
Prostate M10 ***Reference***	tx = 0.73 cm rx = 0.8° ty = 0.41 cm ry = 359.9° tz = 0.32 cm rz = 359.9°	tx = 0.25 cm rx = 0.4° ty = 0.07 cm ry = 359.1° tz = -0.06 cm rz = 358.6°	tx = 0.38 cm rx = 0.4° ty = -0.01 cm ry = 1.0° tz = 0.32 cm rz = 358.2°
Prostate M10 Fast	Δtx = 0.00 cm Δrx = +0.1° Δty = +0.01 cm Δry = +0.1° Δtz = 0.00 cm Δrz = -0.1°	Δtx = 0.00 cm Δrx = -0.1° Δty = -0.01 cm Δry = +0.1° Δtz = 0.00 cm Δrz = 0.0°	Δtx = 0.00 cm Δrx = -0.1° Δty = -0.01 cm Δry = 0.0° Δtz = 0.00 cm Δrz = +0.1°
Bladder A	Δtx = -0.01 cm Δrx = +0.1° Δty = +0.01 cm Δry = +0.1° Δtz = 0.00 cm Δrz = 0.0°	Δtx = 0.00 cm Δrx = 0.0° Δty = 0.00 cm Δry = +0.1° Δtz = 0.00 cm Δrz = 0.0°	Δtx = -0.01 cm Δrx = 0.0° Δty = 0.00 cm Δry = +0.1° Δtz = 0.00 cm Δrz = +0.1°
Bladder B	Δtx = 0.00 cm Δrx = 0.0° Δty = +0.01 cm Δry = +0.1° Δtz = -0.01 cm Δrz = -0.1°	Δtx = 0.00 cm Δrx = 0.0° Δty = 0.00 cm Δry = +0.1° Δtz = 0.00 cm Δrz = 0.0°	Δtx = -0.01 cm Δrx = 0.0° Δty = 0.00 cm Δry = +0.1° Δtz = 0.00 cm Δrz = +0.1°
Bladder C	Δtx = 0.00 cm Δrx = +0.1° Δty = +0.01 cm Δry = +0.1° Δtz = 0.00 cm Δrz = -0.1°	Δtx = 0.00 cm Δrx = -0.1° Δty = -0.01 cm Δry = +0.1° Δtz = 0.00 cm Δrz = 0.0°	Δtx = 0.00 cm Δrx = 0.0° Δty = 0.00 cm Δry = +0.1° Δtz = -0.01 cm Δrz = 0.0°

Measured irradiated doses of the presets

The irradiated doses of the presets sufficient for imaging patients with bladder cancer using the information about image quality was measured as described in section 4.4.1. Using the preset called Bladder A, the measurements were made three times by the chamber positioned in the middle of the CT thorax phantom. The measured doses were 7.5, 7.5 and 7.2 mGy. With the preset Bladder A also the doses on the surface at three different positions were measured. The dose close just above the treatment table was 11,0 mGy, on the lateral side of the phantom 11.5 mGy and in the opposite direction from the table 11.7 mGy. So, the dose measurements on the surface of the phantom were made in the opposite side from the treatment table. The results of the measurements are shown in table 5.

Table 5: Measured absorbed doses in the middle of the CT thorax phantom and at the maximum dose point on the surface of the phantom using the presets.

Preset:	Dose at Isocenter (mGy)	Dose max. on surface (mGy)
Prostate M10	20.5	35.7
Prostate M10 Fast	11.2	18.5
Bladder A	7.5	11.7
Bladder B	4.0	6.7
Bladder C	3.0	4.5

5.4.2 Results of automatic matching accuracy with grey-value algorithm

The investigations were realized as planned in section 4.4.2. During the investigations, where concentration was focused only on one direction at a time, the largest margins between planned position correction and the recommended one was 0.08 cm in translational directions and 0.2° in rotational directions. The investigation using a displacement of 2.0 cm in the lateral direction was repeated three times. The sizes of the recommendations were 2.02 cm, 2.00 cm and 2.08 cm, and the average of these was calculated to be 2.03 cm. The investigation using a displacement of 2.0° around the vertical axis was repeated three times. The sizes of the recommendations were 2.0°, 1.8° and 1.9° and the average of these was calculated as 1.9°. In the investigations, where the displacements were realized in four dimensions together with smaller investigated margins, the sizes of recommendations were almost as accurate as in the investigations of one direction in each case, but with larger margins the recommendations were unrealistic. All the results are shown in table 6.

Table 6: Results of investigations into automatic matching accuracy with grey-value algorithm.

Direction of the displacement	Size of the displacement	Size of the recommendation
Lateral (tx)	0.50 cm	0.45 cm
	2.00 cm	2.03 cm
Longitudinal (ty)	0.50 cm	0.54 cm
	2.00 cm	2.05 cm
Around lateral axis (rx)	0.5°	0.7°
	2.0°	2.1°
Around vertical axis (rz)	0.5°	0.5°
	2.0°	1.9°
tx, ty, rx and rz	tx = 0.50 cm rx = 0.5° ty = 0.50 cm ry = 0.0° tz = 0.00 cm rz = 0.5°	tx = 0.42 cm rx = 0.7° ty = 0.38 cm ry = 0.1° tz = 0.07 cm rz = 0.6°
	tx = 2.00 cm rx = 2.0° ty = 2.00 cm ry = 0.0° tz = 0.00 cm rz = 2.0°	tx = 2.12 cm rx = 2.6° ty = 1.08 cm ry = 346.9° tz = 0.92 cm rz = 5.5°

5.4.3 Results of movement accuracy of Hexapod treatment table using the CBCT system

The investigations were realized as described in section 4.4.3. The recommended position corrections of the software after the first CBCT imaging was recorded and realized by the movements of the Hexapod treatment table. Moreover, the recommended position corrections after the second CBCT imaging were recorded. Both recommendations are shown in table 7 in all five cases. The recommendations for patient positioning after the second CBCT imaging are in same magnitudes in four cases, where the recommendations in translational directions are from 0.00 cm to 0.02 cm, and in rotational directions from 0.0° to 0.2°. In one case, the recommendations after the second CBCT imaging differed from the others by larger recommendations.

Table 7: Recommended and realized position corrections after the first CBCT imaging and the recommended position corrections by another CBCT imaging after realizing the position corrections.

Case	Recommended and realized position corrections	Recommended position corrections after 2nd imaging
1	tx = 0.78 cm rx = 0.9° ty = 0.42 cm ry = 0.0° tz = 0.27 cm rz = 359.9°	tx = -0.01 cm rx = 0.0° ty = 0.00 cm ry = 0.0° tz = 0.02 cm rz = 0.0°
2	tx = 0.36 cm rx = 0.6° ty = 0.33 cm ry = 0.9° tz = 0.01 cm rz = 0.6°	tx = 0.03 cm rx = 0.2° ty = 0.01 cm ry = 359.2° tz = 0.07 cm rz = 0.0°
3	tx = 0.38 cm rx = 0.7° ty = 0.34 cm ry = 0.1° tz = 0.07 cm rz = 0.6°	tx = 0.02 cm rx = 0.0° ty = 0.01 cm ry = 0.0° tz = 0.01 cm rz = 359.9°
4	tx = 0.47 cm rx = 0.4° ty = -0.02 cm ry = 1.0° tz = 0.58 cm rz = 359.1°	tx = -0.01 cm rx = 0.0° ty = -0.01 cm ry = 359.9° tz = 0.00 cm rz = 0.0°
5	tx = -0.61 cm rx = 0.2° ty = -0.28 cm ry = 0.1° tz = 0.26 cm rz = 359.4°	tx = 0.00 cm rx = 0.0° ty = -0.01 cm ry = 359.8° tz = 0.02 cm rz = 0.1°

5.5 Instructions for the radiation therapy process of patients with bladder cancer and first clinical experiences

Between February and May 2011 at HUCH there were in total five patients treated radically for bladder cancer using radiation therapy. In two of the cases the whole bladder and in three of the cases only part of the bladder wall was treated. For all of the patients lipiodol was injected into the tumour area in bladder wall and CT imaging was performed as described in section 4.5. For two of the patients only three different targets, instead of the intended four, were designed, because of the relatively small changes in bladder volume between CT images. The planned target doses were between 52.5 and 64 Gy. The first three patients were treated using photon energy of 6 MV. After receiving calculation data for the treatment planning system with photon energy of 10 MV from manufacturer, the other two patients were treated with this energy. The other properties and parameters of the treatment planning system were adjusted individually for each treatment plan of every patient. For all the patients suitable

treatment plans were planned according to the goals, and by considering the limitedness of realizing them all together comprehensively, as discussed in section 4.5. In all cases the absorbed doses in the PTVs were optimized between 95 % and 107 % of the planned dose. By struggling to minimize the dose in organs at risk in the vicinity of PTVs, there was small cold- and hot-spots aloud to the PTV in three cases. In partial bladder cases the edges of the PTVs, especially inside the bladder, were not considered as definite in order to minimize the dose in organs at risk. However, in two of the cases the coverage of the whole PTVs were at least 95 % of the planned dose, and in three others the areas of cold-spots were not over 4 % of the PTV of the case. Image 22 shows the isodoses in the treatment planning of a whole bladder case at isocenter level, and the dose-volume histogram of the case. In all of the cases the treatment times were between five and seven minutes. Using the experiences a workable template for the treatment planning process in bladder cases was determined. The template includes suitable work-flow for treatment planning with the properties and parameters used in it. The template is introduced in Appendix A as a part of the instructions for the radiation therapy treatment of patients with bladder cancer.

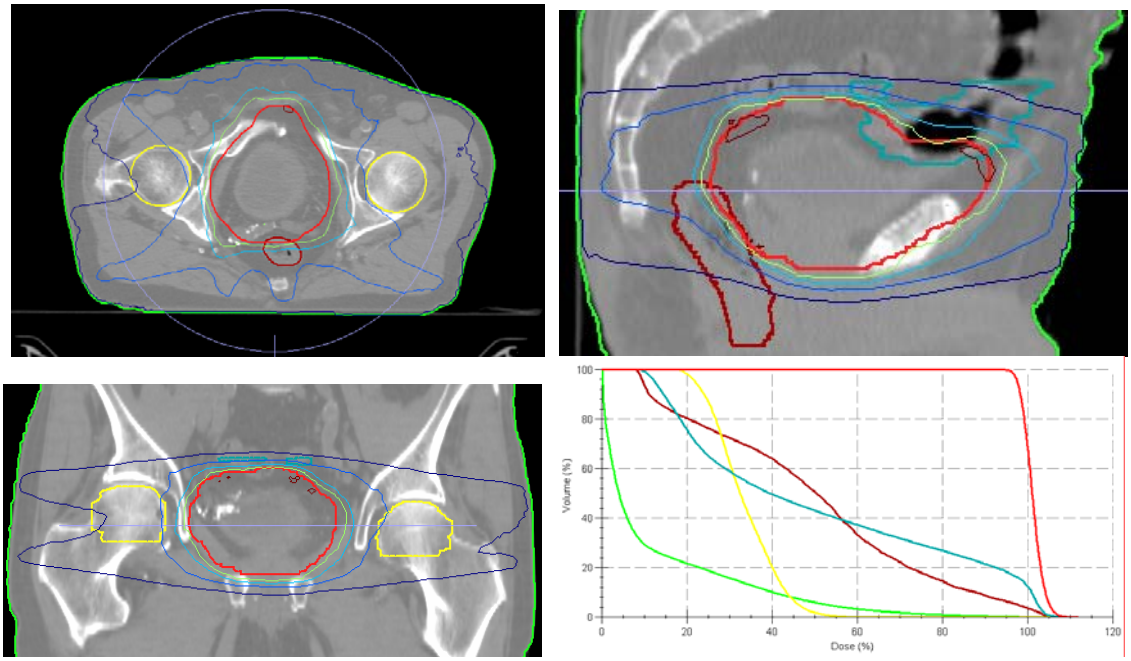

Image 22: Planned dose distribution in a case, in which the whole bladder was treated. The amounts of doses in contoured structures can be seen in DVH, where red indicates the PTV, yellow the hip bones, turquoise blue the bowels, brown the rectum and green the body. In the slices of planning CT images the 107 % isodose is dark red, 95 % green, 80 % light blue, 50 % blue and 20 % dark blue.

Using these results, introduced in section 5.3, of the 360° VMAT treatment plan verification measurements with the created system, a strategy for plan verification was created and used in all five cases. In the plan verification process all of the actual treatment plans are measured and analyzed by the created system. In addition, one plan of each patient is measured and analyzed also by the quality assurance mode without gantry rotation before starting treatment. If a plan measured only by the created system does not pass the set accuracy limits, it is measured and analyzed also by quality assurance mode without gantry rotation. One extra plan of two patients was measured also without gantry rotation to ensure the reliability of the specific plans. Using the measurements with the created system, the calculated percentage of ionization chambers, which had accepted measured doses inside the areas of about 50 % isodoses

were between 93.8 % and 99.7 % with the 6 MV energy plans and between 93.6 % and 99.5 % with the 10 MV energy plans. The percentage of passed point doses inside the areas of about 10 % isodoses were between 93.8 % and 98.7 % with the 6 MV energy plans and between 92.6 % and 98.3 % with the 10 MV energy plans. Also by the information of these investigations, the dose distributions measured using the original plans and without gantry rotation are congruent. All of the plans were accepted for treatment.

The positioning of the patients, the treatment table and the frame of the infrared reflectors were realized as suggested in section 4.5. Using the results of accuracy tests between different presets, also the created presets were included into clinical use. Relatively small doses irradiated by some of the presets enabled CBCT imaging also after the treatment in cases, where image quality was good enough with the created presets. A strategy for determination of an appropriate CBCT imaging preset for each patient individually was created by the results of CBCT investigations. Using the strategy patients are imaged with the preset Prostate M10 before, and with the preset Prostate M10 Fast after, the first fraction. If the image quality in the image performed after the fraction is sufficient, the preset will be used before the second fraction, when the image after the fraction is performed with the preset Bladder A. This is continued till the preset Bladder C or as long as image quality remains sufficient. Also the strategy is introduced in Appendix A by details. The strategy determined a suitable preset for CBCT imaging for each individual patient. In images 23 - 27 are shown CBCT images of a patient to whom the image quality of the preset Bladder C was sufficient.

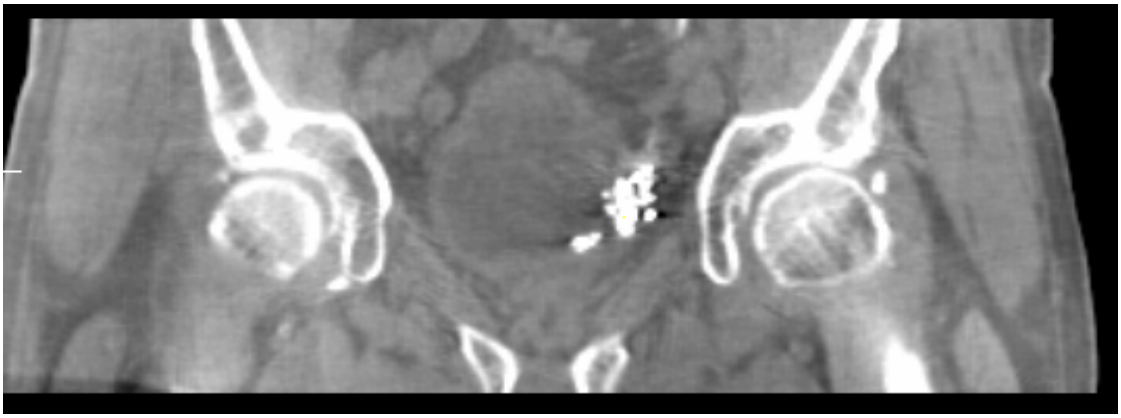

Image 23: Coronal view of a CBCT image using preset Prostate M10. Bladder of the patient can be seen in the middle of the image. Lipiodol is visible in the image as light area on the lateral wall of the bladder.

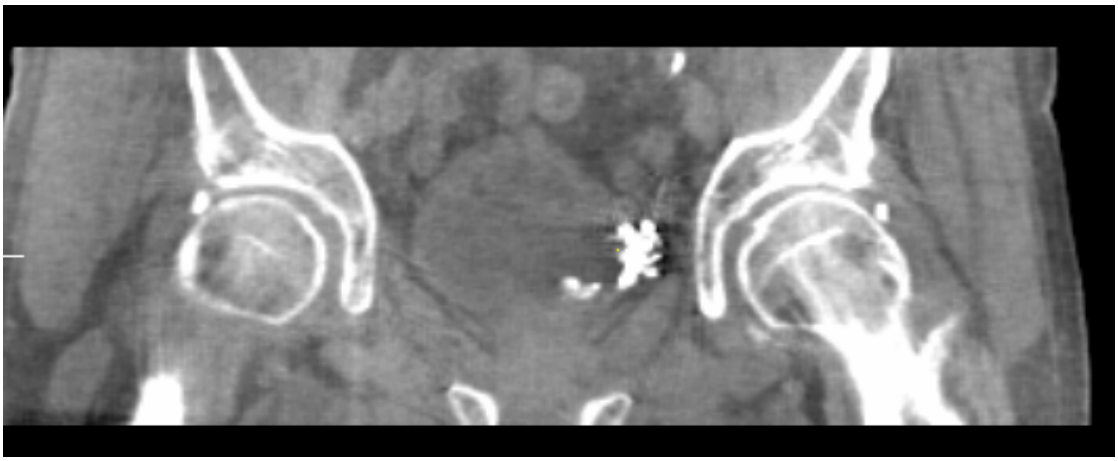

Image 24: Coronal view of a CBCT image using preset Prostate M10 Fast.

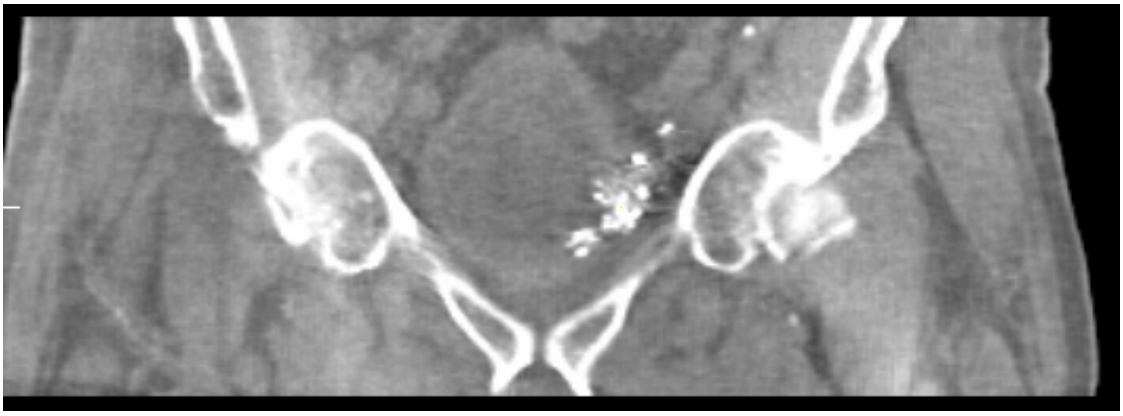

Image 25: Coronal view of a CBCT image using created preset Bladder A.

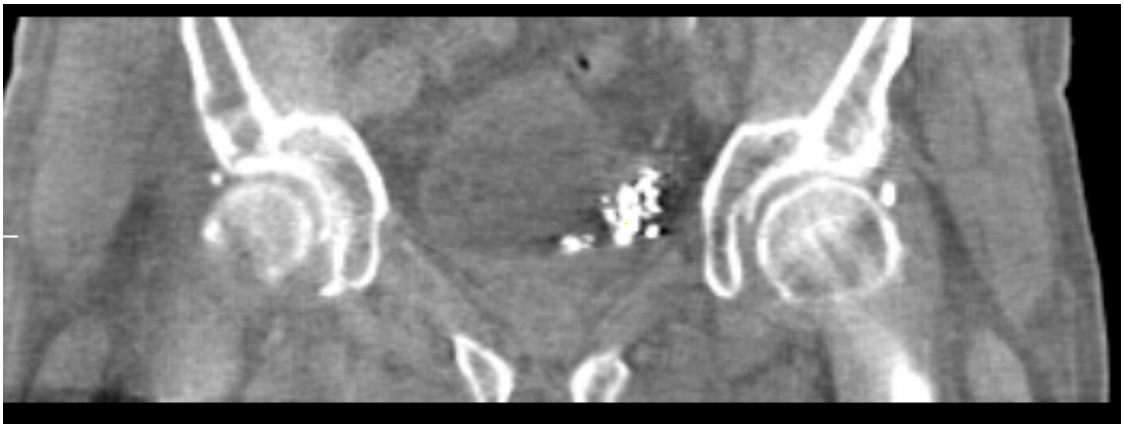

Image 26: Coronal view of a CBCT image using created preset Bladder B.

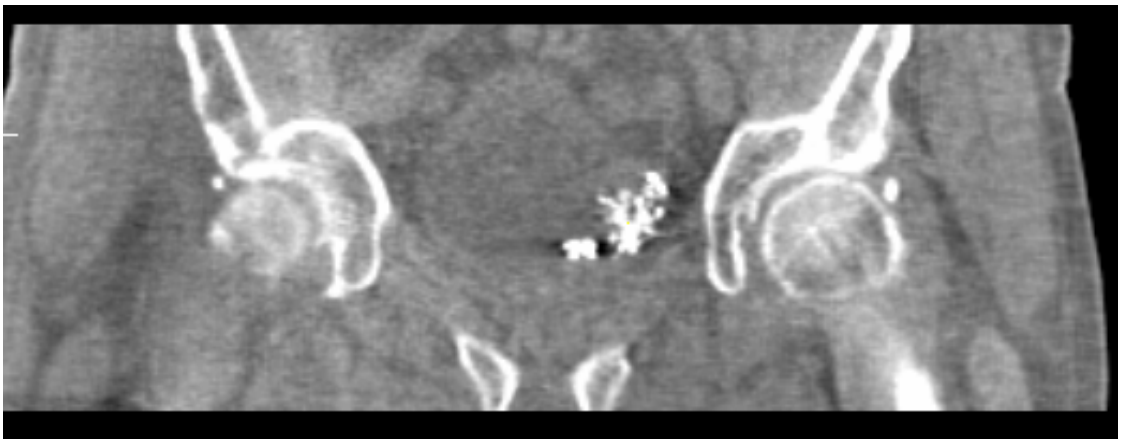

Image 27: Coronal view of a CBCT image using created preset Bladder C.

The strategy for patient positioning with CBCT images was also planned using the results of the CBCT investigations. Automatic matching using the grey-value algorithm with the matching area suggested in section 4.5 was realized with all the patients. The results of automatic matching were reviewed manually always before deciding about the position corrections of a patient. Using the results of matching, the position corrections were done by the motorized Hexapod treatment table in six degrees of freedom with a range of corrections of 0.1 mm and 0.1°. After the corrections had been realized, the treatment was delivered. Also this part of the instructions for radiation therapy of patients with bladder cancer is introduced in Appendix A.

6 Analyses of the Results

6.1 Investigations on the created verification system

6.1.1 Accuracy of the matrix as measuring device

The investigations considered many issues relating to the measurement accuracy of the matrix as measuring device for VMAT treatment plan verification. The measured dose using the matrix was firstly, compared to the measured dose using the chamber of absolute dosimetry. Secondly, the repetitive measurement accuracy of the matrix was determined, and thirdly, the angle dependence of the chambers of the matrix was evaluated. Repetitive measuring accuracy was determined by ten measurements, which enable evaluation of the short term reproducibility of the matrix. It was noticeable during the investigations, that the first measurements by the matrix show relatively smaller doses. From this observation all the investigative measurements were started after the matrix had been switched on at least for ten minutes and the measured dose of daily dose rate measurements were stabilized. However, when the matrix was warmed up, the short term precision was only 0.2 % possible deviations of the mean, which is the same as in the investigations of Spezi et al also with PTW's matrix [33]. However, these measurements were done only for the middle chamber of the matrix. Even though all the chambers are similar, there could be exceptional individuals. However, from the daily dose rate measurements with a 10.4 · 10.4 cm field and dose distribution measurements, there was no particular chamber noticed, which would have been repetitively showing a separate kind of dose according to the others.

Also the comparable measurement for the absolute dosimetry was made by the middle chamber of the matrix. In the investigations the amount of solid water set on top of the matrix was adjusted so that the depth to the measuring point of the middle chamber was the same as in the absolute measurements in water. In these measurements, as in the chambers' angle dependence measurements, the electron density of PMMA, which is the material in the matrix, was not considered to be different to the electron density of water. The equivalent depth for 5.0 mm of PMMA is 5.9 mm layer of solid water [23][24]. The effect of this on the results can be analyzed by the measured percentage depth doses shown in image 12. At the depth of about 10 cm the doses decrease 0.38 percentage units per mm by 6 MV and 0.28 percentage units per mm by 10 MV. The effect of this on the factor to make the matrix comparable to the absolute dosimetry is, however, only a couple of thousandths decrease. Also this kind of 0.9 mm error could occur during positioning of the measurement devices by the lasers. This is one reason why this was not taken into consideration for these investigations, but a more relevant one, is the difficulty to determine the exact equivalent depth in solid water in investigations of the measuring angle dependence of the matrix. Especially from the gantry angles, where from radiation traverses through the other ionization chambers of the matrix, the determination of the exact equivalent depth in water would have been impossible. Also investigations about the relation between the used energy and measuring angle dependence of the chambers should be investigated. However, the same kind of results, firstly about the matrix showing relatively more than absolute measurements, and secondly about the angle dependence of the chambers of the matrix, have been introduced also by other investigations [23].

6.1.2 Analyses of investigations concerning the factor for eliminating the effect of attenuation by the treatment table

In the investigations measurements were made by intervals, which enabled determination of a factor for eliminating the effect of attenuation by the treatment table in all the variable shape areas of it. Using these values, and by the graph made out of these, it is also possible to determine a factor for different sizes of VMAT arcs. However, also these investigations were done only using the middle chamber of the matrix. The effect of the treatment table is obviously different, for example, to a chamber five centimetres laterally aside from the middle chamber. The convenience of the factor for other chambers can be discussed, but the similarity of the treatment table in both lateral directions might cause the overall effect to be about the same as the other chambers as to the middle chamber in cases, where the VMAT arc includes the whole interval of gantry angles from 110° to 250°.

The effect of attenuation by the treatment table was investigated in order to determine a correction factor for the created verification system, but the results of the investigation make it also possible to analyze the effect of attenuation by the treatment table in actual patient treatment. The amount of the effect of attenuation by the treatment table increase along the traversed distance of radiation through the table. The measurement point in the investigations was 8.5 cm above the surface of the table, so for targets higher than that, the effect of the treatment table is smaller from the lateral sides of the table, and the amount of gantry angles, from which the treatment table is in between the radiation source and target, decrease. Concerning targets close to the table, the effects

are opposite. However, in the treatment of patients with bladder cancer, the targets are normally about 10 cm, or more, above the treatment table.

6.1.3 Accuracy of the established calibration factor for the measured dose distributions

In order to determine the calibration factor for dose distributions measured using the created VMAT treatment plan verification system, all the main effects were considered, which would disturb the reliability of the measured doses. The factors were determined by specific investigations, which involved considerations of the effects of different particular elements. During the investigations the goal to determine a calibration factor for VMAT treatment plans, which would be accurate enough for these purposes, was kept in mind, instead of digressing to concentrate on specifications of a certain feature in the measurement system. One reason for avoiding extremely precise investigations for a certain feature is the nature of the productions of VMAT treatment plans. The absorbed dose in a particular volume in matter might be produced only by radiation from certain directions even with a 360° arc. The calibration factor was determined at the middle chamber of the matrix by considering all the effects from all 360°, and averaging them to make it a generally functional estimation. For the measured doses using some chambers away from the middle chamber, the determined factor could be too inaccurate in cases where also the direction of radiation is only from the lateral to back direction, where the effect of attenuation by the treatment table and the angle dependence of the chambers have higher effects. However, it is more probable that the effects average each other out, and the calibration factor is relatively accurate enough in all areas of the volume, where the absorbed dose is high. In spite of all, it is important that the user keeps in mind these issues while analyzing the measured data, instead of drawing too hasty conclusions.

6.1.4 Analyses of the measurements and calculations made with the created system

From the results of these investigations and by the comparable graphs drawn by them, it is possible to visually analyse the effect of attenuation by the treatment table and the measuring angle dependence of the chambers of the matrix, but most of all to analyze the accuracy of the matrix as measuring device by comparing the measured doses with the calculated ones. Using the graphs, showed in image 15 in section 5.1.1, it is possible to perceive the shapes of the system and also to analyze the effects of the materials through which radiation traverses from different directions, and how these effect the graphs. So, also the properties of the calculation algorithms can be analyzed.

The angle dependence of the chambers of the matrix can be perceived by comparing the graph of the measured doses and the one measured only from the gantry angle of 0° with a relative amount of solid water. This investigation proves the measuring angle dependence of the chambers, because the graph measured only from the gantry angle of 0° with a relative amount of solid water is at the same overall level and by similar shapes with the calculated ones. However, the measured point doses using a gantry angle of 0° with a relative amount of solid water are larger than the calculated ones using the analytical anisotropic algorithm of Eclipse. This might be because there was

not set solid water in order to consider also the amount of PMMA from different directions. Anyway, the point doses calculated using the analytical anisotropic algorithm show less particularly in areas, where radiation has to traverse through the matrix and the chambers to get to the measuring point. From the investigations about making the chambers of the matrix comparable to the absolute dosimetry, it was shown that the chambers of the matrix measure a little more than the absolute chamber. This might also be a reason why the measured doses are a slightly higher than the calculated dose graphs. It is not the case with Monte Carlo algorithm of Monaco in all directions. The reason, why the calculated point doses by Monte Carlo are higher at some points than the measured ones, might be the capability of it to consider heterogeneities in matter, for example build ups, when radiation traverses from solid or liquid material into gas. Also in calculations using the Monte Carlo algorithm there are relatively large differences between point doses due to Monte Carlo variance. Due to these reasons also the accuracy of the user to record point doses in the right place from the calculated dose distributions is even more important with the Monte Carlo algorithm than with the analytical anisotropic algorithm. This can be seen also by larger changes in the graph of the Monte Carlo algorithm compared to the analytical anisotropic algorithm one in image 15.

6.2 Analyses of the Ball Test

6.2.1 Analyses of the comparisons between calculated plans

By challenging the treatment planning system to optimize challenging cases as in the ball test, there was found limitations of the optimization module. These limits are obviously very dependent on the individual case, so the most noteworthy issue in this part of the test is that the system will be able to offer information about the infeasibility of the set parameters. However, the treatment planning system will not inform the user about any infeasibility in inserted parameters, if the targets are not failed very radically. Also as seen from tables 1 and 2 in section 5.2.1, the targets, or constraints, set by the user are not durable. Of course this is a matter of parameters, but here, however, the limits of the constraint doses were set as primary, and still the limits were crossed in all cases. This shows that the calculation system is battling between the inserted targets and constraints, and calculating compromises between these challenges, if all the goals and limitations are not reachable.

By comparing the statistics of the calculated dose distributions of the ball test with tables 1 and 2, there are not significant differences in reached doses between energies 6 and 10 MV in similar plans. However, small overall issues are noticeable. Using energy of 10 MV the target doses were reached in bigger volumes of the targets in most cases. This, however, meant a little bit higher hot-spots as well. Using energy of 6 MV the absorbed doses in the constraint volume were slightly smaller. In this kind of test, where the constraint is inside the target volume, these noticed issues were impending by the different properties of depth doses between the two photon energies. By paying attention especially to the tests where the dose limits of the constraint ball were not adjusted lower than the target dose, the treatment planning system were not able to produce an objective dose to the very sides of the target especially to the last CT slices. The reason for this cannot be too tight constraint outside the target ball, because these parameters did not challenge optimization at all. The reason, therefore, might be

unattainable for the user. There should be paid attention to the issue in the clinical treatment planning process. One effective way avoiding this could be by adding a target volume with about 2 mm wider margins in all directions than the actual PTV in the optimization.

From a clinical point of view, the results of the tests slightly favour using energy of 10 MV in the treatment planning of patients with bladder cancer, because with the use of 10 MV energy, target doses were reached a little better. This effect will grow the deeper in matter the target is situated. In the pelvic area the distance to the bladder from the surface of the body is relatively greater than the distances with the created system. It seems by these investigations, that using smaller energy the absorbed doses in constraints could be kept slightly smaller, but however, this kind of challenging cases, where the constraint would be inside the target area, are not involved in the treatment of patients with bladder cancer. Obviously with higher energy the radiation which traverses through the target volume to organs at risk influence more these organs than with lower energy. However, with higher energy less monitor units are needed, and so the absorbed dose on the way to the target is smaller. In the actual treatment planning process of patients, the optimization parameters are adjusted suitable for each case by the user so that the target volume, organs at risk and interactions in matter with the used energy are taken into consideration.

6.2.2 Analyses of the comparisons between calculated and measured dose distributions

Analyses using the results of measurements made with the matrix

There was no distinct way how the chambers, which measured doses that did not pass the accuracy limits, distributed in the matrix. However, in the high gradients, there were bigger differences overall in the accuracy of the measured and calculated point doses. In these areas the average differences were about 2 - 3 %, but in point doses at chambers in the constant dose area the average differences were usually 0 - 2 %. It was also possible to recognize from the profiles, that the gradients were slightly sharper in the calculated ones. However, this observation was done only in the outer gradients of the target ball, while the remainder of the dose distribution area acted very similarly between the calculated and measured ones. Therefore, the chambers which did not pass the accuracy limits of 3 mm and 3 % were positioned quite randomly in the dose distribution area. But as it is possible to compare percentages of the passed measuring points, it is noticeable that the percentage is higher when taking into account the 225 most centrally located chambers. One reason for this might be in the calibration factor for measured dose distributions using the created system, because of the chambers' dependence on the measuring angle. The factor was adjusted using the measurement results for the middle chamber, which was irradiated from all 360° of rotation. The chambers outside the target ball were not irradiated from the direction where their accuracy is at best, from in front. So, the further away from the target the inspected chamber is, the larger the correction factor should be for it. In addition, some of the calculation parameters might affect the accuracy of the calculated dose distribution. These parameters, however, were adjusted to be in the same scales as in treatment planning for bladder cancer patients. Furthermore, the Monte Carlo algorithm of

Monaco follows Poisson's statistics which signifies that the point dose deviation gets smaller while absorbed dose gets higher.

Even though all the measured treatment plans passed the accuracy objectives, it is noticeable that equivalence between the calculated and measured dose distributions becomes a little poorer in the plans which forced the treatment planning system to struggle close to its limits. This is possible to recognize by comparing the measured dose distribution of plan R3D66% to the one of plan R3D60% with both used energies shown in table 3 in section 5.2.2. This can be noticed also by letting the treatment planning system optimize the dose distribution without considering the constraint ball inside the target one, as in plan R3D100%, in which all of the point doses passed the limitations close to the target area with both energies.

Repetitive measurements of dose distribution with plan R3D66% show that the accelerator is able to produce one plan after another accurately. It seems that the matrix had been about 1 mm in a different position after re-positioning. Possible positioning errors of about 1 mm, caused by the user while positioning the matrix using the lasers and field light, are worth taking into account while analyzing the results.

Analyses using the results of measurements made with radiochromic film and the matrix together

The most essential theme of the measurements by radiochromic film was the evaluation of the sharpness of gradients compared to the ones measured by the matrix. To make the evaluation more distinct, the measured profile graphs using the matrix are re-drawn in a different way. The middle points of the point doses measured by the chambers are connected to the next ones by graphs especially at the areas of gradients. These re-drawn graphs are shown in images 28 and 29 using black lines. It can be observed that the matrix is not capable of showing exact shapes of the gradients especially in cases of very rapid changes in dose distribution. However, by concentrating the point doses at the measurement points of the chambers, it can be discovered that at these points the measured doses correlate very well with each other. The point doses correlate very well also in other measurement areas especially by taking into account the 0.5 cm difference in measuring levels. Actually the only area where there is significant error in dose can be observed in the high dose area in the profile in image 28. By observing the isodose of the film measurement shown in image 19 in section 5.2.2, it can be double-checked, that in the same area there is a very high dose area. By evaluating the equivalence between the dose distribution overall, this inconsistent dose area may have affected by the fragility and structural discrepancies of the film [22]. There is also noticeable rapid change in dose at the very end of the profile measured by the film shown in image 29. At that area the film was destroyed because there was drawing ink inserted by the user for the film positioning. However, the equivalence in dose distributions between the radiochromic film and the matrix measured together strengthens the observations of the suitability of the created verification system for reliable dose distribution measurements.

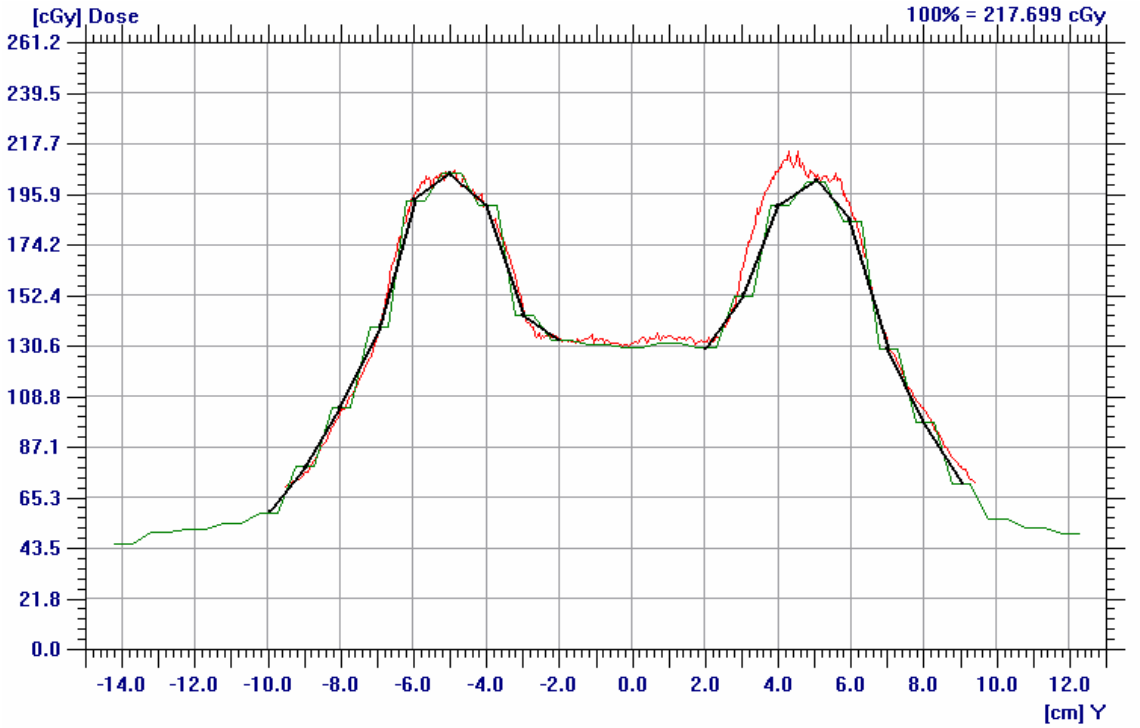

Image 28: Profiles of left to right directions of measured dose distributions of the plan R3D60%6MV. The red line signifies the measured dose profile by film, the green line the measured point doses using the chambers and the black line is connecting the middle points of the measured doses of each chamber.

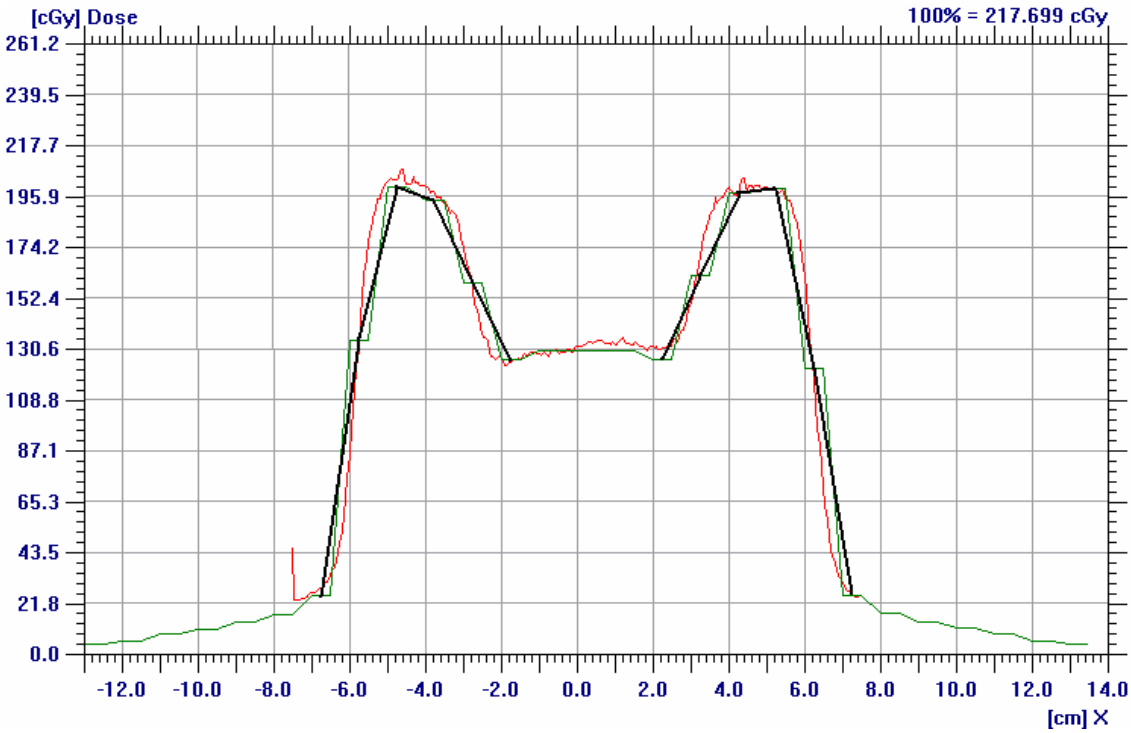

Image 29: Profiles of gantry to table directions of measured dose distributions of the plan R3D60%6MV. The red line signifies the measured dose profile by film, the green line the measured point doses by the chambers and the black line is connecting the middle points of the measured doses of each chamber.

6.3 Analyses of the VMAT treatment plan verifications with the created system

All together there were 28 clinical VMAT treatment plans measured by the created verification system during the project. The goal that 95 % of the ionization chambers of the matrix should pass the accuracy limits of 3 % and 3 mm at least inside about the area of 50 % isodose was reached in almost all the plans. The plans that did not pass this limit had however at least 93.8 % passed point doses. It was noticeable that almost all the failed chambers were in the areas of high gradients. In these areas, the accuracy of the device cannot be absolutely trusted most of all because of the gaps between the chambers. It was also estimated, that the percentage of accepted point doses inside the area of about 10 % isodose were almost as high as close to the target area. The failed point doses outside the target area had almost beyond exception smaller measured doses than the calculated ones. The reasons that measured doses were smaller relatively far away from the target area are probably the same as those discussed for the ball test. However, from a clinical point of view, it is more desirable that the measured doses outside the target volume are smaller than expected, rather than the other way around.

Also by these clinical verification measurements, the calibration factors calculated for the VMAT treatment plan verification system seem to be correct. It was noticeable that within the treatment plans, which were measured also by the quality assurance mode without gantry rotation, the dose distributions areas where the accuracy limits were not reached correlated very well to the measurements done with gantry rotation. In addition, a concern that the common calibration factor for the measured dose distributions might be too strong for some chambers and too weak for some chambers, indicating to have been too strong. By investigating the areas of dose distributions, which did not pass the accuracy limits, there was not found evidence that the direction of radiation into the area would have been the cause for the inaccuracies. This was investigated by comparing the measurement results using the original plan to the ones using quality assurance mode without gantry rotation. In addition, it was investigated using the Monaco treatment planning system to analyze the plan segment by segment, in order to check are the absorbed doses in a certain irradiated volume from certain directions much higher than from the other directions. This way can be analysed have the correlation factors for eliminating the effect of attenuation by the treatment table and the angle dependence of the chambers been appropriate for some particular areas of chambers in each case.

Using these experiences, it seems that the created verification system is a reliable tool for the VMAT treatment plan verification process. However, the long-term experiences and, furthermore, even more specific investigations using the system are desired in order to use only the created system in the VMAT treatment plan verification process. Especially the experiences on suitability of the common calibration factor for the measured dose distributions in the VMAT treatment plans, in the cases where small segments are used, and so the absorbed doses might include the irradiation only from particular directions, should be collected.

6.4 Analyses of the CBCT equipment in patient positioning

Using the results of the investigations, it is possible to state that the CBCT equipment is suitable for the clinical use in patient positioning. The quality of the images was sufficient for visualizing the internal organs, the accuracy of the automatic matching with the grey-value algorithm was shown precise and the recommended movements using the CBCT system and the Hexapod treatment table were shown also accurate. In addition, the possibility to create imaging presets was introduced. The created presets were investigated in order to assure also their reliability in the clinical environment. Using the results, the presets Bladder A, B and C were introduced for the clinical use.

6.4.1 Analyses of the automatic matching accuracy between the presets

From the results of the automatic matching, done by using the CBCT images with the presets Prostate M10, Prostate M10 Fast and the created ones, the parameters of these presets not affected the accuracy of the automatic matching. The equivalence between the original ones indicates that by decreasing the number of the frames to 330 from 660, and furthermore, the imaging time to 60 seconds, not affect the automatic matching accuracy even though visually the image quality suffers a little. Moreover, as long as the image quality is visually good enough for the clinical use, decreasing the tube voltage, current or time, do not affect the accuracy of the automatic matching. Using the manual re-matching, the adjustments done using the automatic matching were shown precise in all the cases with every preset. Using the manual matching, the matching was not possible to make as precisely or at least not as quickly, as using the automatic matching.

6.4.2 Analyses of the irradiated doses using the presets and clinical significance of the results

Using the created presets in imaging, the irradiated doses decreased comparing to the irradiated doses using the original presets, as it was desired. Using the created preset Bladder C, the absorbed dose in the maximum point on the surface of the phantom was less than 15 % of the dose using the preset Prostate M10 and less than 25 % of the dose using the preset Prostate M10 Fast. In practise, for example in the treatment of 35 fractions, in which the CBCT imaging is performed before and after each fraction, using the created preset Bladder C, the absorbed dose in the maximum point on the surface is in total 0.315 Gy which is 2.184 Gy less than with the preset Prostate M10 and 0.980 Gy less than with the preset Prostate M10 Fast. Using these numbers in analyses, it has to be kept in mind that the CT thorax phantom is not equivalent by shapes and matter with the patients, and that every patient is different by the body shapes. However, these results are suggestive. Furthermore, in order to use, for example, the preset Bladder C in imaging of a patient, the image quality has to be sufficient in the case.

It can be discussed that how worthwhile it is to decrease the irradiated dose of the CBCT imaging, because the relation of the decrease is relatively small by comparing to the total treatment doses. However, one of the main goals in the radiation therapy is to be able to treat the target with the planned dose with as little absorbed dose as possible

in the other parts of the body. So, even small dose decrease in the healthy tissues is preferable. In the treatment of patients with bladder cancer the CBCT imaging before the treatments is essential, but the worth of the imaging always after the fractions can be discussed. With the absorbed dose caused by using the created preset Bladder C, the decision whether or not to perform CBCT imaging also after the fractions can be done easier.

6.4.3 Accuracy and reliability of the automatic matching with grey-value algorithm

From the results of the investigations which considered only one directional error at a time, it was noticed that all the recommended position corrections were not over than the exactitude of the setting accuracy of the phantom by the user. In addition, there was no differs in the accuracy of the recommendations between the smaller and bigger made up error in the same direction. With the setting accuracy of the phantom it is not possible to investigate the capability of the automatic matching algorithm with the minimum scale of the recommendations. However, this investigation was accurate enough to analyze the accuracy and reliability of the automatic matching in the significant scales for patient treatment, in which the automatic matching using grey-value algorithm seems to work well.

The exact realization of the position error in multiple directions was not even as precise as to one direction at a time. It was, however, also accurate enough to make possible analyses of the accuracy of the automatic matching in the significant scales for patient treatment. Using the 0.5 cm and 0.5° errors in four directions together, the position correction recommendation was reasonable by using the automatic matching. The result seemed precise using manual matching. In the case where the phantom was positioned 2.0 cm in two of the translational directions and 2.0° in two of the rotational directions away from the isocenter, the recommendations using the automatic matching were obscure. However, using manual matching, the localization image was moved close to the exact position in the translational directions and then re-using automatic matching, the recommendations were more expected. The result seemed precise by reviewing the images. This case is shown in table 8. The results of the case indicate that the positions between the localization and reference images might have been too far from each other for the automatic matching algorithm. However, by this one obscure result in these investigations, it is not possible to claim a specific reason for the confusion in the automatic matching or to draw conclusions about uncertainty in the work of it. In order to do so, there should be done an extensive investigation and also get acquainted with the matching algorithm. Furthermore, in order to investigate the accuracies of the automatic matching precisely in submillimetre scale the phantom should be attached to a micrometer adjustment device the way it would not disturb the imaging. In addition, even though the box of expanded polystyrene is suitable for keeping the interior stable, the material of the box is a little soft outside, which might lead to inaccuracies while adjusting the phantom repeatedly. However, using the results of these investigations, even though the automatic matching worked precisely in all the other parts of the investigations, it is reasonable to recommend reviewing the results of the automatic matching manually before performing the position corrections and delivering the treatment of patients.

Table 8: Recommendations using the automatic matching before and after manual adjustments in the case of set error of 2.0 cm in two of the translational directions and by 2.0° in two of the rotational ones.

Directions of the displacement	The size of the displacement	The size of the recommendation	The size of the recommendation after manual adjustment
tx, ty, rx and rz	tx = 2.00 cm rx = 2.0° ty = 2.00 cm ry = 0.0° tz = 0.00 cm rz = 2.0°	tx = 2.12 cm rx = 2.6° ty = 1.08 cm ry = 346.9° tz = 0.92 cm rz = 5.5°	tx = 2.02 cm rx = 2.2° ty = 1.89 cm ry = 0.1° tz = 0.00 cm rz = 1.8°

6.4.4 Reliability of positioning accuracy of Hexapod treatment table using the CBCT system

In four of the five cases the recommendations for the patient repositioning were not more than 0.02 cm or 0.2° as shown in table 7 in section 5.4.3. Even though these recommendations are one step higher than the steps of the scale, they are not alarming, because the size of the recommendations did occur only to one direction out of six in a case. Moreover, those sizes of errors in the patient positioning are clinically insignificant. However, the bigger position recommendations in one case are a little concerning. The recommendations of 0.03 cm and 0.07 cm in two of the translational directions are not yet alarming clinically, but the error of 0.8° in target position is clinically undesired especially in cases, where organs at risk are next to the PTV. The position error was noticeable using manual matching after using the automatic matching with the first CBCT images. Also the recommendations which the software did suggest after using automatic matching with the second CBCT images indicate that the fault of the error was caused by the automatic matching instead of the system controlling movements of the Hexapod treatment table. Using this investigation, there is no reason to make alarming conclusions about the unreliability of the algorithm of the automatic matching. However, also using these investigations, it is recommended to double-check manually the result of the automatic matching. And even though the movement of the treatment table was shown clinically accurate using this investigation, it is also recommended to follow the treatment table realizing the desired movements.

6.5 Analyses of the technical aspects of radiation therapy of patients with bladder cancer using the first clinical experiences with the introduced equipment and instructions

6.5.1 Suitability of the instructions

The work-flow of the complete treatment process was suitable with all the five bladder cancer patients. Each part of the process was realized essentially similarly, and the treatment of patients were delivered as planned. There were, however, special features in the individual cases, which make it reasonable to analyze the possibilities for some alternatives in the work-flow and suggest possible improvements for the future.

In two cases there were not big changes in the bladder volume or shape between the four planning CT images. In these kinds of cases the CT images could be analyzed after

three CT images, and if there is not relatively large shape changes in the bladder, the fourth image could be performed after a longer period of time. However, because the patients are instructed to urinate just before every fraction, in these two cases as in all of the five, the volumes of the bladders during the treatment were not larger than the largest PTVs.

The work-flow of the treatment planning and the parameters used in the Monaco treatment planning system were suitable with the five patients in the ranges introduced in the template. Using these experiences it seems that with 10 MV photon energy it is possible to reach better dose coverage in the PTV while minimizing the absorbed dose in organs at risk comparing to the use of 6 MV photon energy. The values of the other parameters are, however, important to consider individually in every case and concentrate on evaluating and affecting the optimization in each case. In the cases where it was not necessary to achieve planned dose in the edges of the PTV, the dose limits of the constraints could be set very strict in the optimization. But in the cases where the full dose coverage of the PTV was necessary, like in the one shown in image 22 in section 5.5, using an extra contour with margins of two millimetres around PTV assured the dose coverage also in the edges of the PTV. The extra contours could be also created for constraints, and use them in the optimization in order to try to minimize the absorbed dose in organs at risk. For example in the partial bladder cases the healthy part of the bladder wall could be contoured and set as a constraint instead of setting the complete bladder except the part in PTV as a constraint like in the first clinical cases. This could be done because large part of the bladder is urine which is not relevant to try to protect, but the protection of it challenges the optimization in vain. Furthermore, the individual shapes and sizes of the patients are worth to consider in the treatment planning. One of the five patients was obese, which made it more challenging to produce sufficient dose distribution in the PTV, and the limits of the absorbed doses in the constraints had to be loosened, and the treatment time was forced to be extended. In these kinds of cases with the 15 MV photon energy, which is going to be configured for the clinical use in the near future, it might be possible to achieve the planned doses in PTV easier. On the other hand, with increasing the used energy to 15 MV in the VMAT treatment plans, it might raise the amount of neutrons so high that the absorbed doses in the organs at risk might rise too much.

The image quality of the CBCT images made possible to detect the shape and position of the bladder. Using the introduced work-flow, it was suitable to determine individually appropriate imaging preset for every patient. For two of the patients the quality of the images performed using the preset Bladder C was sufficient. That preset was used in imaging also after the fractions with the patients as well with other two ones. However, with these two patients the quality of the images performed using the preset Bladder A was sufficient for the patient positioning. With these two patients the used preset before the fractions were changed to the preset Bladder B after 10 fractions with one and 15 with the other, because decrease of the lipiodol volume reduced artefacts in the images. Using this observation, and by considering the image quality which provides the reliable visualization of the bladder wall, it is possible to question the use of the lipiodol in the complete bladder cases. In the partial bladder cases the use of the lipiodol is still worthwhile in order to determine the exact place of the tumour using the CBCT imaging. With the obese patient the image quality was good enough for the reliable bladder localization only using the preset Prostate M10. Therefore, with

the patient the imaging after the fractions was made only after first five fractions and after that only once a week using the preset Prostate M10 Fast.

The patient positioning using the automatic matching with the grey-value algorithm was precise almost exceptionally, and the capability to use also the rotational position corrections was observed useful. However, there were randomly situations where the results of the automatic matching were not correct. Most of these times the obscure recommendation of the software was easily noticeable, because the localization image was not set even close to the reference one. In these cases there was either relatively large change in the volume of the rectum or displacements in the bladder and the closest bowels next to it compared to the situations in the reference image. In these cases the matching was made manually. Using these experiences, it is recommended to review the results of the automatic matching, and also to consider the size and place of the automatic matching volume in each case.

6.5.2 Analyses of the clinical experiences with the introduced equipment and comparisons between these to experiences with previously used equipment

One of the novelties introduced using the new linear accelerator for the treatment of patients with bladder cancer in HUCH was the capability of the VMAT. Even though the treatment planning of the VMAT is realized with the inverse planning as in the IMRT, the possible advantages of realizing the treatment with a single arc and using the biological optimization with the Monaco treatment planning system were analyzed. Furthermore, the possibility for the patient positioning in the six degrees of freedom was introduced, and the first clinical experiences were gathered. As with the previous treatment method, the CBCT imaging was used for the on-line localization of the bladder. However, the benefits of the CBCT system of Xvi are also discussed in this section.

The treatment planning using the biological optimization with the treatment planning system Monaco was considered practical especially because of the constant interaction between the software and the user during the optimization. The possibilities to set the organs as serial or parallel by their biological properties and to define the tolerance of the organs for irradiation were also considered advantageous. However, it is the formed dose distribution and especially the reliability of it to be delivered as calculated, which matters in the end. In order to evaluate the dose distributions calculated using the introduced treatment planning strategies, also three of the cases were planned with the previously used methods and equipment which are introduced in section 2.2. Two of the cases were partial bladder ones using 6 MV energy in the VMAT treatment plans. One of these cases is shown in image 30. In the third case the complete bladder was treated using 10 MV photon energy in the VMAT treatment plan. The dose distributions of each case were analyzed using isodoses and DVHs. The attention was focused on the 95 % isodose coverage in the PTV compared to the absorbed doses in the rectum, the bowels, the hip bones, the parts of the bladder outside the PTV and the body. In the partial bladder cases the dose coverage in the PTV were about 2 % less in the VMAT treatment plans with 97 – 98 % coverage. In the complete bladder case the PTV dose coverage was 100 % in the VMAT treatment plan, but about 2 % less in the IMRT treatment plan. However, in all the treatment plans the average absorbed doses in all of the organs at risk were at least a little less in the VMAT treatment plans. Using

these evaluations, it seems that with the biological optimization and the use of the VMAT, it is possible to reduce the irradiated volumes of the organs at risk, with acceptable PTV dose coverage. Furthermore, the overall irradiated volumes of the body were less in all the cases. Also with comparing the dose distributions, it was noticeable that the gradients were sharper in most of the directions. These evaluations were done with comparing for example the 80 % isodoses. In addition, the irradiated small dose volume of body seems to be smaller by the VMAT treatment planning, which can be evaluated with comparing, for example, the 20 % isodoses. Also these observations can be seen in image 30. The results of the investigations, which indicate that the Monte Carlo dose calculation is even more accurate than the calculations made using kernel based methods especially in the heterogeneous volumes, support relying on these observations [15]. However, it is rather challenging to analyze the treatment plans made using two softwares with different calculation algorithms. Also the experience of the user to use the equipment might have influenced to the resulted outcomes. Therefore, there should be more investigations done and experiences gathered, and also consider the equivalence between the calculated and delivered dose distributions using both of the systems, before stating these evaluations authentic.

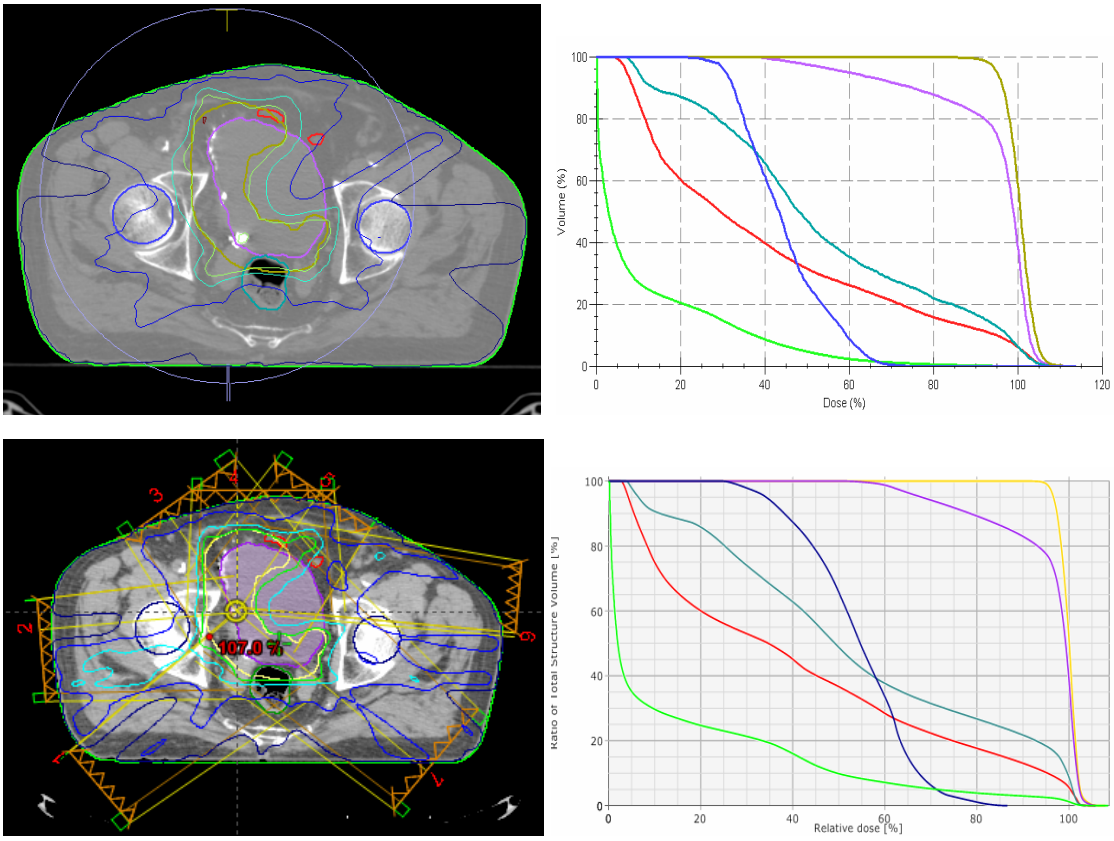

Image 30: The same partial bladder case planned using Monaco with VMAT (on top) and using Eclipse with IMRT (under). In both of the treatment plans the isodoses are represented with the same colours; dark red is 107 %, green 95 %, turquoise blue 80 %, blue 50 % and dark blue 20 %. In both of the DVHs yellow indicates the PTV, violet the bladder, turquoise blue the rectum, red the bowels, dark blue the hip bones and green the body.

The total treatment time including the patient positioning with the six degrees of freedom and the CBCT imaging also after the treatment was almost without exceptions 20 – 25 minutes, which is the same as with the treatment using the previous method in

HUCH. The patient positioning using the Hexapod treatment table was found practical and beneficial especially because the rotational corrections were required as often as the translational ones in these first five bladder cancer cases with the introduced equipment. In addition, the possibility to perform the CBCT imaging also after the fractions with relatively good image quality enough without significant extra irradiated dose can help following the treatment with determining the movements of the organs during a fraction, and so to contemplate possible improvements for the target planning. With the previous method the dose delivery time was five minutes by average, so using single arc there is no profit in the treatment time with these clinical experiences. However, with a single arc the delivery time is constant, because the working paces of the radiographers do not matter as much in the realization of a VMAT treatment plan as in the delivery of seven IMRT fields. The average amount of monitor units decreased from about 1000 - 1100 monitor units irradiated with the IMRT treatment plans to 700 – 900 monitor units irradiated with the VMAT treatment plans. [7]

With comparing the performance of the CBCT system of Xvi to the previously used CBCT system of OBI in treatment of patients with bladder cancer, there are noticeable improvements in the image quality, but also in the possibility to decrease the irradiated dose of the imaging. The OBI system was used with two different settings for the imaging of bladder cancer patients, which both performed the imaging in about 60 seconds. The decision about which one to be used in the imaging have been made with the quality of the images performed in the individual cases. Using the results of the dose measurements made in HUCH in 2009 with a CT head phantom and measuring also the absorbed doses using the introduced presets of Xvi with the same phantom, it is possible to compare the irradiated doses produced by the CBCT imaging with the two systems. The results of the measurements are shown in table 9. Using these results, it is possible to calculate that with one of the settings, named here as Setting A, of OBI the irradiated dose is a little less than with the preset Prostate M10 of Xvi, and with the other setting, named here as Setting B, of OBI the dose is approximately the same as with the preset Prostate M10 Fast. The irradiated dose with the preset Bladder C in Xvi is about 25 % of the irradiated dose using Setting B of OBI. In the CBCT images of the OBI the field of view is larger, and so is the irradiated volume of the body. The image quality was significantly better in the CBCT images performed using the original presets of the Xvi than with the settings used in the OBI, especially if considering the visibility of the intestines. Also in cases where the rectum or bowels contain a lot of gas, the quality of the CBCT images performed with the OBI suffer strong artefacts, which have not noticed to be a problem with the Xvi. In the image 31 is shown a CBCT image performed using Setting A of the OBI. It can be compared with the images 23 - 27 shown in section 5.5, in which there are shown images performed with the presets of the Xvi used in the bladder cases with the same size of a patient as in image 31.

Table 9: The measured irradiated doses with the CT head phantom in the middle and on the surface of the phantom using three presets of the Xvi and two settings of the OBI used in bladder cases in HUCH.

Preset or Setting:	Dose at Isocenter (mGy)	Dose on surface (mGy)
Prostate M10 / Xvi	65.0	67.5
Prostate M10 Fast / Xvi	33.5	35.2
Bladder C / Xvi	8.5	9.0
Setting A / OBI	52.0	55.0
Setting B / OBI	33.0	37.0

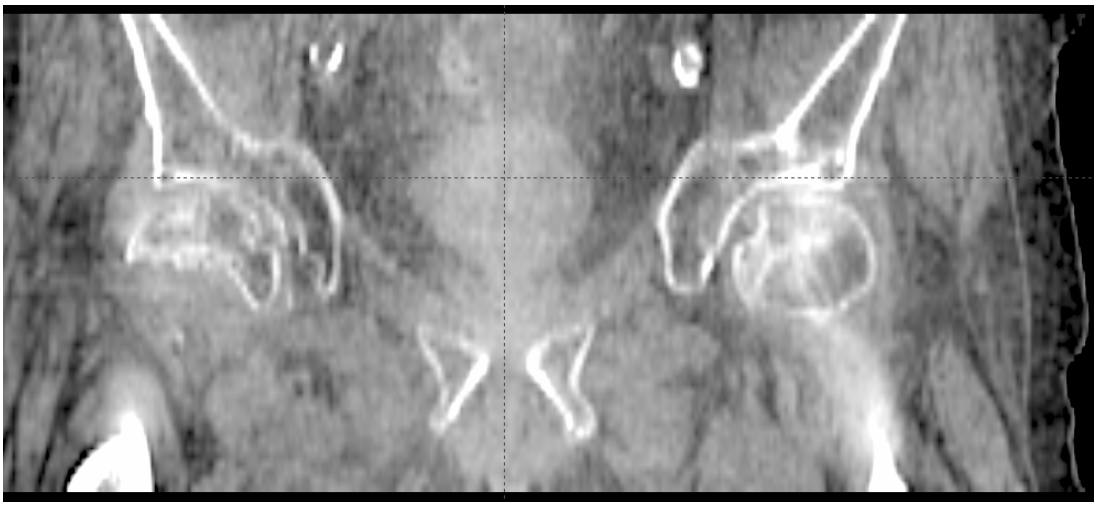

Image 31: Coronal view of a CBCT image performed using Setting A of the OBI.

7 Conclusions

All the goals of the project were reached. The verification system for the VMAT treatment plans was created, and it was found to be a reliable and suitable tool for the dose distribution measurements. Using the created system, the equivalence between the calculated VMAT treatment plans with the treatment planning system Monaco and the delivered plans with the linear accelerator Elekta Axesse were configured using the photon energies of 6 and 10 MV. The new presets were created for the CBCT imaging, which were found to be clinically worthwhile by their capability to perform high quality images with relatively small irradiated doses. The operations of the CBCT system with the Hexapod treatment table were determined precise as well with the created presets as the original ones. In addition, the suitable template for the VMAT treatment planning using Monaco treatment planning system was introduced. Using the results of the investigations on introduced equipment, the instructions for the radiation therapy process of patients with bladder cancer; including the strategies for VMAT treatment planning, CBCT imaging and patient positioning, were created.

During the project the experiences of daily clinical work were gathered. There came up several issues related on working with the equipment, which had to be solved. Using

the solutions and experiences, clinical work with the equipment became more practical. For example, instructions in order to use the Hexapod treatment table and the CBCT system overall were introduced in HUCH. Using the experiences of creating the imaging presets in the Xvi, new presets for clinical use with the other cases as well were considered. For example, new presets were created also for imaging the prostate carcinoma patients which have gold seeds inserted in the prostate. Based on the preset Prostate Seed, the new presets were created to perform images, in which also the walls of the prostate are clearly visible without exposing the patient for greater amount of radiation. Furthermore, the experiences gathered during the project of the work with the treatment planning system Monaco were shared in the clinic, and used for improving the planning strategies also for the treatment of patients with other carcinomas.

The results of the investigations during the project construct strong basis for some further investigations. The investigations done in order to create the verification system for VMAT treatment plans could be continued in extremely precise level. Instead of using the calibration factor for the complete measured dose distribution, the calibration factors could be defined individually for the measured point doses in particular situations. It is not possible, however, to insert different calibration factors for each chamber of the matrix, but with the pre-determined factors for the different situations and with examining the dose distribution, the analyses of the dose distributions could be made specifically for the different point doses. In addition, the effect of attenuation by the treatment table could be investigated using various measuring points above the treatment table in order to evaluate the effects in different kinds of treatments. Furthermore, it would be beneficial to investigate the function accuracy of the CBCT system, especially using the automatic matching, in depth. In those investigations should be concentrated also on the operational principles of the automatic matching algorithms in order to develop them instead of just examining their performance in different cases. The created internal organ phantom was discovered suitable for the CBCT investigations. However, in order to use the phantom in very specific investigations on the CBCT system repositioning accuracy with the Hexapod treatment table the capability of positioning it by the user should be able to be done reliably and extremely accurately. Moreover, it is desirable to reduce the treatment times of the treatment of patients with bladder cancer. Using the treatment planning system Monaco, the users should gather the experiences and try to focus on finding the suitable parameters for the optimization in order to decrease the treatment times while maintaining the qualities of the dose distributions. In addition, the treatment of the first five patients with bladder cancer using the equipment could be analyzed more precisely. The quality of the CBCT images performed using the Xvi make possible to reconstruct the actually delivered dose distributions with the treatment planning system Monaco. For example, the irradiated volume of the bowels could be calculated. Using the data, the benefits of using the equipment in treatment of bladder cancer patients could be analyzed by comparing the data with the ones calculated from the treatment of bladder cancer patients with the previously used equipment in HUCH by Tuomikoski et al [7]. The CBCT images which were performed after the fractions could be also taken into the analyses. Using those images, it could be investigated is there some sort of statistical changes in the bladder volume and shape during the fractions. Moreover, using the CBCT images, it could be reconsidered sufficient margins for the PTV in the treatment of bladder cancer patients with the new treatment unit.

In the near future also the 15 MV photon energy of Elekta Axesse is going to be introduced for the clinical use. The configuration process can be done using the created verification system with the introduced work-flow. Furthermore, the verification system can be adjusted for the dose distribution measurements with the other linear accelerators as well. This could be beneficial especially if the prospective new accelerators for HUCH in couple of years are capable for VMAT. It is also interesting to receive new versions of the used equipment. For example, there are high expectations that using the expected new version of Monaco treatment planning system it is possible to plan the treatment of patients even more practically. However, the work using the introduced equipment is in the very beginning of their life cycles. The experiences of the users with the introduced equipment and methods in the radiation therapy of patients with bladder cancer are essential to be gathered in the long run in order to keep the wheels of improvements running.

8 References

[1] Tenhunen. 2007. Sädehoidon Fysiikka ja Tekniikka. Opetusmoniste. The number of pages: 189. Department of Oncology, HUCH.

[2] Khan. 2010. The Physics of Radiation Therapy. Fourth Edition. Philadelphia. Lippincott Williams and Wilkins, Wolters Kluwer business. ISBN 978-0-7817-8856-4. The number of pages:531.

[3] Yu et al. 2011. Intensity-modulated Arc Therapy: Principles, Technologies and Clinical Implementation. Physics in Medicine and Biology. Vol.56, p.R31-R54. doi:10.1088/0031-9155/56/5/R01

[4] Bortfeld and Webb. 2009. Single-Arc IMRT? Physics in Medicine and Biology. Vol.54, p.N9-N20. doi:10.1088/0031-9155/54/1/N02.

[5] Otto. 2008. Volumetric Modulated Arc Therapy: IMRT in a Single Gantry Arc. Medical Physics. Vol.35, p.310-317. doi:10.1118/1.2818738.

[6] Mihaylov et al. 2010. Biological Optimization in Volumetric Modulated Arc Radiotherapy for Prostate Carcinoma. International Journal of Radiation Oncology Biology Physics. Vol.16, iss.5, p.1-7 doi: 10.1016/j.ijrobp. 2010.06.020.

[7] Tuomikoski et al. 2011. Adaptive Radiotherapy in Muscle Invasive Urinary Bladder Cancer – an Effective Method to Reduce the Irradiated Bowel Volume. Radiotherapy and Oncology. Vol.99, iss.1, p.61-66. doi:10.1016/j.radonc. 2011.02.011

[8] Halperin et al. 2008. Principles and Practise of Radiation Oncology. Fifth edition. Philadelphia. Lippincott Williams and Wilkins, Wolters Kluwer Business. The number of pages: 2106. ISBN-13:978-0-7817-6369-1.

[9] Pos and Remeijer. 2010. Adaptive Management of Bladder Cancer Radiotherapy. Seminars in Radiation Oncology. Vol.20, iss.2, p.116-120. doi:10.1016/j.semradonc.2009.11.005.

[10] Elekta. 2010. Elekta Axesse Specifications and the Linear Accelerator Specific Documentation, 358-090904-318. Department of Oncology, HUCH.

[11] Meyer et al. 2007. Positioning Accuracy of Cone-beam Computed Tomography in Combination with a Hexapod Robot Treatment Table. International Journal of Radiation Oncology Biology Physics. Vol.67, iss.4, p.1220-1228. doi:10.1016/j.ijrobp.2006.11.010.

[12] Wilbert et al. 2010. Semi-robotic 6 Degree of Freedom Positioning for Intracranial High Precision Radiotherapy; First Phantom and Clinical Results. Radiation Oncology. Vol.5, iss.42, p.1-11. doi:10.1186/1748-717x-5-42.

[13] Meeks et al. 2005. Optically Guided Patient Positioning Techniques. Seminars in Radiation Oncology. Vol.15, iss.3, p.192-201. doi:10.1016/j.semradonc. 2005.01.004.

[14] Wu et al. 2002. Optimization of Intensity-modulated Radiotherapy Plans Based on the Equivalent Uniform Dose. International Journal of Radiation Oncology Biology Physics.Vol.52, iss.1, p.224-235. doi:10.1016/s0360-3016(01)02585-8.

[15] Fotina et al. 2009. Advanced Kernel Methods vs. Monte Carlo-based Dose Calculation for High Energy Photon Beams. Radiotherapy and Oncology. Vol.93, iss.3, p.645-653. doi:10.1016/j.radonc.2009.10.013.

[16] Elekta CMS Software. 2010. Monaco Training Guide 2.0.3. CMS GmbH, Freiburg, Germany. Document number: LTGMON0203. Part number: 98961. Department of Oncology, HUCH.

[17] International Atomic Energy Agency (IAEA). 2000. Absorbed Dose Determination in External Beam Radiotherapy. Technical Reports No. 398. STI/DOC/010/398. IAEA. Vienna, Austria.

[18] IBA-Dosimetry. 2011. Blue Phantom^2 with Omni-Pro-Accept (V7). IBA Dosimetry GmbH. 25.4.2011. http://www.iba-dosimetry.com/sites/default/files/ ressources/Brochure_Blue%20Phantom2.pdf

[19] PTW. 2011. 2D-Array seven29 with 729 Ion Chambers. PTW Freiburg GmbH. 30.5.2011. http://www.ptw.de/2d-array_seven29.html?&cId=3510

[20] IBA-Dosimetry. 2011. Matrix detectors. IBA Dosimetry GmbH. 31.5.2011. http://www.iba-dosimetry.com/complete-solutions/radiotherapy/imrt-igrt-rotational-qa/matrixxes

[21] International Specialty Products. 2009. Gafchromic EBT2 Self-developing Film for Radiotherapy Dosimetry. ISP International Specialty Products. NJ, USA. 2.5.2011. http://online1.ispcorp.com/_layouts/Gafchromic/content/products/ ebt2/pdfs/GAFCHROMICEBT2TechnicalBrief-Rev1.pdf

[22] Butson et al. 2003. Radiochromic Film for Medical Radiation Dosimetry. Materials Science and Engineering. Vol. 41, iss. 3-5, p.61-120. doi:10.1016/s0927-796x(03)00034-2.

[23] Van Esch et al. 2002. Acceptance Tests and Quality Control (QC) Procedures for the Clinical Implementation of Intensity Modulated Radiotherapy (IMRT) Using Inverse Planning and Sliding Window Technique: Experience from Five Radiotherapy Departments. Radiotherapy and Oncology. Vol.65, iss.1, p.53-70. doi:10.1016/s0167-8140(02)00174-3.

[24] Poppe et al. 2006. Two-dimensional Ionization Chamber Arrays for IMRT Plan Verification. The International Journal of Medical Physics Research and Practise. Vol.33, iss.4, p.1005-1015. doi:10.1118/1.2179167.

[25] PTW. 2010. Acrylic and RW3 Slab Phantoms. PTW Freiburg GmbH. 23.4.2011. http://www.ptw.de/acrylic_and_rw3_slab_phantoms0.html

[26] STUK – Säteilyturvakeskus / Radiation and Nuclear Safety Authority of Finland. 2009. Calibration certificate of Ionization chamber Farmer NE 2571, serial number 1840. Department of Oncology, HUCH.

[27] Kosunen et al. STUK – Säteilyturvakeskus / Radiation and Nuclear Safety Authority of Finland. 2005. Sädehoidon Annosmittaukset, Ulkoisen Sädehoidon Suurenergisten Fotoni- ja Elektronisäteilykeilojen kalibrointi. Vantaa. Dark Oy. 29 pages. STUK-STO-TR1. ISBN: 951-712-928-9.

[28] Thompson and Martinson. 1993. Matematiikan käsikirja. Helsinki – Tampere. Kustannusosakeyhtiö Tammi ja DTP-partners Oy. The number of pages: 426. ISBN:951-31-0028-6.

[29] PTW. 2010. LinaCheck Monitor Test Device. PTW Freiburg GmbH. 23.4.2011. http://www.ptw.de/linacheck_monitor_test_device.html

[30] Vidar. 2011. DosimetryPRO Advantage Densiometer. Vidar Systems Corporation. 23.4.2011. http://www.vidar.com/film/dosimetrypro-advantage-red.html.

[31] Chai et al. 2010. Behaviour of Lipiodol Markers During Image Guided Radiotherapy of Bladder Cancer. International Journal of Radiation Oncology Biology Physics. Vol.77, iss.1, p.309-314. doi:10.1016/j.ijrobp.2009.08.019.

[32] Landberg et al. International Commission on Radiation Units and Measurements. 1993. International Commission on Radiation Units and Measurements Report 50: Prescribing, Recording and Reporting Photon Beam Therapy. Maryland, U.S.A. Library of congress cataloguing-in-publication data. Second series. The number of pages: 71. ISBN:0-913394-48-3.

[33] Spezi et al. 2005. Characterization of a 2D Ion Chamber Array for the Verification of Radiotherapy Treatments. Physics in Medicine and Biology. Vol.50, iss.14, p.3361-3373. doi:10.1088/0031-9155/50/14/012.

Appendix A

The instructions for the radiation therapy process of the bladder cancer patients in Helsinki University Central Hospital. Department of Oncology, HUCH.

Virtsarakkosyövän kuvantaohjattu adaptiivinen sädehoito (IGART)

Tässä ohjeessa esitettävää hoitotekniikkaa käytetään T2-T4aN0 -virtsarakkosyövän kuvantaohjatussa adaptiivisessa sädehoidossa (IGART = image-guided adaptive radiotherapy) potilailla, jotka eivät sovellu kystektomiaan. Sädehoitoa edeltävinä tutkimuksina on virtsarakon MRI ja/tai varjoainetehosteinen TT. Lisätutkimuksina voidaan käyttää kystoskopiaa ja lipiodol-merkkausta niihin soveltuville potilaille. Annossuunnittelu-TT (TTA) suoritetaan natiivikuvauksena 0, 20, 40 ja 60 minuuttia virtsarakon tyhjennyksestä (miktion jälkeen potilaalle juotetaan 8 dl vettä). TT-simulointi (TT-SIM) suoritetaan 1. TTA-kuvauksen yhteydessä. Virtsarakon seinämään voidaan kuvantaohjausta varten implantoida röntgenpositiivista merkkiainetta (lipiodol) rakon päivittäisen paikantamisen helpottamiseksi kartiokeilakuvauksessa (CBCT:ssä). Tästä johtuen voidaan ohjeessa kuvattua tekniikkaa soveltaa ainoastaan kiihdyttimessä, joka on varustettu CBCT-laitteistolla. Linac 3:ssa hoidettavien potilaiden IMRT-hoidon suunnittelu ja toteutus on esitetty kohdassa A). Linac 6:ssa hoidettavien potilaiden VMAT-hoidon suunnittelu ja toteutus on esitetty kohdassa B).

Kohdealueet:

PTV 1 (punainen):	Virtsarakko 1 + marginaali
PTV 2 (sininen):	Virtsarakko 2 + marginaali
PTV 3 (vihreä):	Virtsarakko 3 + marginaali
PTV 4 (keltainen):	Virtsarakko 4 + marginaali

Mahdollisten booster-suunnitelmien kohdealueet:

PTV Booster 1 (punainen):	Booster-alue 1 + marginaali
PTV Booster 2 (sininen):	Booster-alue 2 + marginaali
PTV Booster 3 (vihreä):	Booster-alue 3 + marginaali
PTV Booster 4 (keltainen):	Booster-alue 4 + marginaali

Kriittiset rakenteet:

Kolmiulotteinen rajaus, annosjakaumatarkastelu sekä annostilavuushistogrammit:

- mahdollinen virtsarakon säästettävä osa
- peräsuoli
- suolisto (**B**owels **S**egment & **I**ntestinal **C**avity)
- lonkkanivelet

Tyypillisiä fraktiointeja:

PTV1-4: yhteensä 25 x 1,8 Gy, 5 fr./viikko
PTV booster 1-4: yhteensä 10 x 2,0 Gy, 5 fr./viikko. Kokonaisannos:65 Gy

PTV1-4: yhteensä 22 x 2,0 Gy, 5 fr./viikko
PTV booster 1-4: yhteensä 10 x 2,0 Gy, 5 fr./viikko. Kokonaisannos:64 Gy

PTV1-4: yhteensä 21 x 2,5 Gy, 5 fr./viikko. Kokonaisannos:52,5 Gy

A) Linac 3

IMRT-suunnittelu Eclipse:llä

Suunnittelussa huomioitavaa:

a) CBCT-kuvausta varten kannattaa luoda oma hoitojakso (course; esim. ”CBCT”). Siinä TT-SIM:n isosentripisteeseen lisätään suunnitelma ”CBCT”, joka koostuu asetuskentästä ja teknisistä syistä lisättävästä hoitokentästä. Hoitokenttää ei kuitenkaan todellisuudessa tule koskaan hoitaa, ja sen annokseksi asetetaan pieni luku (esim. 0,01Gy ≅ 1 MU).

b) Todellisia hoitokenttiä varten luodaan oma hoitojakso (course; esim. ”IGART”). Siinä TT-SIM:n isosentripisteeseen tehdään neljä suunnitelmaa ”RAKKO_punainen”, ”RAKKO_sininen” jne., joita käytetään virtsarakon päivittäinen täyttöaste huomioiden.

Kenttäjärjestely:
Potilas selällään
Isosentripiste TT-SIM:n mukaisesti: Pituus: PTV:n keskellä
Leveys: Keskilinja
Korkeus: PTV:n keskellä

Energia: 6 – 15 MV.
Kenttäkoko: PTV#+0.6 cm.
Suojat: PTV#+0.6 cm, outside.

Virtsarakkosyövän sädehoidon suunnittelussa voidaan tilanteesta riippuen käyttää joko FIMRT- tai IMRT-tekniikkaa. Hoitotekniikan valinnassa voidaan soveltaa seuraavia ohjeita: ”Prostatan sädehoidon annossuunnittelu” ja ”Lantion alueen IMRT-hoidot”. Mikäli hoitotekniikan valinnassa päädytään IMRT-hoitoon, yleensä 5-7 kenttää (ei kuvauskenttiä) tuottaa sopivan annosjakauman. Tällöin kenttäjärjestely voi olla esim. seuraavanlainen:

Alkuosa: 25 x 1.8 Gy, PTVa-d: 100% ≙ 1.8 Gy
7 IMRT-kenttää (6 MV):

Kenttä		Kanturi	Keilanrajain	Annoskertymäalueet
1	DEX -takaviisto	230°	0° tai 90°	PTVrakko, PTVboost
2	DEX-viisto	265°	0° tai 90°	PTVrakko, PTVboost
3	DEX-etuviisto	325°	0° tai 90°	PTVrakko, PTVboost
4	AP	0°	0° tai 90°	PTVrakko, PTVboost
5	SIN-etuviisto	35°	0° tai 90°	PTVrakko, PTVboost
6	SIN-viisto	95°	0° tai 90°	PTVrakko, PTVboost
7	SIN-takaviisto	130°	0° tai 90°	PTVrakko, PTVboost

Loppuosan suunnitelmat (booster yhteensä 10 x 2 Gy, PTVe-h: 100% ≙ 2 Gy) tehdään vastaavalla menetelmällä kohdealueisiin PTVe, PTVf, PTVg ja PTVh. CBCT-kuvaus on erillisessä hoitojaksossa, ja hoitokenttien hoitojaksossa TT-SIM:n isosentripisteeseen tehdään neljä suunnitelmaa ”BOOSTER_punainen”, ”BOOSTER_sininen” jne., joita käytetään virtsarakon päivittäinen täyttöaste huomioiden.
Hoito: virtsarakko tyhjänä
Hoito: 1h virtsarakon tyhjennys + 6dl vettä / kemosädehoidon nesteytys

B) Linac 6

VMAT-suunnittelu Monaco:lla

Ennen suunnittelun aloittamista:

- Tarkasta, että struktuurit ovat siirtyneet Monaco:on oikeilla nimillään.
- Tarkasta, että struktuurit (BS&IC) on piirretty korkeintaan pari cm etäisyydelle kraniaalisesti suurimmasta PTV:stä. Jos ei, poista kraniaaliset osuudet rakenteista.
- Muokkaa struktuurien värit, etenkin PTV:t edellä mainittujen ohjeiden mukaisiksi.
- Luo optimoinnissa käytettävät PTV:t
  -> *CT*-tilassa: *Contouring -> Auto Margin*, nimeä OptPTVx, joka muodostuu lisäämällä 2 mm marginaali kaikkiin suuntiin PTVx:stä.

Suunnittelu:

- Luodessa uuden suunnitelman, valitse *IMRT* ja seuraavassa vaiheessa toisen kierroksen laskenta-algoritmiksi *Monte Carlo*. Käytössä myös template:ja. Alla esitetty suunnitelma Monaco:ssa Template:na nimellä: ”RakkoVMAT360”.
- Tarkista isosentri. Huomioi, että isosentrin on oltava paikassa, joka mahdollistaa suurimmankin PTV:n mahtumisen kenttäkokoon (16*21cm) kaikissa hoitosuunnissa.

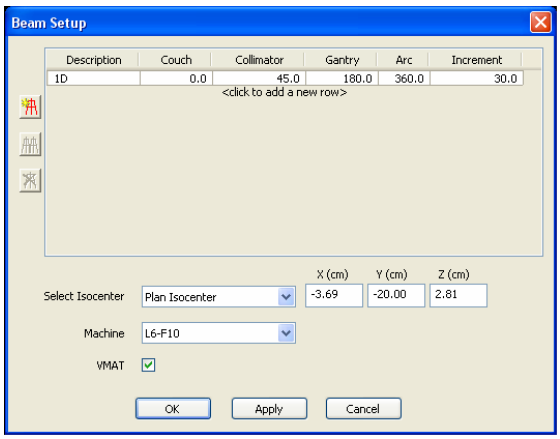

Kuva 1: Beam Setup

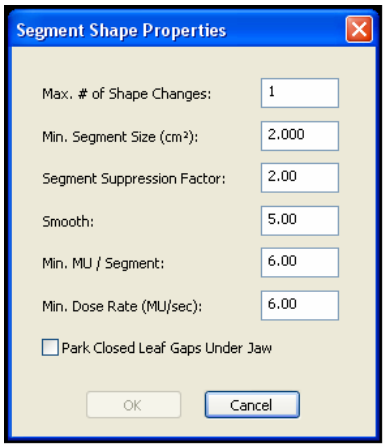

Kuva 2: Segment Shape Properties

Beam Setup (Kuva 1), huomioitavaa:

- Nimeä kenttä PTV:n mukaisesti, esim. PTV1:lle kentän nimeksi 1A. PTV2:lle 1B jne.
- Energia: 10x (*Machine:* L6-F10)
- Kollimaattorikulmaksi 0°, kunhan kattaa PTV:n kaikista suunnista.
- 360° VMAT, *Increment*:iä ei kannata pienentää alle 30°.

Segment Shape Properties (Kuva 2), huomioitavaa:

- ÄLÄ MUUTA: ”*Max. # of Shape Changes* = 1”, “*Min. Segment Size* = 2” ja “*Segment Suppression Factor* = 2”
- “*Smooth*”: 5 (Monaco 2.04 versiossa Medium). Pienentäminen ei paranna juurikaan annosjakauman tarkkuutta, mutta segmenttien määrä kasvaa ja hoitoaika pitenee. Smooth:n suurentaminen huonontaa selkeästi annosjakaumaa.
- ”*Min. MU/Segment*” ja ”*Min.Dose Rate*” väliltä 5-7. Pienentäminen: Tarkempi jakauma, mutta pidempi aika. Suurentaminen: Heikompi annosjakauma, mutta nopeampi hoidon toteutus.

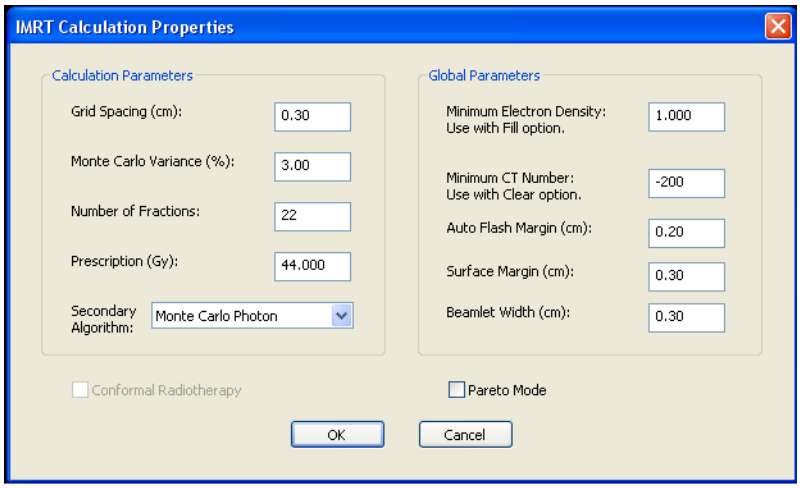

Kuva 3: IMRT Calculation Properties

IMRT Calculation Properties (Kuva 3), huomioitavaa:

- ”*Grid Spacing*” ja ”*Beamlet Width*” arvot on oltava samoja. Aseta myös *DVH-properties* -> ”*Grid Size*”:n arvo samaksi (Max. 1mm eri).

  Huom! ”*Prescription*” -> ”....*Complication Models*” -> ”*Shrink Margin*” toimii vain ”*Grid Spacing*”:n arvon monikertoina. Eli tässä tapauksessa “*shrink Margin*” toimii arvoilla: 0.0, 0.3, 0.6, 0.9 etc.

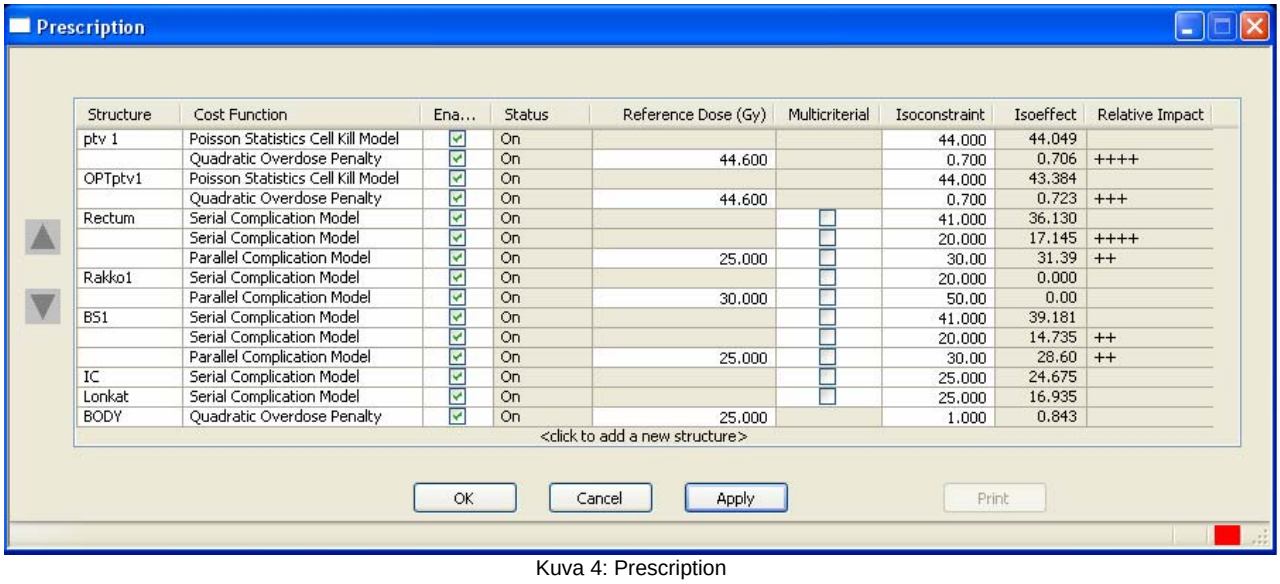

Kuva 4: Prescription

Prescription (Kuva 4), huomioitavaa:

- Jos Rectum:ssa (tai suolistossa) on reilusti ilmaa PTV:n alueella, kannattaa asettaa ainakin PTV:n tai jopa kyseisten ilmaa sisältävien struktuurien ”*Minimum Electron Density*”: 0.

- PTV:t -> ”*Poisson Statistics Cell Kill Model*” -> “*Cell Sensitivity*”: 0.75.
  -> “*Quadratic Overdose Penalty:*” target-annos + 0.5 – 0.8 Gy
  -> “*Isoconstraint*”: 0.600 – 1.000
  -> Voi asettaa todella tiukoiksi etenkin pienille PTV:ille.
  -> vähentää sekä hot- että cold-spot:ja.

- Rectum: Kun osittain PTV.ssä tai sen välittömässä läheisyydessä:

-> 1. *"Serial..."* -> "*Isoconstraint*": noin 0,95 * target-annos
-> "k": 12
-> Klikkaa: *"Optimize Over All Voxels"*
-> 2. *"Serial..."* -> *"Isoconstraint"*: noin 0,5 * target-annos
-> "k": 10
-> "*Shrink Margin*": 0,6 cm
-> *"Parallel..."* -> *"Ref.Dose":* noin 0,65 * target-annos
-> *"k"*: 3
-> "*Shrink Margin*": 0,6 cm

- Rectum: Kun kauempana PTV:stä (esim. rakon anteriorisen seinämän hoito):
Rectumin paikka "*Prescription*:ssa" vasta rakon ja BS jälkeen.
-> *"Serial..."* -> "*Isoconstraint*": noin 0,5 * target-annos
-> "k": 10

- Rakko: Kun hoidetaan koko rakko, ei laiteta rakon struktuuria "*prescription*:iin".
Kun hoidetaan osa rakosta:
-> *"Serial..."* -> *"Isoconstraint*": noin 0,5 * target-annos
-> *"k"*: 8
-> *"Shrink Margin"*: 0,6 cm
-> *"Parallel..."* -> *"Ref.Dose*": noin 0,65 * target-annos
-> *"k":* 2.5
-> "*Shrink Margin*": 0,6 cm

- BS: -> 1. *"Serial..."* -> *"Isoconstraint*": noin 0,95 * target-annos
-> *"k"*: 10
-> Klikkaa: "*Optimize Over All Voxels*"
-> 2. *"Serial*..." -> *"Isoconstraint*": noin 0,5 * target-annos
-> *"k":* 1 (Joissain tapauksissa toimii hyvin k=10)
-> "*Shrink Margin*": 0,6 cm
-> *"Parallel*..." -> "*Ref.Dose*": noin 0,65 * target-annos
-> *"k":* 2.5

IC: -> *"Serial*..." -> "*Isoconstraint*": noin 0,65 * target-annos
-> *"k":* 1 (Joissain tapauksissa toimii hyvin k=10)
-> "*Shrink Margin*": 0,6 cm

Body: -> "*Quadratic Overdose Penalty:*" noin 0,7 * target-annos
-> "*Isoconstraint*": 1.000
-> "*Shrink Margin*": 0,9 cm

Optimointi:

- 1. Kierros (Pencil Beam):
-> Mallaile parametreja niin, että algoritmi joutuu haasteisiin, mutta kuitenkin sen verran löysästi, että lopussa minkään parametrin kanssa ei joudu tappelemaan täysillä.
-> Tarkkaile tilannetta *"Console:n", "Prescription:n" ja "DVH Statistics:n"* avulla.
-> Jo tässä vaiheessa on syytä keskeyttää laskenta, jos havaitsee, että on syytä muuttaa parametreja, joita ei laskennan aikana voi mallailla.

-> Kun laskenut ensimmäisen kierroksen, tarkastele *"Prescription" ja Sensitivity*" taulukoita. Ei kannata lähteä toiseen kierrokseen liian tiukoilla vaatimuksilla.

- 2. Kierros (Monte Carlo):
  -> Kannattaa laskettaa ensimmäisen kerran löysähköillä vaatimuksilla. Tarkkaile tilannetta *"Prescription":sta,* mutta etenkin kiinnitä huomiota *"DVH Statistics:n"* PTV:n 95%:n annoksen osuuteen. Mallaile parametreja niin, että algoritmi joutuu haasteisiin, mutta kuitenkin sen verran löysästi, että koko PTV:n kattaisi 95% tavoite annoksesta eikä lopussa minkään parametrin kanssa joudu tappelemaan täysillä.
  -> Jos löysähköilläkin parametreilla oli vaikeuksia saavuttaa hyvää annosjakaumaa, voi olla syytä muokata esimerkiksi *Min. MU/Segment*" ja "*Min.Dose Rate". Huomioi myös* "*Console:sta"* segmenttien ja MU määrää sekä arvioitua hoitoaikaa (joka on "beam-on"-aika). Tavoitteena voi pitää suuruusluokkia: Segmenttejä: 80-100, MU: 700-900 ja hoitoaika: 180-280 sekuntia.(Hyvin kohdekohtaisia).
    -> Jos näissä petrattavaa, on syytä muokata etenkin arvoja: "*Min MU/Segment*" ja "*Min.Dose Rate*", jolloin koko laskentaprosessi on aloitettava alusta.
  -> Kun annosjakauma on hyvä löysähköillä *"Prescription*":n kriteereillä, segmentit, MU:t ja hoitoaika ovat ok, voi keskittyä mallailemaan *"Prescription"*:ia. Tällöin voi laskettaa vain 2.kierrosta, jossa samaan aikaa optimoimalla haetaan parasta mahdollista annosjakaumaa.
    -> Muista tallentaa välissä, sillä muokkaamalla jotakin parametria, ja palauttamalla sen takaisin alkuperäiseen, ei välttämättä tule uudestaan sama tulos Monte Carlo algoritmilla lasketettaessa.

Valmiin suunnitelma exportointi:

- Lähetä Linac 6:sen *Xvi*:lle suunnitelma CT-kuvan ja struktuurien kera.
- Lähetä suunnitelma *Mosaiq*:iin
  -> *Mosaiq*:ssa jokainen suunnitelma omaan *Course*:en.
  -> Luo myös kokonaisannoksen kirjautumiseksi summa sarake.

Suunnitelmien annosjakaumien laadunvarmistus:

- Mittaa jokainen suunnitelma matrix:n ympärille kehitetyllä phantomilla.
  -> Kerro mitattu annosjakauma kertoimilla:
    -6 MV: 1,036
    -10 MV: 1,045
- Mittaa myös yksi potilaan suunnitelma QA 0° - suunnitelmana.

Hoito:

- Virtsarakon tyhjennys juuri ennen hoidon aloittamista. (Kemosädehoito: 1h virtsarakon tyhjennys + 6dl vettä / kemosädehoidon nesteytys)
- CBCT-kuvaus *Hexapod*:lla potilaalle sopivalla *CBCT-Presets* asetuksella.
  -> Hexapod pöytä asetettava nolla-kohtaansa.
- Auto-matching Grey-value algoritmilla, PTV:n kokoisella maskilla.
  -> Tarkista Auto-matching:n tulos ja match:aa tarvittaessa manuaalisesti.
- Valitaan CBCT-kuvan perusteella hoidettava kenttä.
- Hoidon jälkeen kuvaus potilaalle sopivalla *CBCT-Presets* asetuksella.

CBCT-kuvaus Xvi:lla:

- Potilaalle pyritään löytämään sopiva Xvi:n *CBCT-Preset* kuvauksiin.
  -> Tarpeeksi hyvä kuvanlaatu mahdollisimman pienellä annoksella.

Work-flow:

1. Fraktio:
   Kuvaus ennen: Prostate M10 Fast CCW
   Kuvaus jälkeen: Rakko A CCW 7,5 – 11,7 mGy

Mikäli *Prostate fast* ei tarjoa tarpeeksi hyvää kuvanlaatua, on jatkossa kuvattava *Prostate* –preset:illä. Tällöin on pohdittava kuinka usein ja millä preset:llä hoidon jälkeisiä kuvauksia suoritetaan.

Mikäli *Rakko A* ei tarjoa tarpeeksi hyvää kuvanlaatua, päädytään käyttämään jatkossa vain *Prostate fast* –preset:iä.

Mikäli *Rakko A* tarjoaa tarpeeksi hyvän kuvanlaadun:

2. Fraktio:
   Kuvaus ennen: Rakko A CCW 7,5 – 11,7 mGy
   Kuvaus jälkeen: Rakko B CCW 4,0 – 6,7 mGy

Mikäli *Rakko B* ei tarjoa tarpeeksi hyvää kuvanlaatua, päädytään käyttämään jatkossa vain *Rakko A* –preset:iä.

Mikäli *Rakko B* tarjoaa tarpeeksi hyvän kuvanlaadun:

3. Fraktio:
   Kuvaus ennen: Rakko B CCW 4,0 – 6,7 mGy
   Kuvaus jälkeen: Rakko C CCW 3,0 – 4,5 mGy

Mikäli *Rakko C* ei tarjoa tarpeeksi hyvää kuvanlaatua, päädytään käyttämään jatkossa vain *Rakko B* –preset:iä.

Mikäli *Rakko C* tarjoaa tarpeeksi hyvän kuvanlaadun, päädytään käyttämään jatkossa vain *Rakko C* –preset:iä.

Huomioi kuvauksien lopullisia *Preset*:ejä valitessa, että ennen hoitoa kuvattaessa on kuvan laadulla suurempi merkitys. Hoidon jälkeisiin ”off-line:na” tarkasteltaviin kuviin riittää heikompikin kuvan laatu.

Taulukko 1: Rakko potilaille käytettävien Xvi-presets:ien annoksia. (Mitattu CT-Thorax phantom:lla, r = 16 cm)

Preset:	Annos isosentrissä (mGy)	Annos max. pinnassa (mGy)
Prostate M10	20,5	35,7
Prostate M10 Fast	11,2	18,5
Rakko A	7,5	11,7
Rakko B	4,0	6,7
Rakko C	3,0	4,5